CIVIL ENGINEERING STUDIES
Illinois Center for Transportation Series No. 13-017
UILU-ENG-2013-2011
ISSN: 0197-9191

IMPROVEMENT FOR DETERMINING THE AXIAL CAPACITY OF DRILLED SHAFTS IN SHALE IN ILLINOIS

Prepared By
Timothy D. Stark
James H. Long
Pouyan Assem

Research Report No. FHWA-ICT-13-017

A report of the findings of
ICT-R27-99
Improvement for Determining the Axial Capacity of Drilled Shafts in Shale in Illinois

Illinois Center for Transportation

May 2013

Technical Report Documentation Page

1. Report No.	2. Government Accession No.	3. Recipient's Catalog No.
FHWA-ICT-13-017		

4. Title and Subtitle

Improvement for Determining the Axial Capacity of Drilled Shafts in Shale in Illinois

5. Report Date
May 2013

6. Performing Organization Code

7. Author(s)

Timothy D. Stark, James H. Long, and Pouyan Assem

8. Performing Organization Report No.

ICT-13-017

9. Performing Organization Name and Address

Illinois Center for Transportation
Department of Civil and Environmental Engineering
University of Illinois at Urbana-Champaign
205 N. Mathews Ave, MC 250
Urbana, IL 61801

10. Work Unit (TRAIS)

11. Contract or Grant No.
ICT R27-99
UILU-ENG-2013-2011

12. Sponsoring Agency Name and Address

Illinois Department of Transportation
Bureau of Materials and Physical Research
126 E. Ash St.
Springfield, IL 62704

13. Type of Report and Period Covered

14. Sponsoring Agency Code

15. Supplementary Notes

16. Abstract

In this project, Illinois-specific design procedures were developed for drilled shafts founded in weak shale. In addition, recommendations for field and laboratory testing to characterize the in situ condition of weak shales in Illinois were developed and presented herein. For this project, weak shale is defined as an intermediate geologic material (IGM) with an unconfined compressive strength of 10 to 100 ksf. These investigation and design improvements are anticipated to lead to safer design and substantial deep-foundation cost savings for IDOT.

17. Key Words	18. Distribution Statement
Drilled shaft, weak IGMs, axial capacity rock, shale, side and tip resistance, predictive method, resistance factor, modified standard penetration test, penetration rate	No restrictions. This document is available to the public through the National Technical Information Service, Springfield, Virginia 22161.

19. Security Classif. (of this report)	20. Security Classif. (of this page)	21. No. of Pages	22. Price
Unclassified	Unclassified	68 plus appendices	

Form DOT F 1700.7 (8-72) Reproduction of completed page authorized

ACKNOWLEDGMENTS

This publication is based on the results of ICT Project R27-99, *Improvement for Determining the Axial Capacity of Drilled Shafts in Shale in Illinois*. The Illinois Department of Transportation provided funding for this study. Research team members would like to thank the Technical Review Panel (TRP) members and TRP co-chairs, Bradly Hessing and Bill Kramer, for their valuable inputs and organizational capabilities that facilitated completion of this research and preparation of the final report for this project. Research team members also want to thank Mike Short of IDOT District 3 and Greg Heckel and Brian Laningham of IDOT District 6 for their valuable contributions to field exploration at IL 23 over Short Point Creek and US 24 over the Lamoine River, respectively. We also want to thank the members of the Technical Review Panel for their support and many review comments:

Bill Kramer, TRP Chair, IDOT Bureau of Bridges and Structures

Bradly Hessing, TRP Co-Chair, IDOT Bureau of Bridges and Structures

Heather Shoup, IDOT Bureau of Materials and Physical Research

Abraham Ramirez, U.S. Department of Transportation (FHWA)

Rob Graeff, IDOT District 9 Geotechnical Engineer

Greg Heckel, IDOT District 6 Materials Engineer

Naser Abu-Hejleh, U.S. Department of Transportation (FHWA)

Mike Short, IDOT District 3 Geotechnical Engineer

Dan Tobias, IDOT Bureau of Materials and Physical Research

Dave Miller, IDOT District 3 Geotechnical Engineer

Terry McCleary, McCleary Engineering

Tom Casey, SCI Engineering Inc.

Riyad Wahab, IDOT Bureau of Safety Engineering

Research team members also want to thank Illinois Center for Transportation staff, particularly Dr. Imad Al-Qadi (ICT Director), Dr. Erol Tutumluer, James Meister, and James Pforr, for their cooperation and for providing resources and assistance with laboratory triaxial compression testing of weak shale core specimens at the Advanced Transportation Research and Engineering Laboratory (ATREL). Research team members want also to thank Wang Engineering, Inc., for performing pressuremeter tests at three IDOT bridge sites and providing pressuremeter data for comparison with laboratory data.

DISCLAIMER

EXECUTIVE SUMMARY

For project ICT R27-99, Improvement for Determining the Axial Capacity of Drilled Shafts in Shale in Illinois, the research team studied load transfer mechanisms of drilled shafts that are fully or partially embedded in weak, clay-based sedimentary rocks (e.g., weak shales) encountered in Illinois and developed a design procedure that will improve safety and reduce IDOT's deep-foundation costs for future bridge structures.

The main objectives of Task 1 of this study were to review existing literature and develop a drilled shaft load test database for weak, clay-based sedimentary rocks and to evaluate existing design methods. Objectives of Task 2 were to perform field exploration and laboratory tests at five IDOT bridge sites to develop new methods for characterization of weak shale encountered at shallow depths in Illinois. Objectives of Task 3 were to use the load test database compiled herein and data from five IDOT bridge sites to develop new correlations for the design of drilled shafts in weak shale. Also in Task 3, resistance factors were developed for designing drilled shafts using a load and resistance factor design (LRFD) framework. Drilled shafts at three IDOT sites were re-designed as a part of Task 3 to demonstrate the effectiveness of developed design correlations. The following paragraphs summarize major findings of this project.

DEVELOPMENT OF NEW PREDICTIVE METHODS

Published drilled shaft design literature and drilled shaft load test data since 1962 in rock were reviewed to create a database of drilled shaft static load test data for unit side resistance and tip resistance of drilled shafts in weak cohesive rocks (e.g., shales). This database includes the most recent drilled shaft load tests conducted in shale and other clay-based and cohesive sedimentary weak rocks, including shales in Illinois. This database was used to show that existing methods are not suitable for design of drilled shafts in weak cohesive rocks and was employed to develop a new design method.

UNIT SIDE RESISTANCE

Some of the findings related to drilled shaft unit side resistance are as follows:

- A linear function is recommended to be used to predict unit side resistance in weak shales instead of the power functions that are commonly used to correlate rock unconfined compressive strength to measured unit side resistance in a drilled shaft load test.
- Side resistance does not change significantly with changes in shaft diameter.
- After ultimate unit side resistance is mobilized, additional drilled shaft displacement along the drilled shaft/weak rock interface does not significantly decrease unit side resistance.
- More instrumented load tests on drilled shafts in weak Illinois rocks are required to develop better Illinois-specific predictive methods.

UNIT TIP RESISTANCE

Some of the findings related to drilled shaft unit tip resistance include the following:

- Available predictive methods (with exception of the methods of Abu-Hejleh et al. [2003], Abu-Hejleh and Attwooll [2005], and the *Canadian Foundation*

Engineering Manual [Canadian Geotechnical Society 2006]) correlate only measured tip resistance in load tests to unconfined compressive strength of weak rock.

- Analysis of load test data gathered in this project indicates that mobilized tip resistance is governed not only by unconfined compressive strength of weak rock but also by drilled shaft movement at tip elevation and depth of embedment of a drilled shaft in weak rock. Therefore, predictive methods for tip resistance should account for all of these factors, not just unconfined compressive strength.
- The load test database developed for this project was used to develop a design method that can account for these factors. The new method uses settlement and strength criteria to predict unit tip resistance. This added feature leads to strain compatibility between side and tip resistance.

FIELD EXPLORATION AND LABORATORY TESTING

Field exploration was performed at five IDOT bridge sites to obtain shale core samples for laboratory triaxial compression tests and to determine engineering properties of weak shale in Illinois for drilled shaft design. Pressuremeter testing was performed at three IDOT bridge sites and modified standard penetration tests (MSPTs) were performed at all five sites to measure the in situ properties of weak shale to facilitate correlation with laboratory triaxial values and develop a new design method. Some of the findings related to field exploration and laboratory testing of weak rocks in Illinois include the following:

- For shale specimens with low rock quality designations (RQDs), application of a confining pressure in laboratory triaxial compression tests yielded a higher peak deviator stress than the commonly used unconfined compression tests. For intact specimens (i.e., high RQD), application of a confining pressure did not significantly increase the unconsolidated undrained compressive strength, compared with results of unconfined compressive tests on comparable shale specimens that had comparable water content and RQDs.
- The standard penetration test was modified for use in weak cohesive rocks (e.g., weak shales). An Illinois-specific correlation between MSPT penetration rate and unconfined compressive strength of weak shale was developed and can be used by IDOT for drilled shaft design to reduce the amount of shale coring and laboratory testing required, which will decrease design time and reduce project costs.
- An Illinois-specific correlation between in situ water content and intact Young's modulus was developed for drilled shaft preliminary design phase. This correlation shows that Young's modulus decreases with increasing in situ water content.
- Pressuremeter and laboratory moduli were compared. Pressuremeter moduli are systematically higher than laboratory moduli, which has been observed by other investigators in the past (e.g., Mesri and Gibala [1972]). Young's modulus back calculated from drilled shaft load tests by elastic methods (Poulos and Davis 1974) were also compared with laboratory and pressuremeter modulus. Relationship between unconfined compressive strength and back calculated Young's modulus from drilled shaft load tests is recommended for consistent and economical design.

CONTENTS

CHAPTER 1 INTRODUCTION

1.1 PROBLEM STATEMENT

Use of drilled shafts as foundation units for Illinois bridge structures is increasing. Over a 5-year period (i.e., 2007–2011), the Illinois Department of Transportation's annual budget for pile foundation systems has been approximately constant at $12 million per year. However, over the same time period, use of drilled shafts has increased from less than $0.5 million per year to almost $6.5 million per year because of a lower unit cost, additional scour resistance, and widely available material and equipment to construct.

Drilled shafts are traditionally designed using predictive methods that were developed based on results of load tests in similar soils or rocks. Uncertainty is associated with these methods due to assumptions involved in their development. For major projects where differential settlement of adjacent columns is detrimental, on-site axial load tests are justified to verify the predicted side and tip resistances. However, drilled shaft load tests may or may not be justified for smaller projects, including bridge pier construction or replacement, where the cost of load tests would be a significant percentage of the total cost of the project. As a result, predictive methods are currently used by design engineers for most bridge structures.

Considerable research has been devoted to improvement of drilled shaft design in various types of rocks but not in weak and weathered rocks, such as shale. (During this study, weak and weathered rock is defined as intermediate geologic material (IGM) with unconfined compressive strengths of 10 to 100 ksf). Thus, side and tip load transfer characteristics in weak rocks are not well understood and was the motivation for this study.

Other state departments of transportation (DOTs) (e.g., Colorado and Missouri) have addressed this knowledge gap by conducting load tests on drilled shafts in weak, clay-based rocks (e.g., shale, mudstone, and claystone) and developed state-specific predictive methods for such foundations. These state-specific correlations have resulted in more accurate drilled shaft designs and considerable cost savings for the corresponding state DOTs. Currently, IDOT uses correlations developed in other states or design methods that are developed for stronger rocks, which could result in conservative designs.

1.2 DESIGN ISSUES

Some of the issues addressed during this study regarding current predictive methods for side resistance in drilled shafts in Illinois shales include the following:

- Predictive methods for side resistance that use a power function overpredict side resistance for very weak IGMs and underpredict for stronger IGMs.
- Effect of post-failure shaft movement on ultimate unit side resistance is not well understood and affects whether or not both side and tip resistance contribute to axial capacity.
- Effect of drilled shaft size (e.g., diameter and length) is not well understood for weak cohesive IGMs.

Some of the issues addressed related to current predictive methods for tip resistance in drilled shafts in Illinois shales include the following:

- Impact of embedment depth, diameter, and shaft movement on mobilized drilled shaft tip resistance. These factors are not accounted for in many existing drilled shaft design methods.
- Some design methods are based on an assumed tip displacement that could impact serviceability, so a new method is proposed herein.
- Some design methods recommend drilled shafts be designed as friction bearing or tip bearing but not both. Either approach can lead to conservative designs so this research investigated the possibility of mobilizing both friction and tip resistance in weak rocks (e.g., shales) in Illinois to reduce the level of conservatism and decrease design expenses.
- Mobilization of both friction and tip resistance is possible because this study has developed a tip resistance predictive method that includes settlement and strength criteria.

Lastly, most, if not all, of the available predictive methods use unconfined compressive strength of rock as the main input parameter. Research has shown that mode of failure in weak rocks is influenced by the amount of applied confining pressure (Williams et al. 1980; Goodman 1989; Terzaghi et al. 1996; Jaeger et al. 2007). Lack of confining pressure in laboratory unconfined compression testing of weathered rocks (which is the current practice in the United States, including Illinois) can lead to premature failure (Jaeger et al. 2007) or premature formation of tension cracks in the laboratory specimen and a conservative estimate of design strength. Laboratory triaxial compression tests conducted during this research verified these observations for Illinois shales and resulted in recommendations for conducting unconsolidated undrained triaxial compression tests to develop less conservative designs when drilled shafts are embedded in weathered cohesive IGMs.

1.3 SCOPE OF THIS RESEARCH

The following paragraphs provide a brief description of the main tasks and outcomes of this research project.

- A database of drilled shaft static load tests in various weathered argillaceous cohesive intermediate geologic materials (IGMs) was developed to evaluate current predictive drilled shaft design methods. Based on this comparison, existing predictive methods were modified to better model observed axial behavior of drilled shafts in weak shales and other weathered clay-based rocks (e.g., clay-shales, claystones, and mudstones).
- The new design method is based on both unconfined compressive strength and settlement criteria. This method allows a design engineer to account for mobilization of tip and side resistance in the drilled shaft instead of only one of these resistances because strain compatibility between side and tip resistances is accounted for in the new design methodology. The new design criteria ensures settlement or serviceability limits states will be met, as axial movement of a drilled shaft occurs to mobilize both tip and side resistance.
- Laboratory unconfined compression and triaxial compression tests were conducted on shale cores from five IDOT bridge sites to investigate the effects of

confining pressure on undrained shear strength and mode of failure of the shale specimen. This task is important because undrained compressive strength of shale is the main input for estimating both side and tip resistances. Results of this task generated recommendations for future laboratory triaxial compression testing of shale specimens, as well as future research topics.

- Modified standard penetration tests (MSPTs) were performed at five IDOT bridge structures investigated during this project to develop an Illinois-specific relationship between shale unconfined compressive strength and MSPT penetration rate. This relationship will allow IDOT engineers to utilize MSPT penetration rate for future drilled shaft design and verification of laboratory undrained shear strength values. This approach is recommended where shale is weathered so penetration rate can be measured and obtaining shale cores is either impossible or involves sample disturbance levels that are not acceptable. The use of MSPT penetration rate for drilled shaft design should reduce design time and costs by reducing or eliminating shale coring and laboratory unconfined compression testing and/or triaxial compression testing.

CHAPTER 2 GEOLOGICAL ASPECTS OF WEAK IGMS

2.1 INTRODUCTION

This section discusses the geological aspects of weak rocks that are important to the design of drilled shafts. Weak rocks or intermediate geomaterials (IGMs), underlie a large portion of the United States (e.g., Alabama, Arkansas, California, Colorado, Illinois, Iowa, Kentucky, Michigan, Missouri, Montana, Oregon, Texas, and Utah). Weak and weathered rock is defined as soil or rock with unconfined compressive strengths of 10 to 100 ksf (O'Neil et al. 1999). Use of drilled shafts in weak rock formations (shale, mudstones, and claystones) is gaining popularity among state DOTs, including Illinois, because of lower cost, ease of construction, limited steel availability and time delays for H-piles, additional scour resistance, and widely available equipment for construction. To effectively design drilled shafts in weak rocks, design engineers must understand the geologic conditions that formed the deposits and be familiar with mineralogy and geological conditions during and after formation. Mineralogy of earth materials affects their physical properties and their mechanical behavior. The geological condition (e.g., fissures and joints) can dominate the behavior and shear strength of weak rocks.

2.2 MINERALOGY OF CLAY- AND SILT-BASED INTERMEDIATE GEOMATERIALS

Shales, claystones, and mudstones are referred to as clay-based IGMs. These geomaterials are formed from nonvolcanic minerals and rock fragments that are called epiclastic sediments (Goodman 1993). These rocks are called argillaceous because the main minerals forming their structure are clays (Goodman 1993). Argillaceous rocks are formed from water-deposited sediments that were weathered/eroded from rocks or from previous mud rocks and precipitated in seawaters. Minerals of argillaceous rocks are mainly clays; however, small portions of feldspar, mica, chlorite, serpentine, iron, and organic matter can also be found (Goodman 1993).

2.3 FORMATION OF INTERMEDIATE GEOMATERIALS

Epiclastic sediments are converted to weak argillaceous rocks (such as shales, mudstones, and claystones) through a lithification process (Goodman 1993). As overburden soil accumulates over time, water and/or air is squeezed out of pore spaces of the sediment, creating a more stable and stronger matrix. Lithification involves consolidation of these sediments if the soil sediments are fully saturated. If the soil matrix is partially saturated, lithification involves squeezing out both air and water, which is termed compaction instead of consolidation.

As consolidation and/or compaction of these sediments occurs due to accumulation of more overburden, these initially loose deposits change into a rocklike geomaterial (e.g., shale, mudstone, and claystone). After lithification, these rock materials can undergo weathering, resulting in an IGM.

2.4 CLASSIFICATION OF ARGILLACEOUS ROCKS

This section presents a classification system for identifying argillaceous rocks. A classification system is introduced so differences between shales, mudstones, and claystones can be described in the field and design. This classification system is based on

the degree of fissility of these rocks and their constituent particles. A fissile rock is one that tends to break apart along closely spaced sets of surfaces inherent in the rock mass. Fissility becomes significant in any argillaceous rock lacking a substantial content of calcareous or siliceous material because the strength of the material is controlled by the strength along the preexisting surfaces (Ingram 1953; Goodman 1993).

An argillaceous rock is referred to as shale if it shows fissility (Goodman 1993) and as a mudstone if it does not. Mudstones, however, are bedded. The term claystone is used interchangeably with mudstone. If a mudstone dissolves in water, it disaggregates to particles of clay and silt. A claystone, on the other hand, disaggregates in water to mainly clayey particles with little or no silt (Goodman 1993).

In summary, shale, mudstone, and claystone are all clay-based IGMs, with different degrees of fissility and different mineralogies. The degrees of fissility and mineralogy are reflected in unconfined compressive strength and/or blow count of the IGM that are used in the design process.

2.5 SECONDARY STRUCTURE OF WEAK SHALES

Shear strength of saturated clays can be measured with reasonable accuracy from undisturbed specimens in the laboratory because they do not contain secondary structure, such as joints and fissures. Clay soils are usually fairly homogeneous because the clay particles are deposited in shallow water deposits, which tend to create uniformly graded materials.

Weak argillaceous rocks, however, include secondary structure (e.g., joints and fissures) that controls their mechanical behavior. However, height of triaxial specimens that is commonly used in practice is smaller than fissure spacing and thus laboratory shale specimens rarely capture this secondary structure. Therefore, the mobilized in situ shear strength of the shale is usually lower than the strength of small, laboratory triaxial compression specimens of the same material (Terzaghi et al. 1996). This is due to failure in situ may occur along fissures whereas failure in laboratory is forced to occur within intact rock material.

Because of the secondary structure of weak rocks, full-scale field tests are the best means for determining the shear strength of such rocks. These full-scale tests involve a quantity of material large enough to ensure that the effects of the joints and fissures are accounted for in the engineering properties of the IGM. If full-scale tests are not possible or affordable, large samples of these rocks are required to capture a representative sample of the secondary structure.

The following sections describe the effects of secondary structure on the behavior of weak rocks and give recommendations for quantifying the effects of this secondary structure on the engineering properties required for drilled shaft design in weak shales.

2.5.1 Secondary Structure and Its Indicators

The term secondary structure refers to any set of joints or fissures that exist in a mass of weak rock. Epiclastic sediments (i.e., nonvolcanic materials) are deposited and transformed into rocklike materials by a lithification process. Joints and fissures can form after lithification due to stress relief and weathering, hence the name secondary structure (i.e., after lithification). A secondary structure is any type of discontinuity along which the mechanical behavior of the rock mass becomes discontinuous (Turner 2006). Joints are present in all rock masses but at varying degrees. These joints have strength, permeability,

and deformability characteristics that are different from the intact rock (Palmstrom 1982). Among many types of discontinuities affecting the mechanical behavior of rock masses, the most common are faults, joints, shear planes, foliations, and beddings. These secondary structures are identified by four main factors: (1) orientation of the joint, (2) joint surface roughness and shape, (3) joint filling material, and (4) joint aperture, or opening.

Orientation of a discontinuity surface can be described by the dip and the dip direction of this surface. Dip is defined as the maximum angle of this surface to the horizontal direction (Turner 2006). To measure dip and dip direction, one may use oriented boreholes so the direction of discontinuity can be identified with respect to the orientation of obtained rock cores.

Surface roughness of these discontinuities can be described using the following terms, according to the Turner (2006) manual on rock-socketed drilled shafts:

- slickensided
- smooth
- slightly rough
- rough
- very rough

These terms are used to describe qualitatively the degree of discontinuity roughness.

In addition to the degree of roughness, joint surface shape, or geometry, is important for drilled shaft design. Turner (2006) uses the following terms to describe shape of these discontinuities:

- wavy
- planar
- stepped
- irregular

The type of material filling the joint (e.g., clay, silt, sand, etc.) is also important to estimate the strength mobilized along the joint surface.

The last important factor for describing secondary structure is joint aperture, which is a measure of joint openness. Turner (2006) describes the degree of openness of these joints in terms of joint width:

- wide: 12.5–50 mm
- moderately wide: 2.5–12.5 mm
- narrow: 1.25–2.5 mm
- very narrow: less than 1.25 mm
- tight: 0 mm

2.5.2 Effects of Secondary Structure on Mechanical Behavior of Weak Shales

The secondary structure of weak rocks reduces their shearing strength. Therefore a weak rock specimen that is tested in the laboratory should contain a representative number of joints and fissures. Sample sizes that are commonly used in the United States and IDOT rarely capture a representative sample of these joints and fissures. Therefore, field methods, such as standard penetration tests or pressuremeter tests, may be more suitable for measuring the shear strength of weak rocks because they are influenced by the secondary structure of rock. Both of these field tests were used during this study, and it is recommended subsequently that IDOT consider the modified version of the standard penetration test for drilled shaft design in Illinois.

Weak rocks are confined in the field. However, it is common practice to measure undrained compressive strength of weak rock using unconfined compression tests. If fissures are captured in the test specimen, sliding along fissures is possible, with zero confining pressure condition (Goodman 1993). This causes a premature failure of a rock specimen and thus leads to an underestimate of in situ shear strength. Therefore, it is recommended that IDOT adopt unconsolidated–undrained triaxial compression tests to measure the laboratory shear strength of weak rock in future drilled shaft projects for design or comparison with modified standard penetration test data and correlations presented in Appendix F.

2.5.3 Characterization of Secondary Structure in Engineering Applications

Rock quality designation (RQD) (Deere and Deere 1988) is used commonly in the design of drilled shafts embedded in weak rocks. (RQD is defined as the percentage ratio between the total length of the core recovered and the length of core drilled for a given run of core is the value of recovery ratio.) For example, O'Neil et al. (1996) uses the RQD as a means for determining the ratio of mass rock modulus to laboratory intact rock modulus. RQD is a modified core recovery ratio that is determined by considering only pieces of core that are at least 4 in. long and are hard and sound. Breaks caused by the drilling and coring process are ignored. The percentage ratio between the total length of the core recovered and the length of core drilled for a given run of core is the value of recovery ratio. The sum of lengths of all of rock core segments greater than 4 inch divided by the total length of rock core run is the RQD. The RQD is used to evaluate rock quality, as tabulated below.

Table 2.1 Rock Quality Designation

RQD (%)	Rock Quality
90-100	Excellent
75-90	Good
50-75	Fair
25-50	Poor
0-25	Very Poor

In addition to RQD, other systems are available for characterization of rock mass properties (e.g., GSI and RMR systems). These methods require additional information on the in situ condition of rock mass (e.g., ground water flow through joints and exact information on spacing of discontinuities). This information is not usually collected in a typical drilled shaft project. Therefore, it is recommended that the rock quality designation be used to identify the in situ condition of rock during field shale coring and in preparation of the resulting boring logs. However, RQD is affected by borehole orientation. Therefore, oriented

boreholes are best suited for measurement of RQD because joints vary, so oriented boreholes are recommended for IDOT's future drilled shaft projects if laboratory testing will be performed.

2.6 SUMMARY

Secondary structure of weak argillaceous rocks, such as shales, claystones, and mudstones, affects their shear strength and Young's modulus. Specimens tested in laboratory triaxial compression tests rarely capture joints and fissures because of the small specimen size. Therefore, in situ methods (e.g., Modified Standard Penetration test for weak IGMs) are the better suited for measuring in situ shearing strength and Young's modulus of fissured rocks.

When in situ tests are not justified, rock quality designation (Deere and Deere 1988) can be used to characterize secondary structure of rock, quantify effects of joints and fissures on shear strength, and qualitatively incorporate these characteristics in drilled shaft design.

CHAPTER 3 DRILLED SHAFT STATIC LOAD TEST DATABASE

3.1 INTRODUCTION

Predictive methods for the design of drilled shafts in soils and rocks are empirical. Many of these predictive methods were developed based on databases consisting of load tests on drilled shafts in different types of rocks. Therefore, the applicability of these soil and rock predictive methods needs to be evaluated for weak rocks (i.e., shales) in Illinois.

A database of drilled shaft side resistance and a database of drilled shaft tip resistance in weak rocks were compiled in this study. The database includes over 45 load tests of relevant drilled shaft load tests since 1960 with 87 values of side and tip resistance. These two databases are used herein to evaluate current design methods and develop an Illinois-specific design method. This database is also used to study the load transfer mechanism in side and tip resistance of drilled shafts in weak, clay-based sedimentary rocks.

3.2 SIDE RESISTANCE DATABASE

The unit side resistance database includes 54 values of side resistance from more than 40 drilled shaft load tests. This unit side resistance database is summarized in Table 3.1. This drilled shaft load test database includes the following:

- Data from Osterberg load tests and conventional top-loaded, drilled shaft load tests.
- Drilled shafts embedded in weak shales, claystones, and mudstones.
- Drilled shaft diameters range from 13 to 78 in. (0.33 to 1.98 m).
- Most of the drilled shafts sockets were drilled normally. Only a few of the drilled shafts had artificially roughened socket walls that increase side resistance. Both of these factors influence the mobilized side resistance.
- Side resistance is defined as the maximum unit side resistance reached before load test termination.
- The ratio of drilled shaft vertical movement to diameter is less than 1.7%.
- The vertical displacement of the drilled shafts is generally less than 1 in. (25 mm).

The side resistance database was used to study the behavior of axially loaded drilled shafts in weak rocks and to evaluate current side resistance predictive methods. This database was then used to develop a design method for drilled shafts in weak, clay-based sedimentary rocks in Illinois.

3.3 TIP RESISTANCE DATABASE

The unit tip resistance database includes 33 values of tip resistance from 33 drilled shaft load tests. This database is summarized in Table 3.2. The drilled shaft load test database includes the following:

- Data from Osterberg load tests and conventional top-loaded drilled shaft load tests.
- Drilled shafts embedded in weak shales, claystones, and mudstones.
- Unconfined compressive strength of weak rocks, at or two shaft diameters below the tip, between 10 to 100 ksf.
- Drilled shaft diameters ranged from 12 to 96 in. (0.30 to 2.44 m).
- In most cases, the bottom of the drilled shaft was cleaned of loose debris (see summary in Table 3.2).
- Tip resistance is defined as the maximum unit tip resistance reached before load test termination.
- Drilled shaft vertical movement at the tip elevation was 0.4 to 4.3 in. (10.2 to 109.2 mm).

This tip resistance database was used to study the behavior of axially loaded drilled shafts in weak rocks and to evaluate current tip resistance predictive methods. This database was then used to develop a design method for drilled shafts in weak, clay-based sedimentary rocks in Illinois.

3.4 SUMMARY

Drilled shaft load test databases for unit side and unit tip resistance were developed in this study and are described in this chapter. These databases include only drilled shaft load tests involving weathered cohesive IGMs, not soils and other rocks. Drilled shaft diameters in the database range from 12 to 96 in. (0.30 to 2.44 m) for the tip resistance database and 13 to 78 in. (0.33 to 1.98 m) for the unit side resistance database.

These databases are used to study load transfer mechanism(s) of axially loaded drilled shafts in weak shales, to evaluate current predictive methods, and to develop an Illinois-specific design procedure for drilled shafts in weak rocks.

Table 3.1 Side Resistance Database from Drilled Shaft Load Tests

Index	Reference	Geomaterial Type	f_{smax} (ksf)	q_u (ksf)	D (in.)	RQD (%)	Test Method	Remarks
1	Matich and Kozicki (1967)	Brown to gray shale and massive	> 6.5	14.4	24	—	Pull-out test	Artificially roughened
2	Corps of Engineers (1968)	Clay-shale	> 5.6	15.2	—	—	—	—
3	Geoke and Hustad (1979): Shaft 1	Gray clay-shale (Caddo formation)	7.5 @ 0.25 in.	21.6	30	—	Compression test	Drilled with rock auger
4	Geoke and Hustad (1979): Shaft 2	Gray clay-shale (Caddo formation)	4.6 @ 0.25 in.	15.8	30	—	Compression test	Drilled with rock auger
5	Wilson (1976) Port Elizabeth, south Africa: West pile	Mudstone from Uitenhage series of Cretaceous system	3.76 @ 0.47 in.	22.8	35.4	—	Pull-out test	Concrete defects due to water entering shaft
6	Wilson (1976) Port Elizabeth, south Africa East pile	Mudstone from Uitenhage series of Cretaceous system	2.51 @ 0.12 in.	22.8	35.4	—	Pull-out test	Concrete defects due to water entering shaft
7	Mason (1960): PC25 USA	Weak shale	8.7	31.3	24	—	Compression test	—
8	Johnston and Donald (1979) Melbourne (F2)	Weathered Melbourne mudstone	19.6	40.3	47	—	Compression test	—
9	Brown and Thompson (2008)	Claystone	> 9.6 @ 0.13 in.	43.2	28	—	Compression test	—
10	Brown and Thompson (2008)	Clay-shale	7 @ 0.61 in.	43.2	20	—	Compression test	—
11	Loadtest (2008) IL 5 over IL 84	Shale	1.4 @ 0.44 in.	5.57	42	—	Compression test	—
12	Loadtest (2008) IL 5 over IL 84	Shale	2.7 @ 0.44 in.	11.7	42	—	Compression test	—
13	Loadtest (2008) IL 5 over IL 84	Shale	13.3 @ 0.45 in.	55.75	42	—	Compression test	—
14	Loadtest (1996) FAU 6265	Shale	1.0 @ 0.1 in.	2.65	62	—	Compression test	—

(table continued, next page)

Table 3.1 (continued) Side Resistance Database from Drilled Shaft Load Tests

Index	Reference	Geomaterial Type	f_{smax} (ksf)	q_u (ksf)	D (in.)	RQD (%)	Test Method	Remarks
15	Pells et al. (1978) PC 29	Weathered Melbourne mudstone	16.6	46.1	43	—	Compression test	—
16	Millar (1976): City Center Perth, W.A.	King Park shale	> 23 @ 1.25 in.	63.9	27	—	Compression test	Drilled under bentonite
17	Millar (1976): Telephone Exchange, Perth, W.A. (TP1)	King Park shale	> 6.3 @ 1.2 in.	20.9	26	—	—	—
18	Millar (1976): Telephone Exchange, Perth, W.A. (TP2)	King Park shale	15.04 @ 0.16 in.	56	31	—	—	—
19	Johnston and Donald (1979) Flinders St., Melbourne (F1)	Weathered Melbourne mudstone	21.9	63.9	47.2	—	—	—
20	Walter et al. (1997)	Mudstone	12.5	66.8	35.4	—	Down-hole jack	—
21	Williams and Pells (1981)	Shale	23	64.7	27	—	—	Drilled and cast under bentonite
22	Williams and Pells (1981)	Shale	15	56.4	31	—	—	—
23	Williams (1980a): PS1 Stanley Ave., Melbourne	Weathered Melbourne mudstone	> 11.7	17.33	26	—	Compression test	Drilled normally
24	Williams (1980a): PS3 Stanley Ave., Melbourne	Weathered Melbourne mudstone	10.65	11.9	44	—	Compression test	Roughened
25	Williams (1980a): PS12 Stanley Ave., Melbourne	Weathered Melbourne mudstone	8.56	12.3	13.2	—	Compression test	Drilled with core barrel
26	Williams (1980a): PS14 Stanley Ave., Melbourne	Weathered Melbourne mudstone	10.4	12.1	15.5	—	Compression test	Roughened
27	Williams (1980a): PS15 Stanley Ave., Melbourne	Weathered Melbourne mudstone	8.6	12.5	15.5	—	Compression test	Roughened

(table continued, next page)

Table 3.1 (continued) Side Resistance Database from Drilled Shaft Load Tests

Index	Reference	Geomaterial Type	f_{smax} (ksf)	q_u (ksf)	D (in.)	RQD (%)	Test Method	Remarks
28	Williams (1980a): PS 16 Stanley Ave., Melbourne	Weathered Melbourne mudstone	> 7.5	12.1	15.5	—	—	Roughened
29	Williams (1980a): M1 Middleborough Rd. Melbourne	Weathered Melbourne mudstone	12.51	51.4	48	—	—	Drilled with bucket auger
30	Williams (1980a): M2 Middleborough Rd. Melbourne	Weathered Melbourne mudstone	13.4	48	51.2	—	—	Roughened
31	Williams (1980a): M3 Middleborough Rd. Melbourne	Weathered Melbourne mudstone	14.8	48	48.4	—	—	Drilled with bucket auger
32	Williams (1980a): M4 Middleborough Rd. Melbourne	Weathered Melbourne mudstone	12.9	48.9	53.15	—	—	Roughened
33	Williams (1980a) Pile WG303/2 Melbourne	Slightly weathered Melbourne mudstone	17.75	72.9	—	—	—	Roughened
34	Leach et al. (1976): Pile A, Kilroot, N. Ireland	Mudstone	4.38 @ 0.23 in.	16.71	29.1	—	—	Drilled with auger
35	Leach et al. (1976): Pile B, Kilroot, N. Ireland	Mudstone	2.5 @ 0.55 in.	19.2	29.1	—	—	Drilled with auger
36	Aurora and Reese (1976): MT1, Montopolis	Clay-shale	8.56	29.6	29	—	Conventional	Drilled with auger, dry
37	Aurora and Reese (1976): MT2, Montopolis	Clay-shale	7.64	29.6	31	—	Conventional	Drilled with auger, dry
38	Aurora and Reese (1976): MT3, Montopolis	Clay-shale	14.4	29.6	29.5	—	Conventional	Drilled with auger, dry
39	Aurora and Reese (1976): DT1, Dallas	Clay-shale	5.8 @ 0.2 in.	12.8	35	—	Conventional	Drilled with auger, dry
40	LT-8718-2, KS Socket (1998)	Gray to dark gray shale with limey seams	3.13 @ 0.78 in.	13	72	40	O-Cell	Drilled with auger
41	LT-9048 Route 116 Over the Platte River (2004)	Gray silt shale	> 15.1 @ 0.66 in.	45.9	48	—	O-Cell	Drilled with auger, dry

(table continued, next page)

Table 3.1 (continued) Side Resistance Database from Drilled Shaft Load Tests

Index	Reference	Geomaterial Type	f_{smax} (ksf)	q_u (ksf)	D (in.)	RQD (%)	Test Method	Remarks
42	LT-8718-1 US 36 Over Republican River Socket (2001)	Dark gray shale (Graneros shale formation)	3.75 @ 1.73 in.	19.7	72	49	O-Cell	Drilled with auger
43	LT-8854 I-235 Over Des Moines River Socket (2002)	Clay-shale	13.05 @ 0.86 in.	56.2	42	93	O-Cell	Drilled by auger and core barrel
44	LT-8816 US 281 Over Solomon River Socket (2001)	Gray to dark gray chalky shale	10.85 @ 0.72 in.	49.6	42	80	O-Cell	Drilled with rock auger
45	LT-8733: Pier 1 West US 75 at 77th Street Socket (2001)	Gray shale with limestone lenses	> 8.6 @ 0.2 in.	21.6	72	—	O-Cell	Drilled in dry with auger
46	Brown and Thompson (2008)	Weathered shale	19.8 @ 0.36 in.	46.1	71	—	O-Cell	—
47	Miller (2003): Lexington, MO TS-1A, O-Cell to SG 2	Hard gray clay-shale	15.2 @ 0.15 in.	44.4	43.75	—	O-Cell	Drilled normally
48	Miller (2003): Lexington, MO TS-2, Lower to Upper O-Cell	Hard gray shale to clay-shale	15.2 @ 0.48 in.	46.9	46	—	O-Cell	Drilled normally
49	Miller (2003): Grandview, MO SG 5 to SG 6	Gray thinly laminated clay-shale	7.6 @ 0.65 in.	19.5	77.8	—	O-Cell	Drilled normally
50	Abu-Hejleh et al. (2003): I-225	Soil-like claystone	> 2.6 @ 1.6 in.	8.3	42	—	O-Cell	Slightly roughened
51	Abu-Hejleh et al. (2003): I-225	Soil-like claystone	> 3.6 @ 1.6 in.	12.3	42	—	O-Cell	Slightly roughened
52	Abu-Hejleh et al. (2003): I-225	Soil-like claystone	> 3.1 @ 1.6 in.	10	42	—	O-Cell	Slightly roughened
53	Abu-Hejleh et al. (2003): County line	Soil-like claystone	> 3.4 @ 0.8 in	10.4	48	—	O-Cell	Slightly roughened
54	Abu-Hejleh et al. (2003): Franklin	Very hard sandy claystone	> 19 @ 0.42 in.	64	42	—	O-Cell	Wet

Table 3.2 Tip Resistance Database from Drilled Shaft Load Tests

Index	Reference	Geomaterial Type	qtmax (ksf)	qu (ksf)	D (in.)	RQD (%)	Socket Length (in.)	Tip Movement (in.)
1	LT-8718-1 US 36 Over Republican River	Geraneros Shale Formation	> 56.9	16.7	72	61	315	1.12
2	LT-8718-2 US 36 Over Republican River	Geraneros Shale Formation, dark gray shale	> 44.1	13	72	33	323	0.62
3	LT-8733: Pier 1 West US 75 at 77th Street	Severy Shale Formation	> 127	36.2	72	__	274	0.68
4	LT-8816 US 281 Over Solomon River	Gray to dark gray shale (chalky)	> 136.7	63.5	42	70	141	1.00
5	LT-8854 I 235 Over Des Moines River	Light gray and moist clay-shale	> 378	81.9	42	94	356.2	1.50
6	LT-9021 US 75 Over Neosho River	Green and gray clayey shale	> 149	84.6	60	__	335	0.91
7	LT-9048 Route 116 Over Platte River	Thinly laminated silt shale, gray	> 134	52.5	48	__	120	0.60
8	LT-8415-2	Gray shale	> 140	93	96	43	413	1.34
9	Abu-Hejleh et al. (2003): County Line	Soil-like claystone	> 54	16.85	48	__	162	4.61
10	Abu-Hejleh et al. (2003): Franklin site	Blue and sandy claysone	> 254.5	46.35	42	__	249.6	2.93
11	Abu-Hejleh et al. (2003): I-225	Soil-like claystone	> 55	13.1	42	__	193.2	2.26
12	Aurora and Reese (1976): DT1	Clay-shale	51	12.8	35	__	76.8	2.31
13	Vijayvergiya et al. (1969)	Clay-shale	122	27.2	30	__	124.5	__
14	Thorburn (1966)	Clay-shale	227	88	48	__	48	0.41
15	Thorburn (1966)	Clay-shale	22.4	84	36	__	150	1.32
16	Henley (1967)	Clay-shale	294	36	18	__	240	2.3

(table continued, next page)

Table 3.2 Tip Resistance Database from Drilled Shaft Load Tests

Index	Reference	Geomaterial Type	q_{tmax} (ksf)	q_u (ksf)	D (in.)	RQD (%)	Socket Length (in.)	Tip Movement (in.)
17	Van Doren et al. (1967)	Clay-shale	32	7.2	__	__	__	__
18	Geoke and Hustad (1979): TS 1	Caddo Formation: gray clay-shale	98	17	30	__	214	0.77
19	Geoke and Hustad (1979): TS 2	Caddo and Kiamichi Formations: gray clay-shale	128	20	30	__	308	0.48
20	Wilson (1976)	Mudstone, cretaceous	143.7	22.8	26.5	__	118	1.84
21	Hummert and Cooling (1988)	Shale, thinly bedded	225.6	39	18	__	120	1.8
22	Jubenville and Hepworth (1981)	Unweathered shale	76.4	17	12	__	60	1.2
23	Aurora and Reese (1976): MT1	Clay-shale	119	29.6	29	__	46	2.6
24	Aurora and Reese (1976): MT2	Clay-shale	107	29.6	31	__	48	2.8
25	Aurora and Reese (1976): MT3	Clay-shale	128	29.6	29.5	__	60	1.8
26	Williams (1980a)	Highly weathered mudstone	133.7	13.6	12	__	__	0.75
27	Williams (1980a)	Highly weathered mudstone	146.2	14	12	__	__	0.67
28	Williams (1980a)	Moderately weathered mudstone	123.2	56	39.5	__	__	0.43
29	Williams (1980a)	Moderately weathered mudstone	137.8	51.2	39.5	__	__	0.27
30	Williams (1980a)	Moderately weathered mudstone	146.2	51.2	39.5	__	__	0.23
31	Williams (1980a)	Moderately weathered mudstone	140	56	39.5	__	__	0.27
32	Williams (1980a)	Mudstone	192	40.3	23.6			3.3
33	Williams (1980a)	Moderately weathered mudstone	148.3	29.2	39.5	__	__	4.3

CHAPTER 4 FIELD EXPLORATION AND LABORATORY TESTS

4.1 INTRODUCTION

Field exploration was performed at five existing IDOT bridge sites to investigate the properties of weak cohesive IGMs in Illinois and to develop recommendations for shear strength input parameters for an Illinois-specific design method for predicting drilled shaft capacity. Bridge piers and abutments at these five sites are founded on drilled shafts embedded in weak cohesive IGMs (i.e., primarily weak shales). The five IDOT bridge sites that were investigated are the following:

- IL 23 over Short Point Creek, Livingston County
- US 24 over the Lamoine River, Brown County
- FAI80 over Aux Sable Creek, Grundy County
- Illinois River Bridge replacement (FAU 6265), LaSalle County
- John Deere Road (IL 5) over IL 84, Rock Island County

Two borings were drilled at each site. These borings were drilled to a depth of approximately two drilled shaft diameters below the tip of the existing drilled shafts to evaluate the shear strength of the weak shale involved in the mobilization of shaft tip resistance.

One of the two borings was used to obtain shale core samples for determination of the recovery ratio, RQD of the rock mass, and vertical spacing of joints. Afterwards, unconfined compression and triaxial compression tests were conducted on representative and comparable shale core specimens to study the effect of confining pressure on the behavior of shale specimens subjected to compressive mode of shear (i.e., loading a specimen in the vertical direction). The shale cores were obtained using an NX (2.00 in rock core) core barrel at IL 23 over the Short Point Creek and US 24 over the Lamoine River and an ND_3 (2.06 in rock core) core barrel at the other three sites. In three of the five borings, Wang Engineering Company, Inc. (Wang Engineering) of Lombard, Illinois performed pressuremeter tests to determine pressuremeter moduli of the weak shale and to provide a means for comparison of field moduli, with moduli determined from laboratory triaxial compression tests.

The second boring was drilled usually about 10 to 15 ft from the first boring to obtain MSPT blow counts at various depths. These data were used to develop a new correlation between unconfined compressive strength of weak cohesive IGMs (e.g., shale) in Illinois and MSPT penetration rate (which is subsequently defined) with depth.

Objectives of the field and laboratory testing were

- To study the effect of confining pressure on undrained compressive strength of weak shales.
- To develop a correlation between unconfined compressive strength of weak shales and field MSPT penetration rate values.
- To measure in situ Young's modulus of weak shales and compare with laboratory values.

- To develop the correlation between Young's modulus, in situ water content, and undrained compressive strength for weak shales in Illinois.

4.2 MAJOR FINDINGS

Laboratory and in situ test results on weak shales for five IDOT bridge sites are presented in Appendices A through E. Appendices A through E correspond to the following bridges, respectively:

- IL 23 over Short Point Creek, Livingston County
- US 24 over the Lamoine River, Brown County
- FAI80 over Aux Sable Creek, Grundy County
- Illinois River Bridge replacement (FAU 6265), LaSalle County
- John Deere Road (IL 5) over IL 84, Rock Island County

The major findings of the field and laboratory testing are summarized herein.

4.2.1 Undrained Compressive Strength

Undrained triaxial compression tests with and without confining pressure were conducted on weak Illinois shale cores to investigate the effect of confining pressure on the measured undrained compressive strength. All triaxial compression tests were performed in accordance with ASTM D 7012 at the Advanced Transportation Research and Engineering Laboratory at the University of Illinois at Urbana-Champaign. Rock quality as represented by RQD of weak rock is known to control the shear strength of weak rocks that have a fractured structure. Rock quality designation of the shale cores was measured in accordance to ASTM D 6032. Relationship between rock quality and effect of confining pressure on mobilized undrained compressive strength is studied.

Figure 4.1 summarizes a number of the triaxial compression test results as a function of RQD. Figure 4.1 shows the effect of confining pressure is significant for shale specimens that have a low RQD because of the presence of joints and fissures. The use of a confining pressure results in an increase in undrained compressive strength because the confining pressure prevents premature failure along the joints and fissures present in the shale. In other words, the confining pressure closes the joints and fissures prior to shear and keeps them closed, at least for the initial portion of the test. This finding is in agreement with published literature (e.g., Golder and Skempton 1948; Williams et al. 1980; Santarelli and Brown 1989; Goodman 1989; Terzaghi et al. 1996; ASTM D 2166-06; Jaeger et al. 2007). Application of a confining pressure leads to closing of fissures and increases the undrained strength. Figure 4.1 also shows that specimens with high RQDs yield similar values of confined and unconfined compressive strengths (i.e., less scatter) because there are few joints and fissures to reduce the strength of the unconfined specimens.

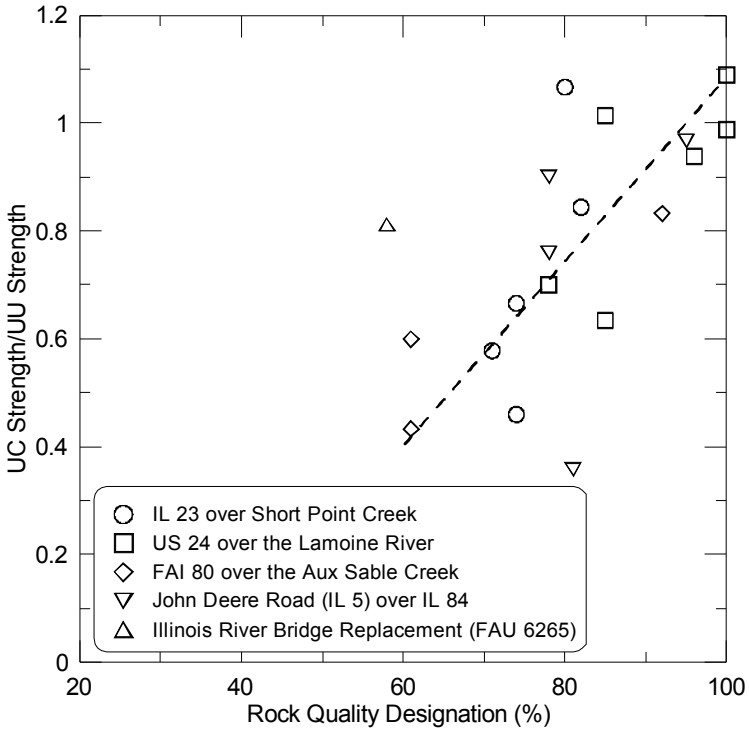

Figure 4.1 Effect of confining pressure on undrained compressive strength of Illinois shale.

4.2.2 Young's Modulus and In Situ Water Content

Young's modulus was measured from results of confined and unconfined triaxial compression tests in accordance to ASTM D 7012. In short, the modulus was estimated from the initial slope of the deviator stress–axial strain relationships obtained in the unconfined and confined triaxial compression tests. In situ water content of rock specimens was measured in accordance to ASTM D 2216-10. These data were used to develop a relationship between undrained Young's modulus and shale in situ water content, which is shown in Figure 4.2. This relationship is expected because in situ water content reflects the mineralogy and structure of soils and rocks (Terzaghi et al. 1996), both of which affect soil stiffness and strength. This results in Young's modulus decreasing rapidly with increasing water content. Thus, when site-specific triaxial compression testing is not available, in situ water content is an index property that can be used to estimate Young's modulus of weak shales using the relationship in Figure 4.2 for preliminary drilled shaft design phase.

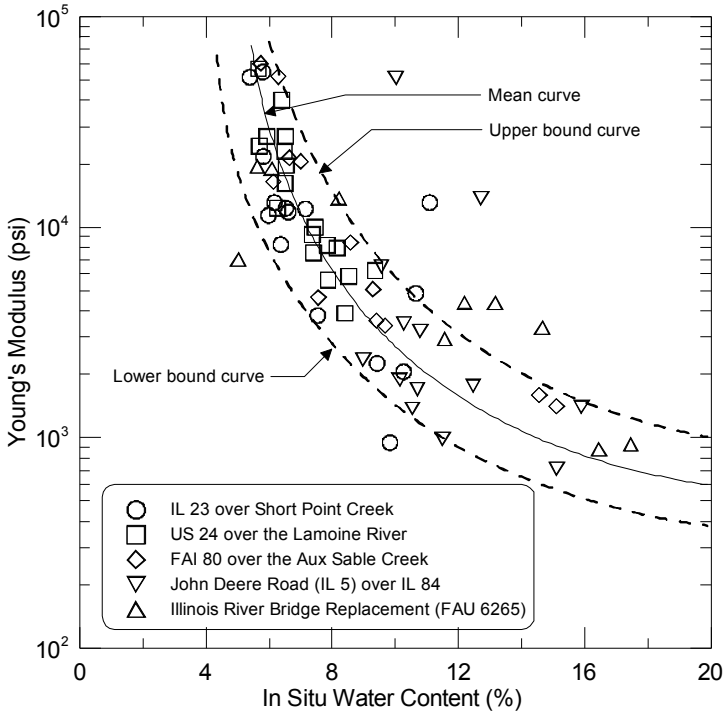

Figure 4.2 Relationship between in situ water content and laboratory Young's modulus for shales in Illinois.

4.2.3 Young's Modulus and Undrained Compressive Strength

Unconfined and confined triaxial compression tests were performed in accordance with ASTM D 7012. The peak deviator stress from each triaxial compression test was used to calculate the undrained compressive strength for each test. The resulting undrained compressive strengths are shown in Figure 4.3 versus Young's modulus. Figure 4.3 shows that Young's modulus and undrained strength are related, which is in agreement with previous studies (e.g., Hendron et al. 1970). Figure 4.3 shows Young's modulus increases rapidly with increasing undrained strength because as strength increases the shale also becomes stiffer. This relationship can be used for preliminary settlement analysis of bridge piers founded on drilled shafts because some of predictive methods require an estimate of Young's modulus.

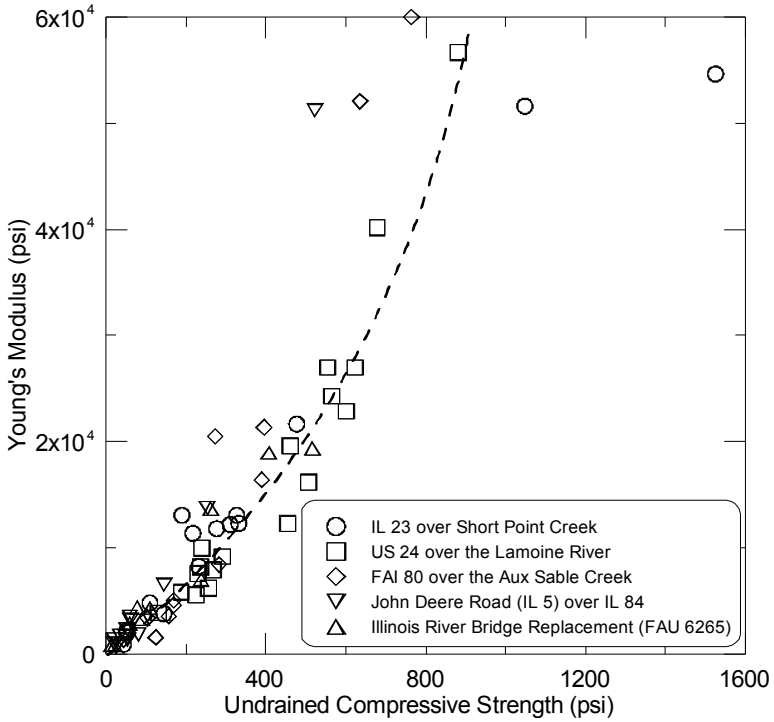

Figure 4.3 Relationship between undrained compressive strength and Young's modulus for shales in Illinois.

4.2.4 Pressuremeter Modulus

Wang Engineering conducted eight pressuremeter tests in weathered shales at three of the IDOT bridge sites investigated (see Appendices C, D, and E). Abu-Hejleh et al. (2003) and Abu-Hejleh and Attwooll (2005) also report pressuremeter test results in soil-like and very hard sandy claystone bedrocks (see Table 4.1). Pressuremeter modulus will be compared with Young's modulus obtained in laboratory and back calculated from drilled shaft load tests.

Table 4.1 Pressuremeter Tests (Data from Abu-Hejleh et al. 2003)

Site	IGM Type	q_u (ksf)	E_m (ksf)
I-225	Soil-like claystone	8.3	970
I-225	Soil-like claystone	13.1	2550
County Line	Soil-like claystone	10.4	1800
County Line	Soil-like claystone	16.8	3200
Franklin	Very hard sandy claystone	64	11050
Franklin	Very hard sandy claystone	41	4700

4.2.5 Recommended Design Young's Modulus

The tip resistance drilled shaft load test database was used to back calculate Young's modulus of weak shale and to develop a relationship with unconfined compressive strength. Figure 4.4 summarizes the pressuremeter, drilled shaft load test, and laboratory modulus values for weathered cohesive IGMs gathered during this study. As expected, pressuremeter moduli are higher than laboratory and drilled shaft load test moduli because pressuremeter compression loads are applied parallel to the plane of rock laminations and laboratory triaxial tests or drilled shaft load tests load the weak rock perpendicular to laminations. This is in agreement with Mesri and Gibala (1972) that show shale is stiffer when it is loaded parallel to plane of laminations. In addition, the pressuremeter tests are testing less disturbed material because the tests are performed in situ instead of in a laboratory, which requires transportation and specimen trimming. This is in agreement with published literature that describes sample disturbance during transport and trimming activities (e.g., Hendron et al. 1970; Mesri and Gibala 1972).

Direction of applied loads in a drilled shaft is similar to the loading in laboratory triaxial compression tests or field load tests and not pressuremeter tests. A drilled shaft load test measures in situ modulus of shale and involves less IGM disturbance than laboratory specimens. Therefore the associated relationship for Young's modulus measured from load test results in Figure 4.4, is recommended for design.

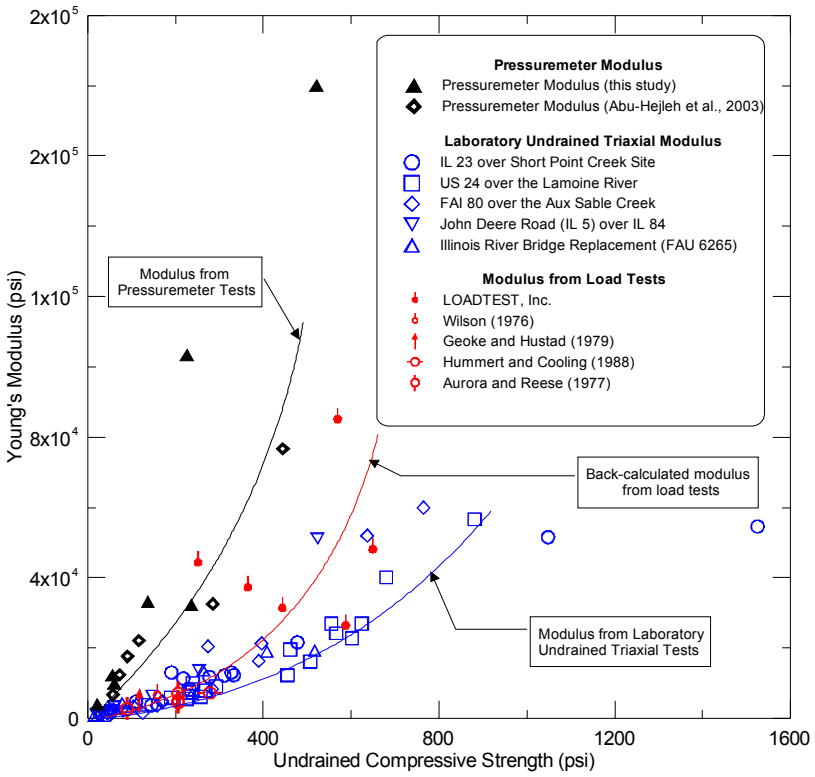

Figure 4.4 Comparison of Young's modulus values from pressuremeter, drilled shaft load, and laboratory triaxial compression tests.

4.2.6 Modified Standard Penetration Test (MSPT) and Unconfined Compressive Strength

Previous investigators (e.g., Stroud 1974; Terzaghi et al. 1996; Abu-Hejleh et al. 2003; Abu-Hejleh and Attwooll 2005) show standard penetration test N-values (ASTM D 1586) and unconfined compressive strength of weak rocks are related. Standard penetration test results presented by Abu-Hejleh et al. (2003) and standard penetration tests performed during this research (i.e., Stark et al. 2013) indicate that 18 in. of penetration (ASTM D 1586) is difficult or impossible to obtain in weak cohesive rocks (e.g., shales). Therefore blow counts obtained from such tests should be extrapolated to those that correspond to 18 in. of penetration. This often requires engineering judgment and involves considerable uncertainty and nonuniformity among different agencies. To eliminate the need for 18 in. of penetration and to reduce uncertainties in interpretation of test results, a modified standard penetration test (MSPT) is proposed herein.

The MSPT utilizes the concept of penetration rate ($\dot{N}$) instead of blow counts, which are dependent on the amount of penetration. In short, penetration rate is the inverse of slope of the linear portion of a plot of penetration distance versus blow count. This proposed test and recommended analysis procedure are discussed in detail in Appendix F. Modified standard penetration tests were performed at five IDOT sites during this study to demonstrate and refine the procedure. These test results show that penetration rate ($\dot{N}$) and unconfined compressive strength of weak rocks are related. Figure 4.5 presents unconfined compressive strengths, penetration rates, and proposed trend line.

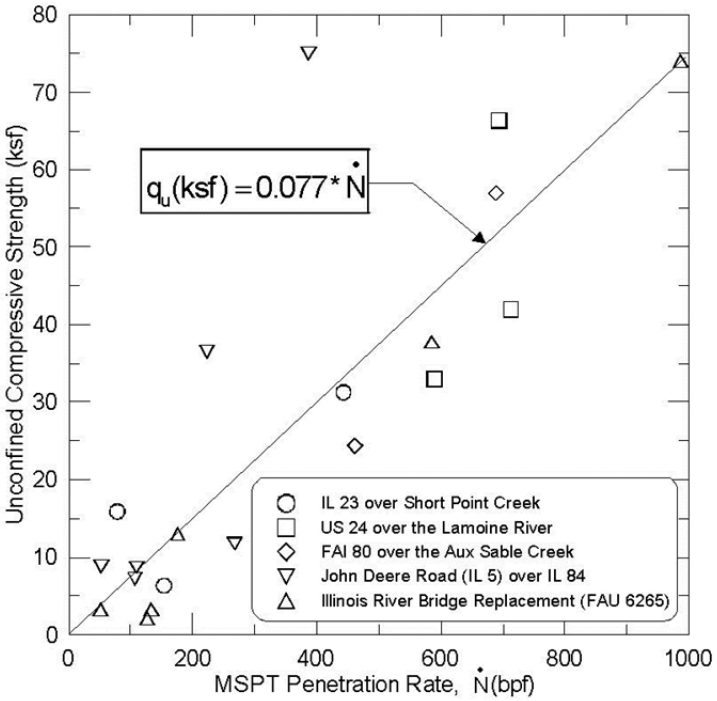

Figure 4.5 MSPT penetration rates and unconfined compressive strength of weak Illinois shales.

Based on Figure 4.5, the following expression can be used to estimate the unconfined compressive strength of weak shales from MSPT penetration rates for drilled shaft design in Illinois:

$$q_u(\text{ksf}) = \zeta * \dot{N}$$

where

q_u = unconfined compressive strength, ksf

$\zeta = 0.077,\ \text{ksf / bpf}$

$\dot{N}$ = penetration rate, bpf

This correlation is advantages for situations where the shale is highly weathered and obtaining high-quality shale cores for laboratory triaxial compression tests is difficult. More important, the use of MSPT penetration rates for drilled shaft design should reduce subsurface investigation and design time and costs by reducing or eliminating shale coring and laboratory triaxial compression testing by IDOT. This proposed test procedure also eliminates the shortcomings of conventional standard penetration tests and thus reduces the uncertainties that are involved in current test result interpretation. All IDOT districts are equipped to perform the modified standard penetration test. Recommended MSPT equipment and test procedures are presented in Appendix F and should be followed to ensure uniformity between different agencies. As a result, it is recommended that IDOT consider the use of MSPT penetration rates for future drilled shaft design in weak shales.

4.3 SUMMARY

Field exploration was performed at five existing IDOT bridge sites to investigate the properties of weak shales in Illinois and to develop an Illinois-specific method for predicting drilled shaft capacity. The following is a summary of the major findings:

- Triaxial compression test results indicate that the use of a confining pressure can increase the undrained compressive strength of weak shale, especially in shales with a low RQD value. Therefore, future research should use unconsolidated undrained tests with confining pressures equal to total overburden stress at the elevation of shale specimen to measure the weathered shale shear strength (Terzaghi et al. 1996; Stark et al. 2013). Side and tip resistance measured in future load tests should also be compared with shale shear strengths that are measured using unconsolidated undrained tests.
- Young's modulus can be correlated with the in situ water content and the undrained compressive strength. These correlations can be used to estimate Young's modulus of shales for the preliminary analysis of settlement of bridge piers when site-specific data is not available or to confirm site-specific data and laboratory test results.
- Pressuremeter modulus values are higher than modulus obtained from laboratory triaxial compression tests and drilled shaft load tests. Young's modulus obtained from drilled shafts load tests provide a better estimate of the in situ Young's modulus of weak rock compared to a triaxial compression modulus. This is due to weak rock in a drilled shaft load test being tested in situ and undergoing less disturbance. Therefore a relationship between unconfined compressive strength

and Young's modulus back calculated from drilled shaft load tests provides the best estimate of in situ modulus of weak rock for design (Figure 4.4).

- A correlation between unconfined compressive strength and MSPT penetration rate was developed for Illinois shale. This correlation can be used with MSPT penetration rate for drilled shaft design, especially when obtaining high-quality shale samples for triaxial compression testing is difficult or impossible. The use of MSPT penetration rates for drilled shaft design should reduce the design time and costs by reducing or eliminating shale coring and laboratory triaxial compression testing by IDOT.

CHAPTER 5 REVIEW OF PREDICTIVE METHODS FOR SIDE AND TIP RESISTANCE

5.1 INTRODUCTION

Drilled shafts socketed into weak rocks are commonly designed to carry the applied structural loads in the following ways: (1) tip resistance only, (2) side resistance only, or (3) a combination of side and tip resistance. If only side resistance or tip resistance is considered in drilled shaft design, the data presented in Chapters 6, 7, and Appendix G show this will lead to a conservative design. Therefore, it is appropriate to include both side and tip resistance to determine the allowable applied loads (Zhang and Einstein 1998; Stark et al. 2013). IDOT's current drilled shaft design approach is to rely on only side or tip resistance, whichever provides the largest axial resistance. This leads to conservative designs as is discussed in Appendix G.

Since the 1970s, a considerable number of load tests were conducted on drilled shafts socketed in rocks. Only few researchers (e.g., Williams 1980a), however, compiled a database that focused only on drilled shafts in weak rocks. Therefore, the majority of design methods discussed below were developed using databases that include both weak and strong rocks in their formulation.

Review of the literature further indicates that only few researchers (e.g., Miller 2003; Abu-Hejleh et al. 2003; Abu-Hejleh and Attwooll 2005) studied the applicability of available predictive methods to design of drilled shafts in weak rocks. Although their work provides valuable information on this matter, their databases include a limited number of drilled shaft load tests against which predictive methods for weak rocks can be evaluated.

This chapter presents a review of the literature on available predictive methods for side and tip resistance of drilled shafts in rocks. For each predictive method, the type of rock, the drilled shaft geometry, and the proposed design method are discussed. Chapter 6 uses the database developed herein and described in Chapter 3 to evaluate the applicability of these design methods to drilled shafts in weak shales in Illinois.

5.2 PREDICTIVE METHODS FOR SIDE RESISTANCE

Review of the load test database of Chapter 3 indicates that relatively small displacements are required for mobilization of ultimate unit side resistance. Analytical studies and load test measurements have shown further that side resistance accounts for a large percentage of mobilized axial capacity of drilled shafts socketed in weak rocks (Horvath and Kenney 1979). Therefore, many designers prefer to design drilled shafts to take loads in side resistance, as opposed to accounting for combined side and tip resistance (Miller 2003). It is common in drilled shaft projects that predictive methods are used for determining the magnitude of side resistance. It is important, however, that the designer be aware of the background of available predictive methods and the assumptions involved in their formulation. This section discusses predictive methods for side resistance of drilled shafts in rocks.

5.2.1 Rosenberg and Journeaux (1976)

Rosenberg and Journeaux's (1976) method is one of first for the prediction of side resistance of drilled shafts in rocks (Kulhawy et al. 2005). Rosenberg and Journeaux's (1976) proposed design correlation is

$$f_s / P_a = 1.09 * (q_u / P_a)^{0.52}$$

P_a in the above equation is the atmospheric pressure. This design method is based on a load test database that included only six data points (Kulhawy et al. 2005) and is based on the unconfined compressive strength of intact rock specimens. Rocks included in this database are sandstone, shale, limestone, and andesite, whose unconfined compressive strengths range from 11 to 720 ksf. The recommended correlation equation and its mathematical form are affected by the stronger range of data present in the database of Rosenberg and Journeaux (1976).

5.2.2 Horvath and Kenney (1979)

Horvath and Kenney's (1979) database includes large- and small-scale drilled shafts in field, rock anchors in the field, and small-scale drilled shafts in the laboratory to develop its method. The total number of drilled shaft axial load tests reported in their original paper is 87. Of these data, 50 data points are in the shale family (Kulhawy et al. 2005). Horvath and Kenney (1979) recommend

$$f_s = 0.2 * \sqrt{q_u (\text{MPa})}$$

for drilled shafts with smooth socket walls and

$$f_s = 0.3 * \sqrt{q_u (\text{MPa})}$$

for drilled shafts with rough socket walls. Horvath and Kenney (1979) provide different equations for small-diameter and large-diameter drilled shafts, which suggests the mobilized side resistance slightly decreases for large diameters. Horvath and Kenney (1979) utilize unconfined compressive strength of intact rock specimens measured in the laboratory for development of its predictive method. Unconfined compressive strength values were not reported and had to be estimated for some cases. Unconfined compressive strength of geomaterials in their database ranged from 2 to 846 ksf, which is well beyond the upper bound value (i.e., 100 ksf) for weak IGMs as defined by O'Neil and Reese (1999).

Horvath et al. (1983) discusses the advantages of artificially roughened sockets in their paper. They further point out that artificial roughening is significantly beneficial in the case of drilled shafts in soft rocks (e.g., shales). This fact is evident from Horvath and Kenney's (1979) correlation for rough sockets.

5.2.3 Meigh and Wolski (1979)

Meigh and Wolski (1979) compiled a database of 13 cases. Several of these cases have been used in other correlations, and about half are believed to have uncertain data (Kulhawy et al. 2005). Unconfined compressive strength of intact specimens used in their study ranged from 4 to 420 ksf. Meigh and Wolski (1979) recommend

$$f_s / P_a = 0.55 * (q_u / P_a)^{0.6}$$

for an unconfined compressive strength range of 15 to 265 ksf where P_a is the atmospheric pressure, and

$$f_s = 0.25 * q_u$$

for an unconfined compressive strength range of 8.5 to 15 ksf.

5.2.4 Williams et al. (1980)

Williams et al. (1980) used a total of 36 field load tests that were conducted in Melbourne mudstone and Sydney shale for development of their design method. Their correlation equation for prediction of side resistance is based on the unconfined compressive strength of intact rock specimens.

Peak values of side resistance come from unit side resistance–displacement curves developed from field load tests. Unconfined compressive strength values, however, come from correlation between in situ water content and drained strength parameters (Kulhawy et al. 2005). These unconfined compressive strength values range from 10.6 to 1693 ksf. Upper bound value for their data is well beyond the upper bound defined for weak IGMs. Williams et al. (1980) recommends the following equation for prediction of side resistance:

$$f_s / P_a = 1.84 * (q_u / P_a)^{0.37}$$

5.2.5 Reynolds and Kaderabek (1980)

Reynolds and Kaderabek (1980) were interested in the increase of bearing capacity of shallow foundations in soft Miami limestone by means of shear load transfer along the interface of shallow foundation and adjacent rock. Reynolds and Kaderabek (1980) report a median unconfined compressive strength of 31 ksf for Miami soft limestone for 688 tests. The authors recommend

$$f_s = 0.3 * q_u$$

for prediction of side resistance that can be mobilized at the interface of foundation and adjacent rock.

5.2.6 Gupton and Logan (1984)

Gupton and Logan (1984) recommend the following design method for prediction of side shear transfer:

$$f_s = 0.2 * q_u$$

This design method suggests a linear increase in side resistance by unconfined compressive strength, using a slope of 0.2.

5.2.7 Rowe and Armitage (1987)

Rowe and Armitage (1987) reviewed and summarized existing databases (i.e., Williams et al. 1980; Williams and Pells 1981; Horvath 1982) on side resistance of rock-socketed drilled shafts. The database that they studied includes 80 load tests at more than 20 sites (Kulhawy et al. 2005). This database includes shale, mudstone, claystone, limestone, sandstone, siltstone, chalk, diabase, and andesite. The average unconfined compressive strength of these rocks ranged from 8.5 to 846 ksf. This method was further confirmed using drilled shaft load tests performed in Ordovician aged shale that is found in Canada (Miller 2003).

The method of Rowe and Armitage (1987) assumes the rock socket is clean. However, this method distinguishes between smooth and artificially roughened sockets. Rowe and Armitage (1987) adopt the socket wall roughness classification introduced by Pells et al. (1980). Rowe and Armitage (1987) recommend the following correlation for sockets with roughness classification of R_1, R_2, and R_3 (i.e., groove less than 10 mm deep)

$$f_s = 0.45 * \sqrt{q_u(\text{MPa})}$$

and following equation for rock sockets with wall roughness classification of R_4 (i.e., grooves more than 10 mm deep)

$$f_s = 0.6 * \sqrt{q_u(\text{MPa})}$$

5.2.8 Carter and Kulhawy (1988)

The method of Carter and Kulhawy (1988) is based on 25 axial load tests. This load test database includes compression tests on shear sockets, compression tests on complete sockets, and uplift tests on shear sockets (Carter and Kulhawy 1988). Rock types included in this database are shale, mudstone, chalk, siltstone, sandstone, and limestone. Unconfined compressive strength of these rocks range from 4.2 to 856 ksf, with an average of 124 ksf.

From these data, only 12 load tests reached failure in side resistance; and thus design correlation is based on these tests. Carter and Kulhawy (1988) suggested the following lower bound equation for design purposes

$$f_s / P_a = 0.63 * (q_u / P_a)^{0.5}$$

and the following equation as a best fit to their data.

$$f_s / P_a = 1.42 * (q_u / P_a)^{0.5}$$

Carter and Kulhawy (1988) further explain that values of unit side resistance in excess of $0.15q_u$ should be used only when load test results are available.

5.2.9 Toh et al. (1989)

Toh et al. (1989) based their design method on nine load tests (i.e., one instrumented micropile and eight instrumented cast-in-place bored piles), with diameters ranging from 25 to 48 in. that were conducted in the Kenny Hill Formation in Malaysia. This design method was further verified by additional load tests reported by Meigh and Wolski (1979).

The database of Meigh and Wolski (1979) was already discussed. Kenny Hill Formation has layers of shale, mudstone, sandstone, and siltstone, with a range of unconfined compressive strength of 8.4 to 50 ksf.

Toh et al. (1989) recommends the following correlation equation for unit side resistance of drilled shafts socketed in similar rocks:

$$f_s = m * q_u$$

where m is obtained from the right vertical axis in Figure 5.1, reproduced from Toh et al. (1989).

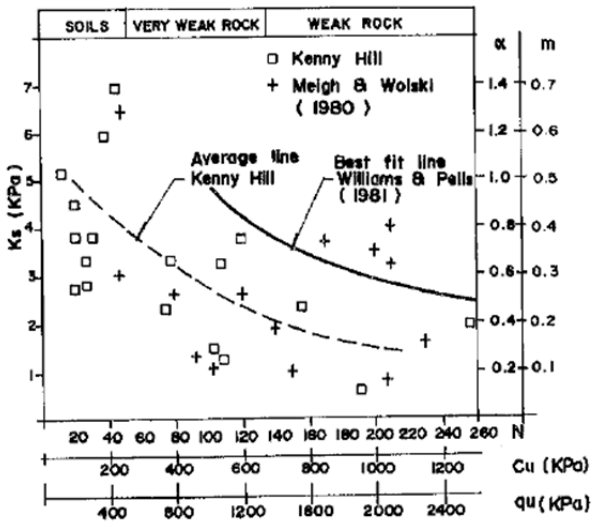

Figure 5.1 Design method for prediction of unit side resistance (after Toh et al. 1989).

5.2.10 Kulhawy and Phoon (1993)

Kulhawy and Phoon (1993) summarized the database developed by Rowe and Armitage (1984) and a database developed for Florida limerocks by Bloomquist and Townsend (1991) and McVay et al. (1992). Their design recommendations are based on 40 data points in the mentioned database. Rock types included in this collection are shale, mudstone, sandstone, limestone, and marl. Kulhawy and Phoon (1993) recommend

$$f_s / P_a = C * (q_u / 2 * P_a)^{0.5}$$

for prediction of side resistance in drilled shafts where C is a constant of proportionality for best fit to collected data that is obtained by the least square method. Kulhawy and Phoon (1993) recommend a value of 2 for C as a mean value, a value of 1 as a lower bound, and a value of 3 as an upper bound for rock sockets with very rough wall interface.

5.2.11 O'Neil et al. (1996)

O'Neil et al. (1996) introduces an alternative method for argillaceous weak IGMs (e.g., clay-shales and claystones). Ultimate unit side resistance can be approximated using

$$f_s = \alpha * q_u$$

where q_u is the unconfined compressive strength of the rock specimen and α is an empirical factor that is a function of q_u and fluid pressure exerted by concrete at the time of pour. α can be obtained from Figure 5.2.

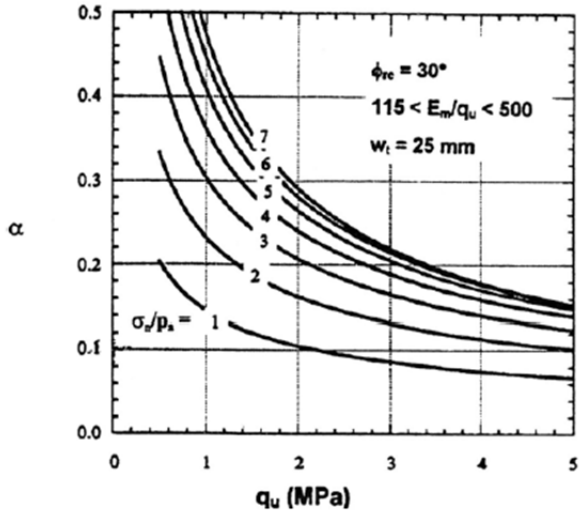

Figure 5.2 α factor for empirical design method for cohesive IGMs by O'Neil et al. (1996).

This method is based on work of Hassan et al. (1997) where detailed modeling and field testing were conducted to study load transfer mechanism in side resistance of drilled shafts in clay-shale of Texas (Turner 2006).

5.2.2 Miller (2003)

Miller (2003) reviewed design correlations of Rosenberg and Journeaux (1976), Horvath and Kenney (1979), Williams et al. (1980), Williams and Pells (1981), Rowe and Armitage (1987), Reese and O'Neil (1988), and Kulhawy and Phoon (1993).

These design methods were then evaluated using static load tests that were conducted in Missouri Pennsylvanian Age shales at three different sites (i.e., Lexington site, Grandview Triangle site, and Waverly site) in Missouri.

Miller (2003) points out that the method of Rowe and Armitage (1987) most closely predicts the measured unit side resistance. This method, however, slightly overestimates unit side resistance. Miller (2003) recommends the following correlation, with minor modifications to the method of Rowe and Armitage (1987) to produce more conservative values, for prediction of unit side resistance in shale formations found in Missouri:

$$f_s = 0.4 * \sqrt{q_u(\text{MPa})}$$

5.2.13 Kulhawy et al. (2005)

Kulhawy et al. (2005) reviewed current predictive methods for side resistance (e.g., Rosenberg and Journeaux 1976; Horvath,1978; Meigh and Wolski 1979; Williams et al. 1980; Rowe and Armitage 1984; Carter and Kulhawy 1988; Reese and O'Neil 1988; Kulhawy and Phoon 1993). The database collected by Prakoso (2002) was considered to be the best one complied and thus was used for evaluation of these design methods. The same database was used for the development of design correlation by Kulhawy et al. (2005).

Kulhawy et al. (2005) recommend the following correlation equation for prediction of unit side resistance of normal rock-socketed drilled shafts:

$$f_s / P_a = 1.0 * (q_u / P_a)^{0.5}$$

Furthermore, Kulhawy et al. (2005) recommend the following relationship as a lower bound to 90% of the data collected by Prakoso (2002)

$$f_s / P_a = 0.63 * (q_u / P_a)^{0.5}$$

5.2.14 Abu-Hejleh and Attwooll (2005)

The method of Abu-Hejleh and Attwooll (2005) is based on results of static load tests, laboratory tests, and SPT tests that were conducted in Colorado. Abu-Hejleh and Attwooll (2005) recommend the following correlations for soft claystone bedrock shale that has an SPT N-value of 20 to 100 bpf and unconfined compressive strength of less than 24 ksf:

$$f_s(\text{ksf}) = 0.075 * N = 0.31 * q_u$$

Abu-Hejleh and Attwooll (2005) further recommend the following correlation for very hard sandy claystone bedrock shale with an SPT N-value of more than 120 bpf and unconfined compressive strength of less than 100 ksf:

$$f_s(ksf) = 2.05\sqrt{q_u}$$

5.2.15 AASHTO LRFD Bridge Design Specifications (2006)

AASHTO LRFD Bridge Design Specifications (2006) recommend the method of Horvath and Kenney (1979) with a minor modification. This method is summarized below:

$$f_s / P_a = \alpha_E * 0.65 * (q_u / P_a)^{0.5}$$

α_E is introduced to account for the difference between rock mass and intact properties. Table 5.1, reproduced from O'Neil and Reese (1999), can be used to estimate α_E.

Table 5.1 Correction Factor for O'Neil and Reese (1999) Design Method

E_m / E_r, rock modulus ratio	α_E
1	1.00
0.5	0.80
0.3	0.70
0.1	0.55
0.05	0.45

5.3 PREDICTIVE METHODS FOR TIP RESISTANCE

Mobilization of tip resistance in rock-socketed drilled shafts requires larger displacements than side resistance. Mobilization of tip resistance also depends on other factors such as embedment depth and undrained compressive strength. Therefore, more uncertainty is involved in prediction of tip resistance than that of side resistance.

Review of the literature (e.g., Geoke and Hustad 1979) indicates that tip resistance accounts for a small percentage of axial capacity of a rock-socketed drilled shaft. For this reason, tip resistance is sometimes ignored in design; and this leads to rather conservative decisions regarding the size of the rock socket. To account for the contribution of tip resistance, a reliable predictive method is needed that accounts for all of the factors mentioned above.

Current predictive methods for tip resistance are discussed below. These methods will be evaluated to identify the most accurate method or the need for development of new methods for drilled shafts in weak rocks (e.g., shales) in the later chapters.

5.3.1 Teng (1962)

Teng (1962) uses a linear function for prediction of tip resistance. The allowable unit tip resistance of rock-socketed drilled shafts is as follows:

$$q_{t-allow} = 0.13 \text{ to } 0.20 * q_u$$

Assuming a factor of safety of 3.0, Teng's (1962) method can be modified to give ultimate values for unit tip resistance:

$$q_t = 0.39 \text{ to } 0.60 * q_u$$

5.3.2 Coates (1967)

Coates (1967) proposes a linear function for tip resistance. This method is based on Griffith's strength theory and assumes shearing strength of rock is mobilized along the entire failure surface at the same time. This equation also assumes that microscopic cracks are present in rock and stress concentrations can develop at the boundary of these discontinuities. Coates (1967) recommends

$$q_t = 3 * q_u$$

for prediction of tip resistance for drilled shafts in rocks. As in the case of Teng (1962), this method does not account for shaft geometry and movement at the tip of the drilled shaft.

5.3.3 Rowe and Armitage (1987)

Rowe and Armitage (1987) reviewed the work of Horvath (1982), Glos and Briggs (1983), and Williams (1980a) and based their recommendations on the results of 12 load tests with diameters greater than 12 in. The ultimate load was not reached in any of these tests. As in the case of Teng (1962) and Coates (1967), Rowe and Armitage (1987) did not account for effects of shaft geometry, shaft movement, etc., in the formulation of their predictive method. Rowe and Armitage (1987) recommend the following correlation for the prediction of unit tip resistance:

$$q_t = 2.5 * q_u$$

5.3.4 Carter and Kulhawy (1988)

Carter and Kulhawy (1988) use the Hoek and Brown failure criterion to develop a correlation for the prediction of tip resistance of a circular foundation on a randomly jointed rock mass. Thus, this method has a semi-empirical nature. Their recommended correlation equation for the prediction of unit tip resistance of a drilled shaft is as follows:

$$q_t = \left(\sqrt{s} + \sqrt{m\sqrt{s} + s} \right) * q_u$$

s and m can be determined from information on rock quality (i.e., RQD), joint spacing, and rock description. A summary of recommended s and m values can be found in the original work of Carter and Kulhawy (1988) or in other texts on drilled shafts (e.g., Reese et al. 2006).

The method of Carter and Kulhawy (1988), however, does not account for the effect of embedment and thus leads to very conservative designs.

5.3.5 ARGEMA (1992)

ARGEMA (1992) correlates tip resistance to strength of rock measured using unconfined compression tests on intact specimens. ARGEMA proposes the following equation for the design of drilled shafts in rocks.

$$q_t = 4.5 * q_u \leq 10 \text{ MPa}$$

ARGEMA (1992) defines an upper bound limit for their method as shown above.

5.3.6 Zhang and Einstein (1998)

Zhang and Einstein (1998) compiled a database that includes 39 load test results. Tip movement for these tests ranged from 0.6 to 20% of shaft diameter, and shaft diameter ranged from 12 to 75.5 in. Rock types included in this database are mudstone, clay-shale, shale, gypsum, till, diabase, hardpan, sandstone, marl, siltstone, and limestone. Unconfined compressive strength of these geomaterials ranged from 11 to 1149 ksf.

Zhang and Einstein (1998) recommend a design of the following form.

$$q_t = \alpha * \sqrt{q_u(\text{MPa})}$$

An alpha coefficient of 4.8 was suggested as a mean to the observed behavior. Zhang and Einstein (1998) also recommend an alpha coefficient of 6.6 for the above equation for an upper bound for the design method and an alpha coefficient of 3.0 as a lower bound for design.

5.3.7 Abu-Hejleh and Attwooll (2005)

The method of Abu-Hejleh and Attwooll (2005) is based on results of load tests, laboratory work, and SPT tests conducted in Colorado. Abu-Hejleh and Attwooll (2005) recommend the following correlation for soft claystone bedrock shales that have an SPT N-value of 20 to 100 bpf and an unconfined compressive strength of less than 24 ksf:

$$q_t(\text{ksf}) = 0.92 * N = 3.83 * q_u$$

Abu-Hejleh and Attwooll (2005) further recommend the following correlation for very hard sandy claystone bedrock shale with an SPT N-value of more than 120 bpf and an unconfined compressive strength of less than 100 ksf:

$$q_t(\text{ksf}) = (1.2 + 0.48 * L/D) * q_u < 4.08 * q_u, \text{ when } L/D > 6$$

The method of Abu-Hejleh and Attwooll (2005) accounts for the effect of embedment in rock, which is considered to be a significant improvement over other predictive methods discussed thus far.

5.3.8 Canadian Foundation Engineering Manual (2006)

The predictive method proposed in the *Canadian Foundation Engineering Manual (CFEM)* (Canadian Geotechnical Society 2006) accounts for effects of drilled shaft

embedment in rock and in situ condition of rock mass on mobilized bearing capacity of drilled shafts. The *CFEM* proposed correlation is

$$q_t = 3 * K_{sp} * d * q_u$$

where

$K_{sp} = \dfrac{3 + c / B_s}{10 * \sqrt{1 + 300 * \delta / c}}$ = empirical factor for condition of rock mass

$d = 1 + 0.4 * L_s / B_s \leq 3$ = depth factor

L_s = socket length

B_s = diameter of socket

c = spacing of discontinuities ≥ 12 in.

δ = aperture thickness ≤ 0.2 in.

q_u = unconfined compressive strength of rock

Use of *CFEM* (2006) requires detailed information on rock mass condition, such as aperture thickness and spacing of discontinuities, which is very difficult to obtain. Such information is not often recorded in typical drilled shaft projects. Moreover, sample disturbance of rock cores associated with drilling procedures currently in use leads to unreliable and rather conservative assumptions regarding the in situ condition of rock.

5.4 SUMMARY

Current empirical and semi-empirical methods were reviewed in this chapter. Their method of development and the databases they used were also discussed. Because these methods are based on empirical data, the design engineer needs to be familiar with databases used in their development. As this review of literature indicates, these methods have not been developed exclusively for shale, with the exception of Miller 2003 and Abu-Hejleh and Attwooll 2005. The majority of empirical methods utilize databases that have geomaterials with unconfined compressive strengths well beyond upper limits defined for weak IGMs by O'Neil and Reese (1999).

A static load test database was recently developed by the UIUC research team and was presented in Chapter 3. This database will be used in the next chapter to evaluate the precision and accuracy of current predictive methods.

CHAPTER 6 EVALUATION OF PREDICTIVE METHODS

6.1 INTRODUCTION

Available predictive methods for the design of drilled shafts in rocks are reviewed in Chapter 5. These methods are empirical and were developed using databases of measured side and tip resistance in weak and strong rocks, so many of the relationships may not be applicable to weak Illinois shales. In Chapter 3, a database of measured side and tip resistance for drilled shafts in weak shales, claystones, and mudstones was developed and then used to evaluate available predictive methods for the design of drilled shafts in weak Illinois rocks. These predictive methods were modified to develop a new design procedure for drilled shafts in weak Illinois shales for use by IDOT.

6.2 PREDICTIVE METHODS FOR SIDE RESISTANCE

Soil constitutive models could be used to study load transfer mechanism(s) in axially loaded drilled shafts. However, these models require input parameters for cohesion intercept, friction angle, normal stiffness, and some quantitative measure of dilatancy of weak rocks. Such information is not routinely collected in field or laboratory tests (Carter and Kulhawy 1988). For this reason, available predictive methods are mainly empirical, using data that is routinely collected during field drilling and sampling and laboratory testing.

These empirical methods use three general mathematical functions to correlate unconfined compressive strength of intact rock specimen to measured unit side resistance of drilled shafts: (1) linear functions, (2) power functions, and (3) piecewise functions (combination of functions).

The database of measured side resistance of drilled shafts in weak rocks developed herein is used below to evaluate existing predictive side resistance methods.

6.2.1 Linear Functions

Reynolds and Kaderabek (1980) and Gupton and Logan (1984) recommend linear functions for prediction of unit side resistance of drilled shafts in rocks. Table 6.1 summarizes these methods. Table 6.1 shows the design equation and the mean and coefficient of variance (COV) of the predicted (denoted by letter p) to measured (denoted by letter m) unit side resistance values, using the drilled shaft database developed herein and described in Chapter 3. In other words, the design equations in Table 6.1 and a q_u value were used to calculate the unit side resistance for the 50 depths at which side resistance was measured in the 45 load tests included in the database. The predicted values of side resistance were then divided by the measured values at the corresponding depths. This produced a ratio of predicted (p) to measured (m) side resistance for the 45 measured values of side resistance at various depths. From these 45 ratios of predicted to measured side resistance, the mean and standard deviation were computed. Once the mean and standard deviation were computed, the coefficient of variance for each predictive method was computed by dividing the standard deviation of the predicted to measured (p to m) values by the mean of the predicted to measured values (p to m). This mean and COV are the values shown in Table 6.1.

Table 6.1 Statistics for Linear Functions for Unit Side Resistance

Design Method	Design Equation	Mean of Ratios of p to m	COV of Ratios of p to m
Reynolds and Kaderabek (1980)	$f_s(ksf) = 0.3 * q_u$	1.03	0.26
Gupton and Logan (1984)	$f_s(ksf) = 0.2 * q_u$	0.69	0.26

Note that the method in the *Canadian Foundation Engineering Manual* (Canadian Geotechnical Society 2006) was not evaluated herein because the discontinuity spacing of weak rock for the majority of data available is smaller than the required value of 12 inch. Field exploration at five IDOT sites further showed that discontinuity spacing for Illinois shale is smaller than 12 inch. Therefore, the method in the *Canadian Foundation Engineering Manual* (2006) is not recommended for use by IDOT.

6.2.2 Power Functions

Rosenberg and Journeaux (1976), Horvath and Kenney (1979), Williams et al. (1980), Rowe and Armitage (1987), Toh et al. (1989), Kulhawy and Phoon (1993), O'Neil et al. (1996), Miller (2003), Kulhawy et al. (2005), and AASHTO LRFD Bridge Design Specifications (2006) use power functions for their predictive methods. Table 6.2 summarizes these methods, with the mean and coefficient of variance (COV) of the predicted to measured unit side resistance values for the drilled shaft database described in Chapter 3. The mean and coefficient of variance for each predictive method was computed as described above under "6.2.1 Linear Functions." The resulting mean and COV values are shown in Table 6.2.

Table 6.2 Statistics for Power Functions for Unit Side Resistance

Design Method	Design Equation	Mean of Ratios of p to m	COV of Ratios of p to m
Rosenberg and Journeaux (1976)	$f_s / P_a = 1.09 * (q_u / P_a)^{0.52}$	1.05	0.37
Horvath and Kenney (1979)	$f_s = 0.2 * \sqrt{q_u(MPa)}$	0.58	0.37
Williams et al. (1980)	$f_s / P_a = 1.84 * (q_u / P_a)^{0.37}$	1.22	0.45
Rowe and Armitage (1987)	$f_s = 0.45 * \sqrt{q_u(MPa)}$	1.3	0.37
Toh et al. (1989)	$f_s(KPa) = m * q_u$	0.7	0.43
Kulhawy and Phoon (1993)	$f_s / P_a = 2 * (q_u / 2 * P_a)^{0.5}$	1.3	0.37
O' Neil et al. (1996)	$f_s(ksf) = \alpha * q_u$	0.55	0.37
AASHTO LRFD (2006)	$f_s / P_a = \alpha_E * 0.65 * (q_u / P_a)^{0.5}$	0.50	0.37
Miller (2003)	$f_s = 0.4 * \sqrt{q_u(MPa)}$	1.15	0.37
Kulhawy et al. (2005)	$f_s / P_a = (q_u / P_a)^{0.5}$	0.92	0.37

6.2.3 Piecewise Functions

Alternatively, Meigh and Wolski (1979), Carter and Kulhawy (1988), and Abu-Hejleh and Attwooll (2005) use piecewise functions instead of linear and power functions for their proposed unit side resistance correlations. Table 6.3 summarizes these methods with the mean and coefficient of variance (COV) of predicted to measured values of unit side resistance for load tests in the drilled shaft database described in Chapter 3. The mean and coefficient of variance for each predictive method was computed as described above under "6.2.1 Linear Functions." The resulting mean and COV values are shown in Table 6.3.

Table 6.3 Statistics for Piecewise Functions for Unit Side Resistance

Method	Design Equation	Mean of Ratios of p to m	COV of Ratios of p to m
Meigh and Wolski (1979)	$f_s = 0.25 * q_u,\ 8.5 < q_u < 15$ ksf $f_s / P_a = 0.55 * (q_u / P_a)^{0.6},\ 14 < q_u < 265$ ksf	0.63	0.3
Abu-Hejleh and Attwooll (2005)	$f_s(\text{ksf}) = 0.075 * N = 0.3 * q_u,\ q_u < 24$ ksf and $20 < N < 100$ $f_s(\text{ksf}) = 2.05 * \sqrt{q_u},\ q_u < 100$ ksf and $N > 120$	1.02	0.27
Carter and Kulhawy (1988)	$f_s / P_a = 0.63 * (q_u / P_a)^{0.5} < 0.15 * q_u$	0.47	0.26

6.2.4 Discussion of Unit Side Resistance Results

The statistics presented in Tables 6.1, 6.2, and 6.3 for the various predictive methods for unit side resistance suggest that linear functions better predict the measured behavior (i.e., load test data). Power functions give inaccurate predictions for the weaker range of IGMs (i.e., power functions commonly overestimate side resistance). Predictive methods by Miller (2003), Kulhawy et al. (2005), and Rosenberg and Journeaux (1976) are superimposed on measured values of unit side resistance from the Chapter 3 database in Figure 6.1. Power functions, in general, overestimate the unit side resistance when the unconfined compressive strength of the rock is less than 40 ksf and underestimate the unit side resistance of drilled shafts when the unconfined compressive strength of rock is greater than 40 ksf. Therefore, power functions exhibit poor fits to the observed relationship between side resistance and unconfined compressive strength and are not recommended.

Piecewise functions are more accurate than power functions; however, they occasionally underestimate the unit side resistance. Furthermore, the same level of accuracy can be obtained in design by using a simple linear function as a predictive method. As a result, it is recommended that a linear function (e.g., modified version of those shown in Table 6.1) be used to predict unit side resistance for drilled shafts constructed in weak Illinois shales.

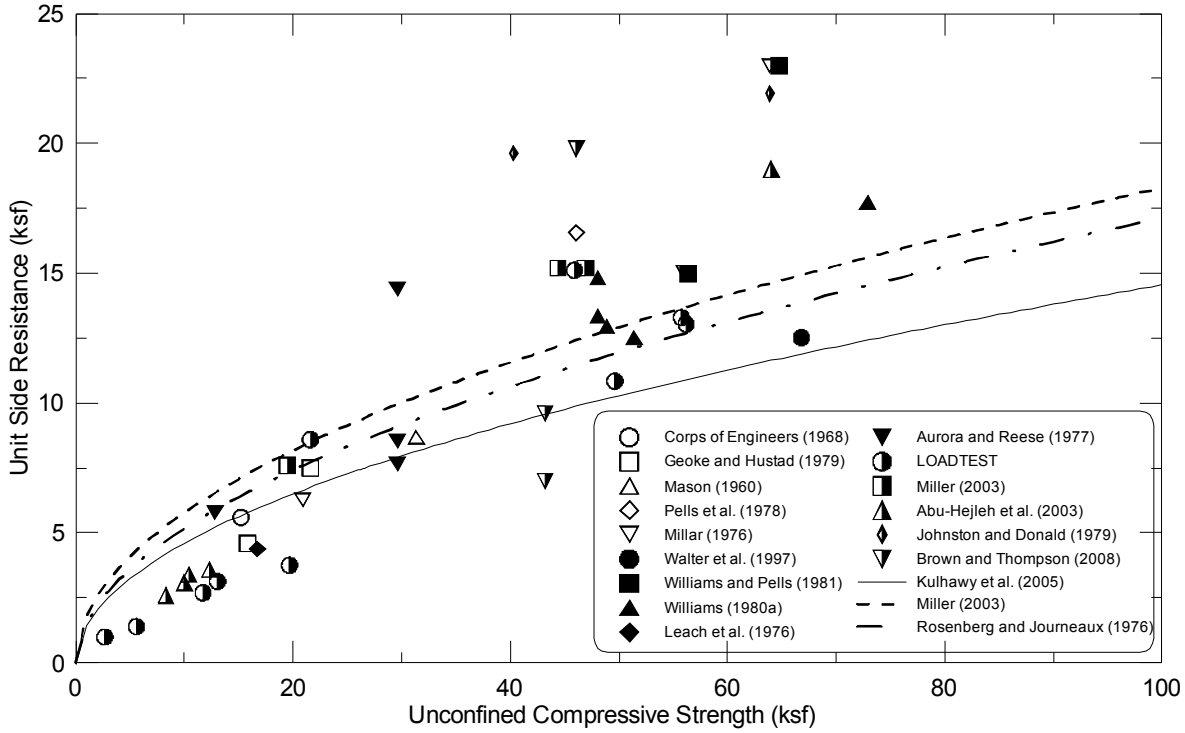

Figure 6.1 Comparison of power function predictive methods and load test database.

6.3 PREDICTIVE METHODS FOR TIP RESISTANCE

Linear functions, power functions, or a combination of both are commonly used to correlate tip resistance of drilled shafts to unconfined compressive strength for the design of drilled shafts in rocks. Drilled shaft load tests from the database described in Chapter 3 whose tip displacements are ≥3% of their tip diameter during the load test were used to evaluate existing predictive methods. A tip displacement of ≥3% of the tip diameter is used to ensure all tip resistance predictive methods are evaluated consistently and to eliminate the influence of tip displacement on the final decision.

6.3.1 Linear Functions

Teng (1962), Coates (1967), Rowe and Armitage (1987), and Carter and Kulhawy (1988) used linear functions for their proposed predictive methods. Table 6.4 summarizes these methods, the design equation to predict the unit tip resistance, and the mean and coefficient of variance (COV) of the predicted to measured unit tip resistance values for load tests in the drilled shaft database described in Chapter 3. The mean and coefficient of variance for each predictive method was computed as described above under “6.2.1 Linear Functions.” The resulting mean and COV values are shown in Table 6.4.

Table 6.4 Statistics for Linear Functions for Unit Tip Resistance

Method	Design Equation	Mean of Ratios of p to m	COV of Ratios of p to m
Teng (1962)	$q_t = 3/5 \text{ to } 3/8 * q_u$	0.12	0.29
Coates (1967)	$q_t = 3 * q_u$	0.60	0.29
Rowe and Armitage (1987)	$q_t = 2.5 * q_u$	0.50	0.29
Carter and Kulhawy (1988)	$q_t = \left(\sqrt{s} + \sqrt{m\sqrt{s} + s}\right) * q_u$	0.01	0.29

6.3.2 Power Functions

Zhang and Einstein (1998) use a power function for their predictive method. Table 6.5 summarizes this method and the mean and coefficient of variance (COV) of predicted to measured values of unit tip resistance for the drilled shaft database described in Chapter 3. The mean and coefficient of variance for each predictive method was computed as described above under “6.2.1 Linear Functions.” The resulting mean and COV values are shown in Table 6.5.

Table 6.5 Statistics for Power Functions for Unit Tip Resistance

Method	Design Equation	Mean of Ratios of p to m	COV of Ratios of p to m
Zhang and Einstein (1998)	$q_t = 4.8 * \sqrt{q_u(\text{MPa})}$	0.92	0.40

6.3.3 Piecewise Functions

ARGEMA (1992) and Abu-Hejleh and Attwooll (2005) use a combination of linear and power functions for different ranges of undrained compressive strength of rocks for their predictive methods. The tip resistance database in Chapter 3 was used to evaluate these methods for the design of drilled shafts in weak rocks (i.e., weak Illinois shales). The values of mean and COV of the predicted to measured tip resistance values are summarized in Table 6.6. The mean and coefficient of variance for each predictive method was computed as described above under “6.2.1 Linear Functions.” The resulting mean and COV values are shown in Table 6.6.

Table 6.6 Statistics for Piecewise Functions for Unit Tip Resistance

Method	Design Equation	Mean of Ratios of p to m	COV of Ratios of p to m
ARGEMA (1992)	$q_t = 4.5 * q_u < 10$ MPa	0.89	0.31
Abu-Hejleh and Attwooll (2005)	$q_t = 0.92 * N = 3.83 * q_u,\ 20 < N < 100$ $q_u < 24$ ksf $q_t = (1.2 + 0.48 * L/D) * q_u < 4.08 * q_u$ when $L/D > 6$ $N > 120$ and $q_u < 100$ ksf	0.69	0.34

6.3.4 Discussion of Unit Tip Resistance Results

Some of the predictive methods underestimate the tip resistance of drilled shafts, which is indicated by their low computed mean (e.g., Teng 1962; Carter and Kulhawy 1988). This leads to a conservative design in which tip resistance is included as one of the components that contribute to total axial capacity. Some other methods have high COVs, and thus they lead to inaccurate estimates of tip resistance (e.g., Zhang and Einstein 1998).

The mobilized tip resistance of drilled shafts in weak rocks is a function of tip displacement allowed, socket length, and unconfined compressive strength of weak rock, as shown in Figure 6.2. Figure 6.2 shows that the greater the tip displacement, the greater the tip resistance, up to a ratio of tip displacement to tip diameter of about 6.

Most of the predictive methods reviewed and evaluated herein ignore allowable displacement of the shaft tip and socket length. A new design method that implicitly accounts for these important parameters was developed herein and will be introduced in Chapter 8.

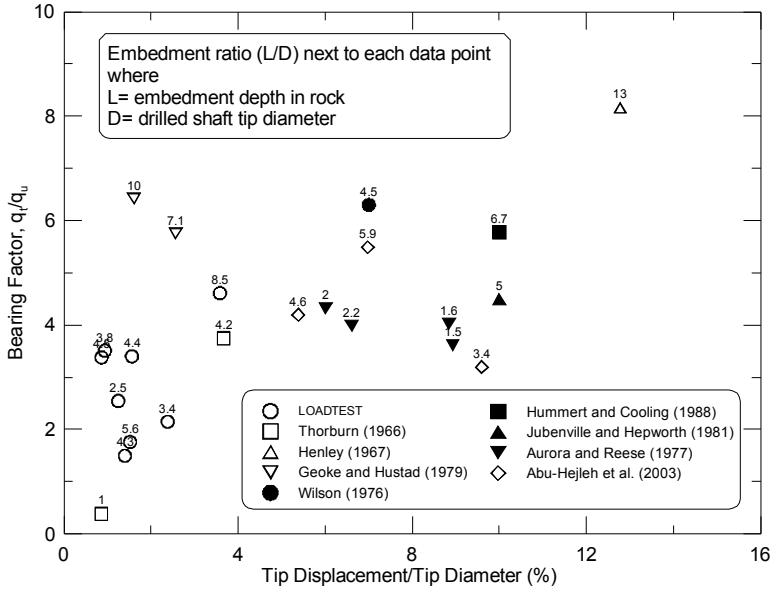

Figure 6.2 Effect of shaft tip displacement and shaft embedment on tip resistance.

6.4 SUMMARY

Predictive methods for side and tip resistance were evaluated. Observations regarding the evaluation of side resistance predictive methods are as follows:

- Power functions overestimate side resistance when unconfined compressive strength is less than 40 ksf and underestimate side resistance when unconfined compressive strength is greater than 40 ksf.
- Piecewise functions provide more accurate predictions than power functions; but they occasionally underestimate unit side resistance, which leads to an overly conservative design.
- Linear functions, with modifications suggested Chapter 8, are the most appropriate type of function, or equation, to predict unit side resistance in weak rocks. Linear equations are simpler and easier to use than piecewise equations and are recommended for use by IDOT to design drilled shafts in weak shales.

Observations regarding tip resistance methods are as follows:

- Tip resistance predictive methods tend to underestimate tip resistance.
- Tip resistance methods assume a predetermined tip displacement, and thus the serviceability of the drilled shafts and bridge cannot be determined. This also leads to designs where strain compatibility does not exist between side and tip resistance.
- Many tip resistance predictive methods ignore the contribution of embedment depth to bearing capacity.
- The load test database developed herein was used to develop a design method that accounts for tip displacement, embedment depth, and unconfined compressive strength. This new method allows the user to include allowable settlement and design shear strength to predict unit tip resistance.

CHAPTER 7 LOAD TRANSFER MECHANISM FOR DRILLED SHAFTS IN WEAK SHALE

7.1 INTRODUCTION

Load transfer mechanism in rock-socketed drilled shafts is a function of undrained strength (e.g., unconfined compressive strength) of rock, drilled shaft tip and nominal diameter, rock-embedment depth, and drilled shaft tip movement. Understanding the load transfer mechanism(s) is important for identifying the important factors in the mechanism that should be included in the predictive method. The load transfer mechanism(s) means the ways in which the load applied to the drilled shaft is transferred to the rock in which the drilled shaft was constructed. The load transfer mechanisms differ for side resistance and tip resistance because these two resistances load the rock differently. For example, the rock at the tip of the drilled shaft is loaded in compression while the rock along the drilled shaft is loaded in shear.

These factors will be discussed and evaluated in subsequent sections of this chapter, using the measured side and tip resistances in the drilled shaft load test database described in Chapter 3.

7.2 LOAD TRANSFER IN SIDE RESISTANCE

Analytical and empirical studies of rock-socketed drilled shafts (Moore 1964; Gibson 1973; Osterberg and Gill 1973; Aurora and Reese 1976; Ladanyi 1977; Geoke and Hustad 1979; Horvath and Kenney 1979; Brown et al. 2010) indicate that side resistance contributes significantly to the axial capacity of drilled shafts socketed in soft rocks. Therefore, it is important to understand the factors affecting load transfer to the sides of the drilled shaft and mobilization of side resistance to support the applied load.

7.2.1 Effect of Construction Methods

Construction techniques have a large influence on the mobilized side resistance in drilled shafts. For example, if the sides of the auger boring are roughed due to a rough auger or by the driller, the concrete can adhere better to the rock walls of the boring and provide a greater side resistance than smooth walls. An empirical adhesion factor is used to quantify the level of adhesion between the rock walls and drilled shaft concrete. A higher adhesion factor means a greater interlock between the rock and concrete and usually reflects that some construction technique was used to increase the bond between the rock walls and the concrete.

Drilled shafts with concrete defects (e.g., water in the shaft preventing full adherence of the concrete to the rock walls, the concrete not being vibrated sufficiently to make contact with the rock walls, or the concrete being contaminated by soil as the casing is withdrawn) can decrease side resistance and are discussed herein. Figure 7.1 shows the side resistance database described in Chapter 3 and demonstrates effects of construction techniques on mobilized side resistance.

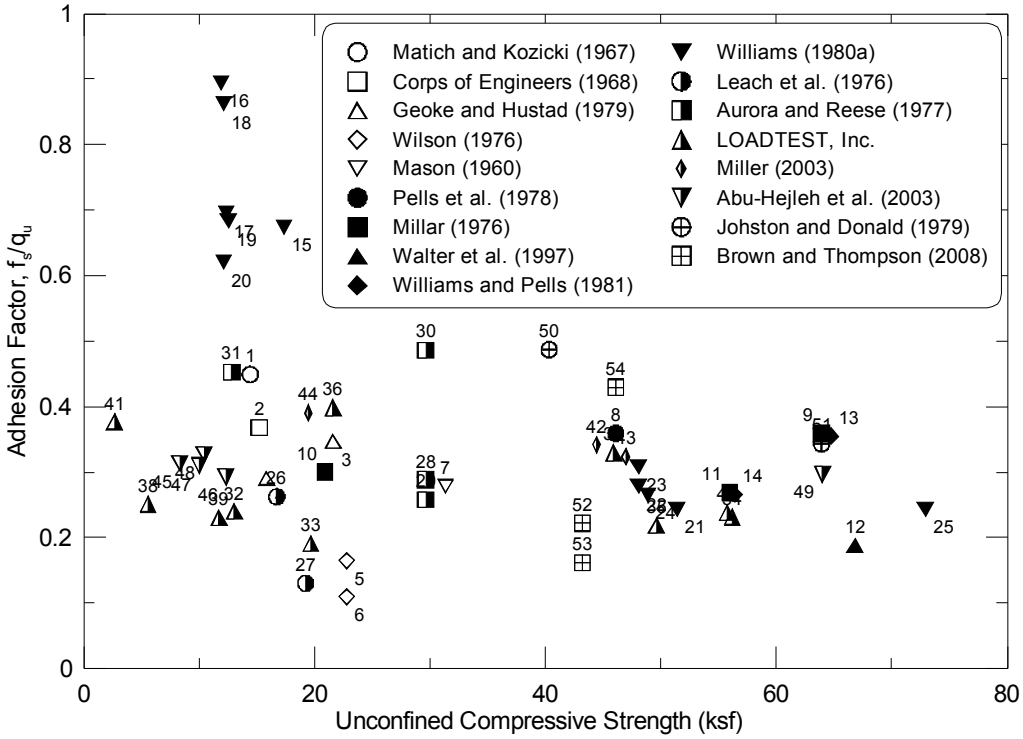

Figure 7.1 Load test database for unit side resistance with various construction techniques.

7.2.1.1 Artificially Roughened Rock Sockets

Data points labeled 15 to 20 in Figure 7.1 were obtained from static load tests performed on drilled shafts socketed in Melbourne mudstone (Williams 1980a). The data point labeled 1 on Figure 7.1 is reported by Matich and Kozicki (1967) and was obtained from static load tests. These data present normalized unit side resistance of drilled shafts with artificially roughened sockets. These data points indicate that load transfer in side resistance can be increased for drilled shafts in weak rocks if the socket or boring walls are roughened by mechanical means, as compared to normally constructed rock sockets that exhibit smoother walls.

7.2.1.2 Concrete Defects and Construction Methods

Data points labeled 5 and 6 in Figure 7.1 were obtained from two static load tests on drilled shafts at Port Elizabeth, South Africa (Wilson 1976). Wilson (1976) points out that there was a concrete defect in these drilled shafts due to water entering shaft hole while the concrete was being poured. This defect in concrete adherence and curing caused significant reduction in the mobilized unit side resistance in these drilled shafts.

The data discussed herein, which are affected by construction techniques, will not be used in subsequent discussions of this chapter and the development of a new predictive method in Chapter 8 because they do not represent the side resistance of a normally constructed drilled shaft. However, this section illustrates the importance of good construction techniques (e.g., dewatering the shaft prior to pouring concrete and adequately vibrating the concrete within the rebar cage, to mobilize full side resistance).

7.2.2 Effect of Shaft Diameter

Figure 7.2 shows the adhesion factor versus shaft nominal diameter for drilled shafts in weak rocks. This figure indicates the adhesion factor is unaffected by drilled shaft diameter and mainly influenced by construction technique. This finding is in agreement with conclusions of Horvath and Kenney (1979) and Brown et al. (2010).

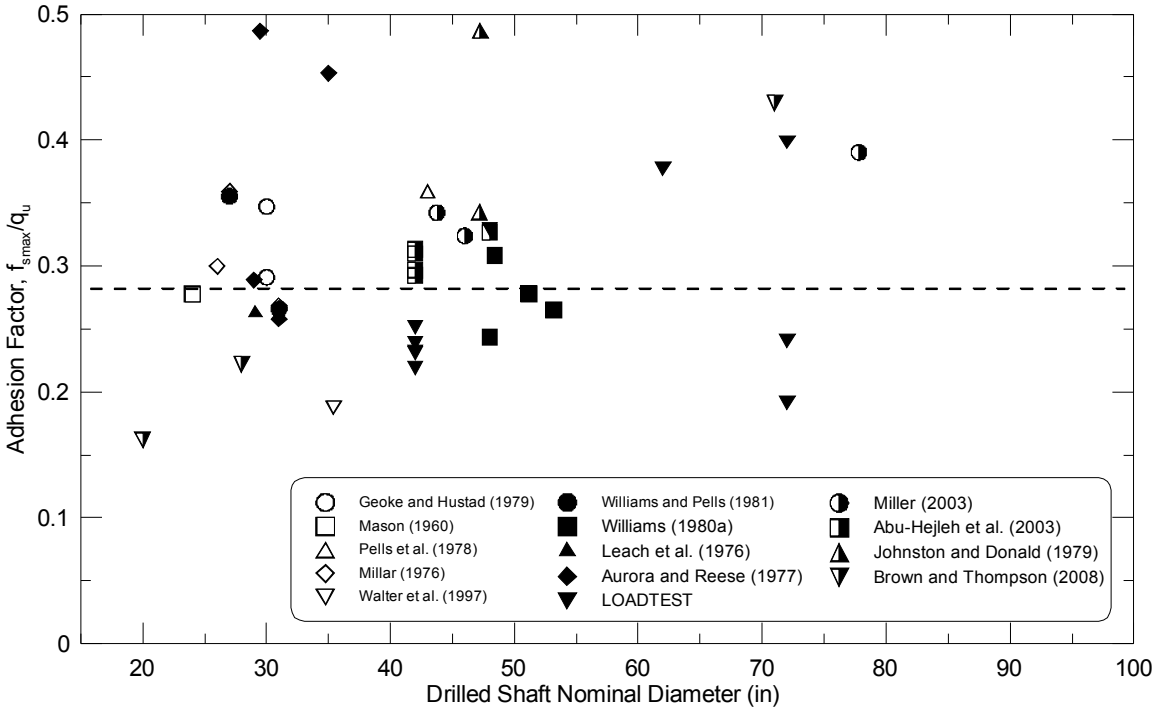

Figure 7.2 Effect of shaft diameter on adhesion factor or mobilized maximum side resistance.

7.2.3 Effect of Drilled Shaft Displacement

Side resistance in drilled shafts is mobilized at small shear displacements. Figure 7.3 presents a relationship between drilled shaft diameter and shaft shear displacement required to mobilize the maximum side resistance, $f_{s,max}$. This data was obtained from the side resistance database described in Chapter 3, representing drilled shaft load tests in which sensors were installed along the drilled shaft to measure the load transfer at different depths along the drilled shaft. Figure 7.3 shows that shaft displacements of less than 1 in. are generally required to mobilize the full side resistance along shaft/rock interface. Review of load tests in Chapter 3 indicates that drilled shafts in soft rocks undergo such displacements under service loads. Therefore, it is assumed that full side resistance is mobilized in drilled shafts in soft rocks for design purposes.

Figure 7.4 shows the ratio of residual side resistance to peak or maximum side resistance ($f_{s,max}$) versus drilled shaft displacement after $f_{s,max}$ is reached. This figure shows that side resistance of drilled shafts in weak rocks remains near the maximum value even after a post-peak shaft displacement of 1.4 in. occurs. This means there is little post-peak decrease in side resistance with increasing drilled shaft displacement. This is in agreement with observations of Williams and Pells (1981). This conclusion is truly significant for drilled shaft design because it means IDOT can use both side and tip resistance in their designs

because there is little post-peak decrease in side resistance. This finding is significant because it is well known that tip resistance requires much more shaft displacement to mobilize the maximum tip resistance, $q_{t,max}$. If there were a large post-peak decrease in side resistance, a designer could not use both side and tip resistance in the design because it would overestimate the total resistance available. In summary, the data in Figure 7.4 show that IDOT can include both side and tip resistance in drilled shaft designs for weak rocks, which will lead to smaller and more cost-effective bridge foundation systems.

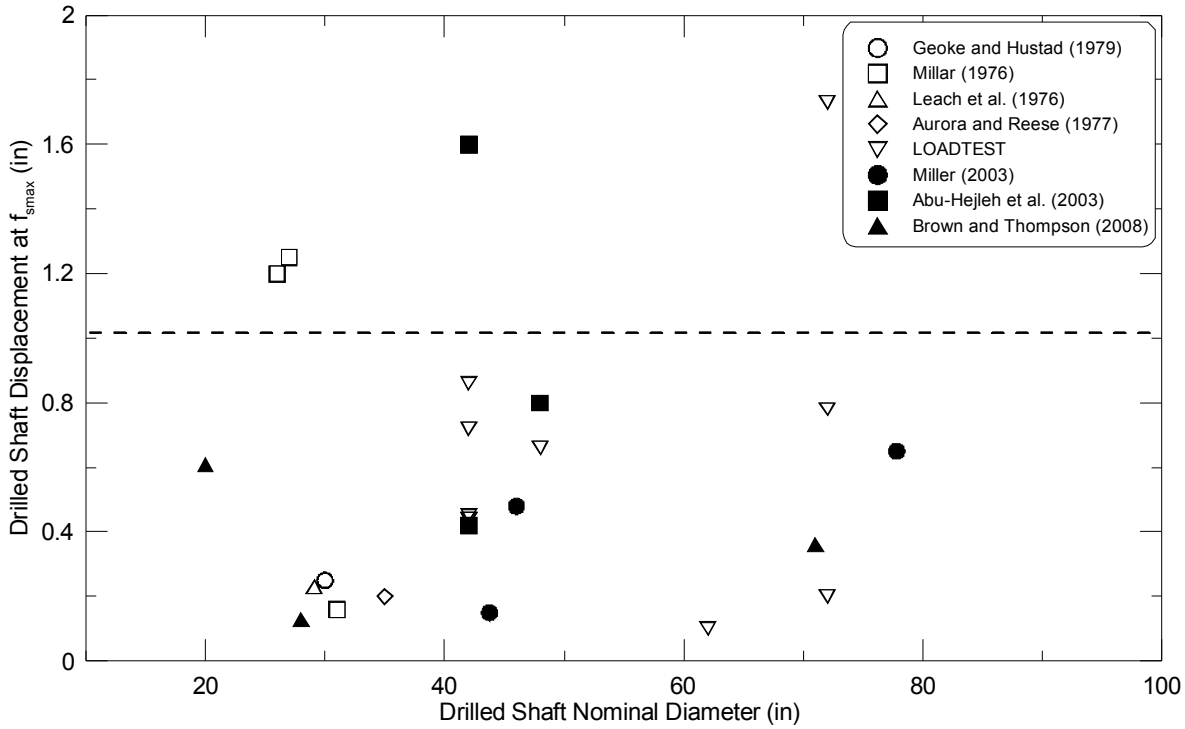

Figure 7.3 Effect of shaft displacement on mobilized side resistance.

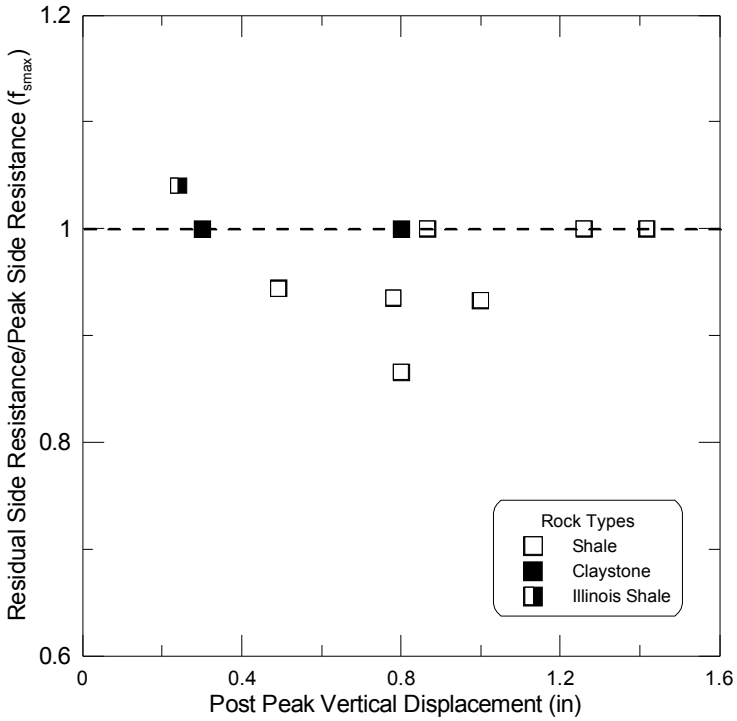

Figure 7.4 Effect of post-peak shaft displacement on side resistance of drilled shafts in weak rocks.

7.2.4 Effect of Rock Type

All available predictive methods (with the exception of Miller 2003; Abu-Hejleh et al. 2003; Abu-Hejleh and Attwooll 2005) combine results of drilled shaft load tests in strong and weak rocks in their databases. This approach was considered a disadvantage of these methods because

- Review of the literature shows the relationship between unconfined compressive strength and measured side resistance is not the same for drilled shafts in weak and strong rocks, so the coefficients in the design methods will be different.
- Different mathematical correlations are needed to predict side resistance of drilled shafts in weak and strong rocks because of different displacements to mobilize maximum side resistance, $f_{s,max}$, and different post-peak behaviors.

This study used only drilled shaft load test results in weak argillaceous sedimentary rocks to develop the design methods proposed herein. Figure 7.5 shows that drilled shafts in these weak argillaceous sedimentary rocks follow the same trend, and thus one form of mathematical function (i.e., linear function or equation) could be used to predict the side resistance in weak shales.

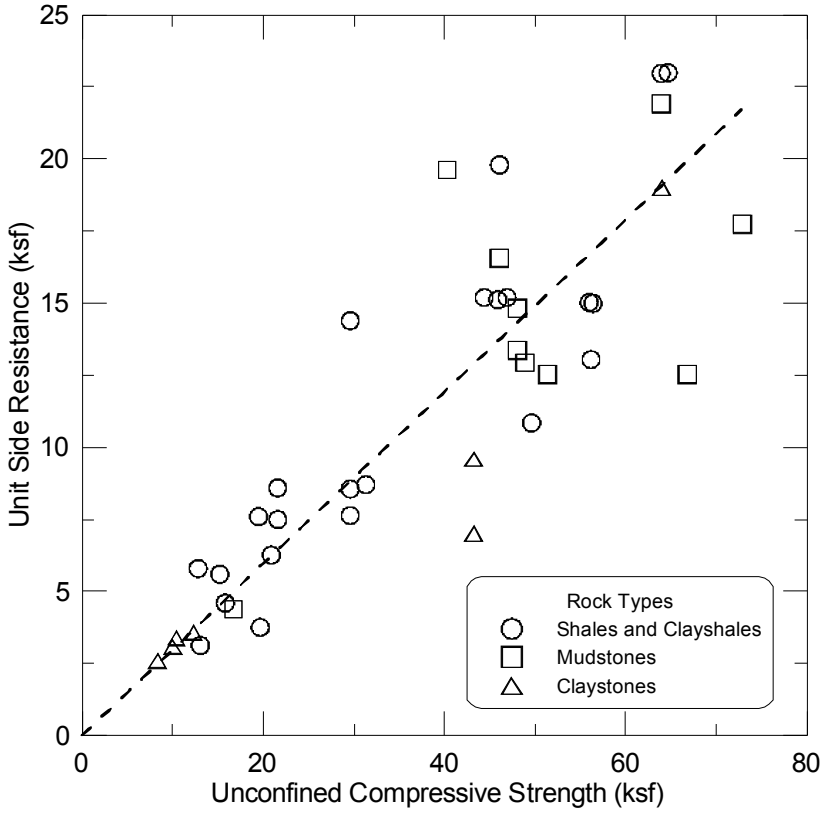

Figure 7.5 Effect of rock type on the relationship between unconfined compressive strength and measured side resistance in weak sedimentary rocks.

7.3 LOAD TRANSFER IN TIP RESISTANCE

Since the mid-1970s, research (e.g., Williams 1980a) has been conducted on the load transfer in tip resistance mechanism of drilled shafts in rocks. However, the first comprehensive study of load transfer in tip resistance was conducted by Zhang and Einstein (1998). They developed a database of drilled shaft load test results in a variety of weak and strong rocks, and developed an empirical method based on rock strength. The Zhang and Einstein (1998) method does not account for the effects of drilled shaft displacement at the shaft tip due to applied loads and embedment depth or length in rock on tip resistance. This omission is unfortunate because Williams et al. (1980a) previously showed that tip resistance of drilled shafts in weak rocks is a function of shaft tip displacement and shaft embedment length in rock.

This indicates that different factors affect the mobilized tip resistance. Therefore, prediction of tip resistance involves more uncertainty, so it is frequently neglected in design. Neglecting tip resistance often leads to conservative designs that produce unnecessary socket lengths of 15 to 30 ft (Rosenberg and Journeaux 1976). A large socket depth, or length, increases foundation costs by increasing drilling costs, increasing construction material costs, and increasing construction time and labor. A longer drilled shaft is more expensive to load test if a load test is desired.

To overcome the omission of tip resistance in drilled shaft design in weak rocks, the authors have developed a database of measured unit tip resistance of drilled shafts that are

embedded in weak argillaceous sedimentary rocks. This database contains information on drilled shaft tip displacement, embedment depth or length, drilled shaft tip diameter, and unconfined compressive strength of weak rocks at or slightly below the tip. This database and existing literature was used to study the contribution of each of these four factors on mobilization of tip resistance in drilled shafts in weak rocks.

7.3.1 Effect of Diameter

Previous research (e.g., Prakoso and Kulhawy 2002; Brown et al. 2010) indicates that normalized tip resistance, q_t, to unconfined compressive strength, q_u, or $N_c^* = q_t / q_u$ does not vary significantly with drilled shaft tip diameter, as shown in Figure 7.6. Because the bearing capacity factor is independent of shaft diameter at the tip elevation, a predictive method for tip resistance of drilled shafts in weak rocks need not to be a function of drilled shaft tip diameter. As a result, the design method developed herein uses drilled shaft tip diameter to normalize tip displacement; but it does include the factors that influence tip resistance.

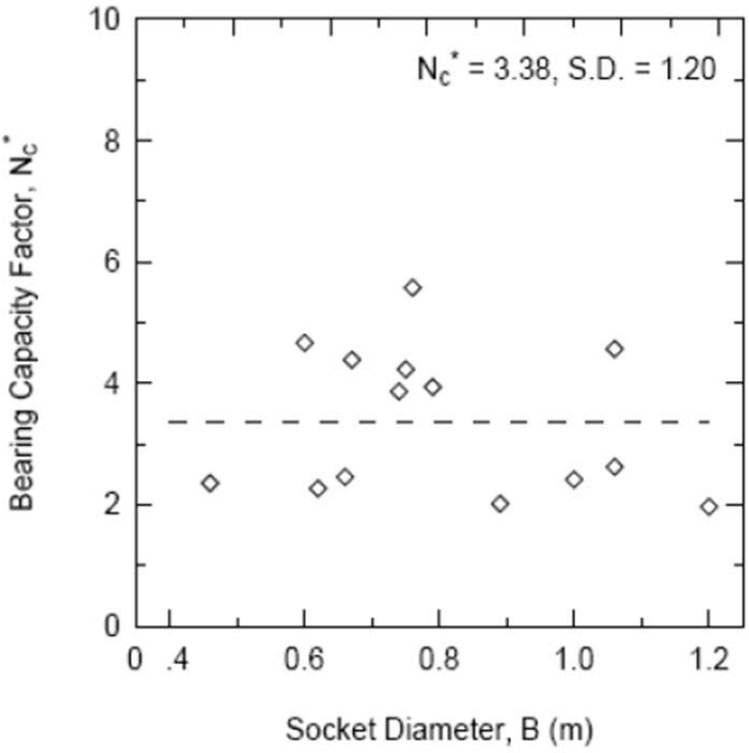

Figure 7.6 Effect of drilled shaft diameter on normalized tip resistance (after Prakoso and Kulhawy 2002).

7.3.2 Effect of Tip Displacement

Vertical movement and differential settlement of drilled shafts are important design criteria because they can affect the serviceability of the supported bridge structure. Figure 7.7 shows that tip resistance of drilled shafts is sensitive to vertical displacement. Figure 7.7 shows considerable scatter, but there is a rough trend of increasing tip resistance with increasing tip displacement. This finding is important because side resistance doesn't

increase or decrease with additional displacement, so the tip can be allowed to displace enough to mobilize the maximum tip resistance. Therefore, the proposed design method is based on rock strength and shaft displacement, or settlement, to prevent excessive settlement and damage to the superstructure while incorporating the increase in tip resistance with increasing tip displacement.

7.3.3 Effect of Shaft Embedment in Weak Rock

Classical bearing-capacity theories account for the effect of foundation embedment on its allowable bearing capacity (e.g., Vesic 1973). Some of the current drilled shaft predictive methods (e.g., Rowe and Armitage 1987; Carter and Kulhawy 1988), however, do not account for this important factor. Figure 7.7 shows the embedment ratio (i.e., embedment length L divided by shaft diameter D, or L/D) for each drilled shaft load test data point and shows that tip resistance increases as the embedment ratio increases. Therefore, the proposed method will account for embedment ratio on tip resistance.

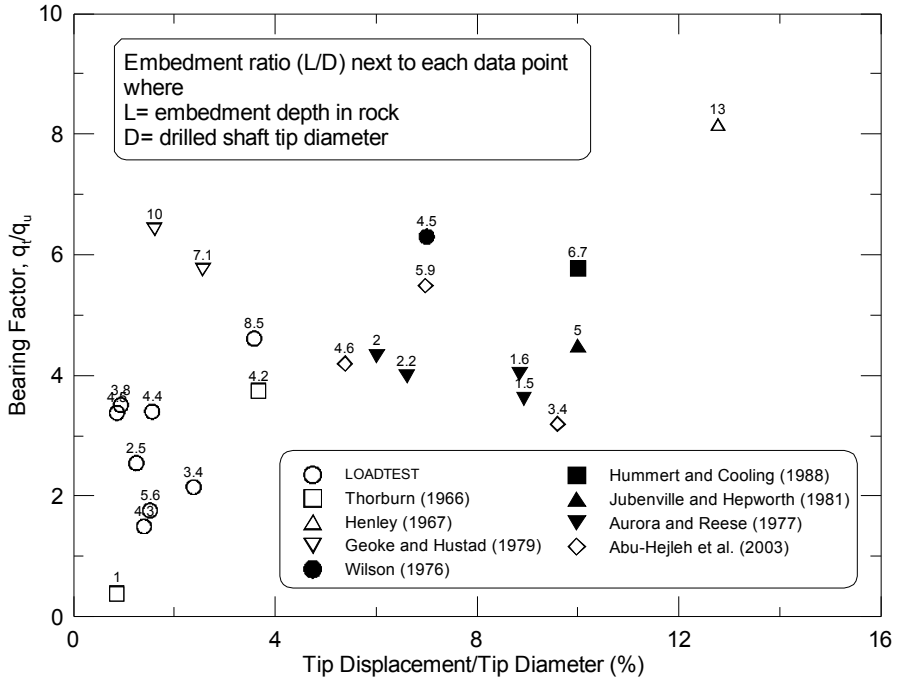

Figure 7.7 Effect of tip displacement and embedment depth on mobilized tip resistance in weak sedimentary rocks for different embedment ratios.

7.4 SUMMARY

Load transfer to side and tip resistance was studied for drilled shafts in weak rocks. The load test data collected herein for weak rocks shows that load transfer in side resistance is independent of shaft diameter, and only a small shaft displacement is required to mobilize full side resistance. Therefore, the proposed design method correlates unit side resistance to unconfined compressive strength to satisfactorily predict the mobilized side resistance in weak rocks. Tip resistance, however, is controlled by unconfined compressive strength of weak rock, tip of shaft displacement, and shaft embedment length in weak rock. Therefore, the proposed predictive method for tip resistance accounts for shaft displacement, shaft embedment length, and unconfined compressive strength of the weak rock.

CHAPTER 8 NEW DESIGN METHOD FOR DRILLED SHAFTS IN WEAK COHESIVE IGMS

8.1 INTRODUCTION

Predictive methods for the design of drilled shafts in rocks were reviewed and evaluated in Chapters 5 and 6. Significant drilling and construction cost savings can be realized by using drilled shafts in weak rocks instead of driven steel piles. However, little attention has been given to the design and construction of drilled shafts in weak sedimentary rocks (e.g., shales) to date, which provided the impetus for this research project. To rectify this design void, methods to predict side and tip resistance for drilled shafts in weak rocks were developed herein. These methods are based on a collection of load test results that include only weak cohesive sedimentary rocks. This chapter presents a new design method that IDOT can use to design drilled shaft foundations in weak Illinois shales for bridge structures.

8.2 PREDICTIVE METHOD FOR SIDE RESISTANCE IN WEAK COHESIVE IGMS

Unconfined compressive strength is the primary engineering property that controls the mobilized unit side resistance in drilled shafts. Chapter 7 shows that the load transfer mechanism in side resistance is not significantly affected by drilled shaft geometry (e.g., drilled shaft diameter). Chapter 7 shows that the ultimate side resistance of drilled shafts in weak rocks is often mobilized with relatively small vertical movements and will not experience a significant post-peak decrease in side resistance with increasing shaft displacement. Review of the literature further indicates that drilled shafts in weak shales, mudstones, and claystones exhibit similar behavior in side resistance. Therefore, the proposed design method uses the unconfined compressive strength of weak cohesive rock to accurately predict unit side resistance of drilled shafts for several types of weak cohesive sedimentary rocks.

8.2.1 Side Resistance Predictive Method

The side resistance database (Chapter 3) was used to select representative and applicable load test data for developing an empirical design method for drilled shafts in weak rocks. Regression analyses were used to determine the line of best fit to the selected side resistance data. Figure 8.1 shows a linear function is used to correlate measured unit side resistance to unconfined compressive strength for the design of drilled shafts in weak rocks.

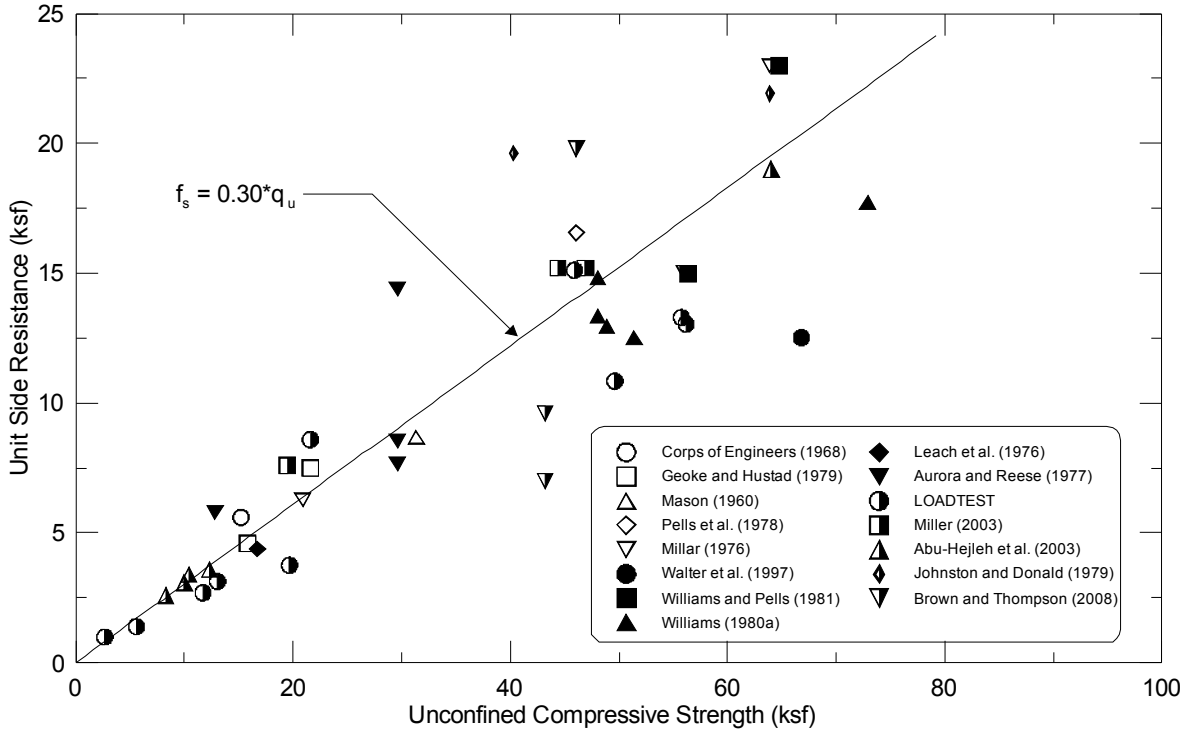

Figure 8.1 Predictive method for unit side resistance of drilled shafts in weak rocks, using a linear function to fit the load test data.

Other researchers suggest a linear function, or equation, to predict unit side resistance in weak rocks (e.g., Reynolds and Kaderabek 1980; Gupton and Logan 1984; Abu-Hejleh et al. 2003; Abu-Hejleh and Attwooll 2005) but recommend different coefficients or adhesion factors in the following equation. As shown below, the new predictive method for side resistance, f_s, in weak Illinois shales uses an adhesion factor of 0.3 and average unconfined compressive strength, q_u, along the shaft wall:

$$f_s(\text{ksf}) = 0.30 * q_u \leq 30 \text{ ksf}$$

where

f_s = unit side resistance of drilled shafts socketed in weak rocks, ksf

q_u = average unconfined compressive strength of rock along socket wall, ksf

0.30 = empirical adhesion factor, dimensionless

8.3 PREDICTIVE METHOD FOR TIP RESISTANCE

Tip resistance in drilled shafts is primarily controlled by the unconfined compressive strength of weak rock. However, a review of the load test database (see Chapter 7) shows that tip resistance is also a function of embedment depth in weak rock and shaft tip displacement. The predictive method for tip resistance that is introduced herein is based on the load test database of Chapter 3 and is a function of all three of these factors.

8.3.1 Tip Resistance Predictive Method

The tip resistance database is summarized in Figure 8.2. The embedment depth of drilled shafts in weak rock is normalized with shaft diameter (see labels next to data in Figure 8.2). The line of best fit to data for the load test data with an embedment ratio of 2 is also shown in Figure 8.2.

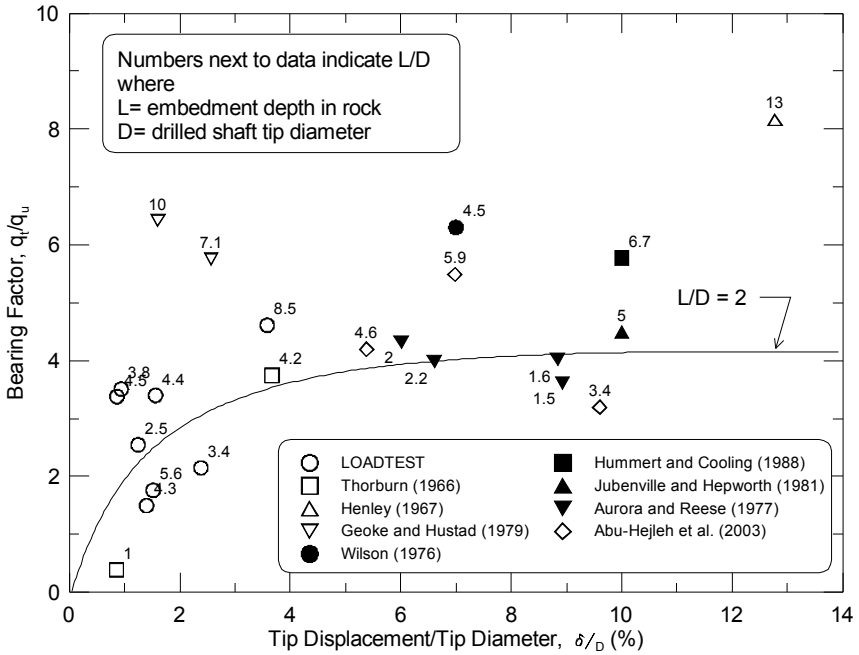

Figure 8.2 Predictive method for tip resistance of drilled shafts in weak rocks using polynomial function to fit the load test data for an embedment ratio of 2.

Regression analyses were used to determine the equation of best fit for an embedment ratio of 2 (shown in Figure 8.2). The expression for the depth correction factor proposed by Vesic (1973) was then used to back calculate the equation for cases for which the embedment depth is zero, which is referred to as the "reference equation." The reference equation and Vesic's depth correction form the proposed design equation for tip resistance. The new predictive method for tip resistance is shown below:

$$q_t = \frac{3.2 * \delta / D}{\delta / D + 1.3} * q_u * d_c \le 2.5 * q_u * d_c$$

where

q_t = tip resistance, ksf

q_u = unconfined compressive strength, ksf

$\frac{\delta}{D}$ = ratio of tip movement to tip diameter, in percent

d_c = Vesic's depth correction factor $= 1.0 + 0.4 * k$, dimesionless

$$k = \begin{cases} k = L/D & L/D \le 1 \\ k = \tan^{-1}(L/D) & L/D > 1 \end{cases}$$

L = embedment depth in weak rock, in.

A displacement equal to 5% of the shaft diameter (O'Neil and Reese 1999) is recommended for evaluation of tip resistance, which can be used to estimate the tip movement, δ, in the tip resistance equation above. Other serviceability limit states (i.e., tip displacements) could be considered if a tip displacement equal to 5% of shaft diameter produces total or differential settlements that are unacceptable for the structural aspects of the design or serviceability.

8.4 MSPT-BASED DESIGN METHOD

A relationship between MSPT penetration rate ($\dot{N}$) and unconfined compressive strength was developed for weak shales based on MSPTs conducted at five IDOT bridge sites (see Appendix F or Chapter 4). This relationship can be substituted in the above drilled shaft side and tip resistance relationships to develop a MSPT-based drilled shaft design method. It is anticipated that IDOT will prefer an MSPT-based design method because it omits expensive and time consuming shale rock coring and subsequent laboratory triaxial compression testing. This will decrease the time and cost required to develop design parameters for drilled shaft design in weak Illinois shales. More important, every IDOT district is equipped to measure MSPT penetration rates in weak Illinois shales, which will facilitate comparison of results and drilled shaft designs. It is anticipated that IDOT will base future drilled shaft designs on the proposed MSPT-based method described below and in Appendix F.

Other SPT based design methods are recommended by Abu-Hejleh et al. (2003) and Abu-Hejleh and Attwooll (2005) but these use limited data in Colorado to develop a correlation between blow count and unconfined compressive strength whereas the method proposed below used five sites in Illinois. In addition, current correlations are only applicable to weak IGMs with unconfined compressive strength of less than 18 ksf. The proposed method can be used in stronger IGMs (i.e., unconfined compressive strength less than 80 ksf). More important, the proposed MSPT method is based on penetration rate and does not require 18 in. of penetration in weak rocks. This eliminates the uncertainties in interpretation of test results for situations where the IGM is so strong that 18 in. of penetration is not possible. The MSPT-based design equation for side resistance is:

$$f_s(\text{ksf}) = 0.30 * \zeta * \dot{N} \leq 30 \text{ ksf}$$

where

f_s = unit side resistance of drilled shafts socketed in weak rocks, ksf

$\dot{N}$ = MSPT penetration rate, bpf

ζ = 0.077 = empirical factor relating MSPT penetration rate and q_u, ksf/bpf

The new MSPT-based method for tip resistance is:

$$q_t(ksf) = \frac{3.2 * \delta / D}{\delta / D + 1.3} * \zeta * \dot{N} * d_c \le 2.5 * \zeta * \dot{N} * d_c$$

where

q_t = tip resistance, ksf

ζ = 0.077 = empirical factor relating MSPT penetration rate and q_u, ksf/bpf

$\dot{N}$ = MSPT penetration rate, bpf

δ = tip movement, inch

D = tip diameter, inch

d_c = Vesic's depth correction factor = $1 + 0.4 * k$, dimensionless

$$k = \begin{cases} k = L / D & L / D \le 1 \\ k = \tan^{-1}(L / D) & L / D > 1 \end{cases}$$

L = tip embedment depth in weak rock, inch

8.5 NEW DESIGN PROCEDURE FOR DRILLED SHAFTS IN WEAK ROCKS

The predictive methods introduced in Sections 8.2, 8.3, and 8.4 were developed for drilled shafts in weak rocks. The proposed design method for side resistance uses only the unconfined compressive strength of the weak rock along the shaft. Tip resistance, however, is based on strength and settlement criteria and also accounts for the effect of socket length. The general Brown et al. (2010) design procedure flowchart shown in Figure 8.3 is recommended for use by IDOT with the side resistance and tip resistance equations presented above for the design of drilled shafts in weak sedimentary rocks.

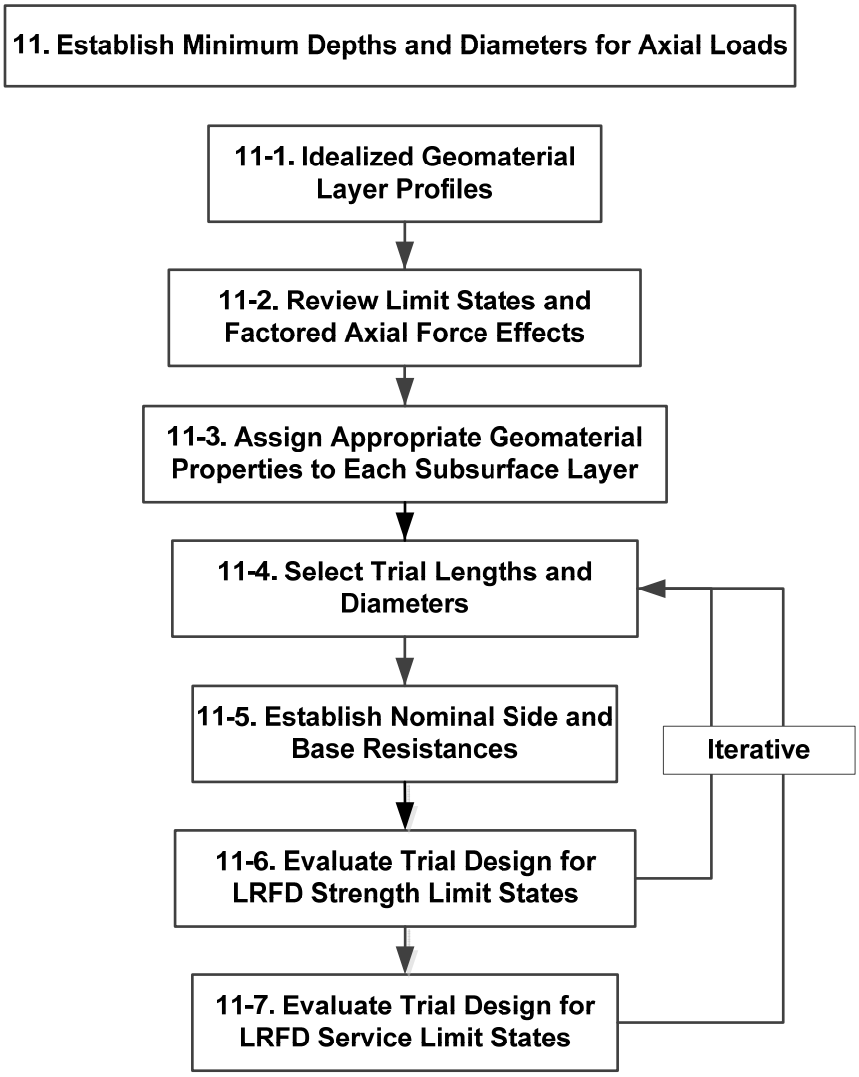

Figure 8.3 General design procedure for drilled shafts (after Brown et al. 2010).

8.6 LOAD AND RESISTANCE FACTOR DESIGN

A resistance factor was developed herein for the new design method for drilled shafts in weak rocks. This resistance factor allows geotechnical engineers to adopt a load and resistance factor design (LRFD) approach to be consistent with the structural design of the bridge superstructure (Brown et al. 2010). Based on the drilled shaft load test database developed herein, a resistance factor of 0.5 is recommended for drilled shaft design in weak rocks. This resistance factor should be applied to the total axial resistance or capacity (i.e., combined tip and side resistance) of the drilled shaft. The resulting equation to estimate the design or allowable applied axial load to the drilled shaft is given by the following:

$$Q_{design} = \varphi * (f_s * P_{socket} * L_{socket} + q_t * A_{tip})$$

where

Q_{design} = design factored resistance,kips

φ = LRFD resistance factor = 0.50

f_s = unit side resistance, ksf

P_{socket} = rock socket perimeter, ft

L_{socket} = rock socket length, ft

q_t = unit tip resistance, ksf

A_{tip} = rock socket tip area, ft^2

8.7 COMPATIBILITY OF SIDE AND TIP RESISTANCE

Rock sockets that are constructed with normal drilling techniques do not experience a large post-peak decrease in side resistance (see Chapter 7). However, displacement or strain softening and a significant reduction in side resistance (i.e., brittle failure) could be a source of concern if the drilling technique (e.g., wet-drilling method) produces smooth sockets (Williams and Pells 1981). Full side resistance is mobilized at displacements of approximately 1.6% of nominal shaft diameter (see Chapter 7). When drilling methods are expected to produce smooth rock sockets or walls, one of the following design approaches should be used.

- Use full side resistance and limit the tip displacement to values δ less than 1.6% of the shaft nominal diameter in the tip resistance equation.
- Use “softened” side resistance as determined from drilled shaft load tests and tip resistance determined from the new predictive for tip displacements that are larger than 1.6% shaft diameter.

The second recommendation, or approach, requires performing a full-scale load test because the new predictive method for side resistance was developed based on load test data that did not experience post-peak softening in side resistance. This load test is used to ensure there is not a large post-peak decrease in side resistance in the weak shale encountered.

8.8 SUMMARY

The new predictive methods for side and tip resistances were developed for use by IDOT in weak Illinois shales. The side resistance predictive method is a function of only the unconfined compressive strength of weak rock. Conversely, the tip resistance method is a function of unconfined compressive strength, tip displacement, and socket length. The drilled shaft design flowchart presented by the Brown et al. (2010) is recommended, with the modifications of Section 8.2 through 8.6 of this report for the design of drilled shafts in weak cohesive sedimentary rocks.

CHAPTER 9 CLOSING REMARKS AND FUTURE RESEARCH

9.1 INTRODUCTION

ICT R27-99, Improvement for Determining the Axial Capacity of Drilled Shafts in Shale in Illinois, studied load transfer mechanisms of drilled shafts that are fully or partially embedded in weak, clay-based sedimentary rocks (e.g., weak shales) encountered in the state of Illinois; and it developed a design procedure that will improve safety and reduce IDOT deep-foundation costs for future bridge structures.

The main objectives of Task 1 of this study were to review the existing literature and develop a drilled shaft load test database for weak, clay-based sedimentary rocks and to evaluate existing design methods. Objectives of Task 2 were to perform field exploration and laboratory tests at five IDOT bridge sites to develop new methods for characterizing weak shale encountered at shallow depths in the state of Illinois. Objectives of Task 3 were to use the load test database compiled herein and data from five IDOT bridge sites to develop new design correlations for the design of drilled shafts in weak shale. Task 3 also developed resistance factors that can be used to design drilled shafts using a load and resistance factor design framework. The following paragraphs summarize major findings of this project.

9.2 DEVELOPMENT OF NEW DESIGN PROCEDURE

Published drilled shaft design literature and drilled shaft load test data since 1962 in rock were reviewed to create a database of drilled shaft static load test data for unit side resistance and tip resistance in weak shales for this study. This database includes the most recent drilled shaft load tests conducted in shale and other clay- based and cohesive sedimentary weak rocks, including shales in Illinois. This database was used to show that existing methods do not accurately predict drilled shaft capacity and was used to develop a new design method.

9.2.1 Unit Side Resistance

Findings related to drilled shaft unit side resistance include the following:

- This study recommends a linear function to predict unit side resistance in weak shales—instead of the power functions commonly used to correlate rock undrained compressive strength to measured unit side resistance in a drilled shaft load test.
- Side resistance does not change significantly with changes in shaft diameter.
- After ultimate unit side resistance is mobilized, additional drilled shaft displacement along the drilled shaft/weak rock interface does not decrease unit side resistance.
- More instrumented load tests on drilled shafts in weak Illinois rocks are required to develop better Illinois-specific predictive methods.

9.2.2 Unit Tip Resistance

Findings related to drilled shaft unit tip resistance include the following:

- Available predictive methods (with the exception of the methods of Abu-Hejleh et al. [2003], Abu-Hejleh and Attwooll [2005], and the *Canadian Foundation Engineering Manual,* [Canadian Geotechnical Society 2006]) correlate only the measured tip resistance in load tests to the unconfined compressive strength of weak rock.
- Analysis of load test data herein indicates that mobilized tip resistance is governed not only by the undrained compressive strength of weak rock but also by drilled shaft movement at tip elevation and depth of embedment of drilled shaft in weak rock. Therefore, predictive methods for tip resistance should account for all of these factors, not just unconfined compressive strength.
- The load test database developed herein was used to develop a design method that can account for these factors. The new method uses settlement and strength criteria to predict unit tip resistance.

9.2.3 Field Exploration and Laboratory Testing

Field exploration was performed at five IDOT bridge sites to obtain shale core samples for laboratory triaxial compression tests and to determine engineering properties of weak shale in Illinois for drilled shaft design. Modified standard penetration tests (MSPTs) were also performed at these sites to measure the in situ properties of weak shale to facilitate correlation with laboratory triaxial values and to develop a new design method. Wang Engineering, Inc. performed pressuremeter tests at three sites to study applicability of this test method to drilled shaft design in weak rocks. Findings related to field exploration and laboratory testing of weak rocks in Illinois include the following:

- For shale specimens with low RQDs, application of a confining pressure in laboratory triaxial compression tests yielded a higher peak deviator stress than the commonly used unconfined compression tests. For intact specimens (i.e., high RQD), application of a confining pressure did not significantly increase the undrained compressive strength, compared to results of unconfined compressive tests on comparable shale specimens.
- An Illinois-specific correlation between MSPT penetration rate and the undrained compressive strength of weak shale was developed and can be used by IDOT for drilled shaft design to reduce the amount of shale coring and laboratory testing required, which will decrease design time and reduce project costs.
- An Illinois-specific correlation between initial water content and Young's modulus was developed herein for drilled shaft design. This correlation shows that Young's modulus decreases with increase in situ water content.
- Pressuremeter, drilled shaft load test, and laboratory triaxial compression moduli were compared, and pressuremeter moduli are systematically higher than drilled shaft load test and laboratory moduli, a finding that was observed by other investigators (e.g., Mesri and Gibala 1972). The unconfined compressive strength-Young's modulus relationship developed based on drilled shaft load test results is recommended for consistent and economical drilled shaft design.

9.3 NEW DRILLED SHAFT DESIGN PROCEDURE

New predictive methods for unit side resistance and tip resistance are presented in Chapter 8. The unit side resistance predictive method is a function of only unconfined

compressive strength, while unit tip resistance is a function of unconfined compressive strength, embedment depth, and tip displacement under applied loads. The drilled shaft design flowchart by Brown et al., (2010) is recommended with the use of the side and resistance equations presented in Chapter 8, for the design of drilled shafts in weak sedimentary rocks (e.g., weak shales in Illinois). Recommendations of Chapter 4 are also anticipated to be used by IDOT for determining the strength parameters.

9.4 RECOMMENDATIONS FOR FUTURE RESEARCH

Little attention has been given to the design of drilled shafts in weak sedimentary rocks. More field and laboratory testing is recommended for improving the new design method presented herein for drilled shafts in weak rocks. Topics for future research are outlined below.

- Measure additional Illinois-specific MSPT penetration rate and undrained compressive strength for weak shales throughout the state of Illinois to further verify and refine the correlation between MSPT penetration rate and unconfined compressive strength presented herein, which is based on five IDOT bridge sites. Additional MSPT data could be collected at other bridge sites that utilized drilled shafts and/or future field explorations in weak shales to improve the current relationship between MSPT penetration rate and the unconfined compressive strength of weak shales. Enhancing this correlation will provide additional confidence for its use in design, and the use of an MSPT-based design method will reduce the amount of shale coring and laboratory testing required for future projects and lower design time and project costs.
- Additional load tests on drilled shafts in Illinois weak shales are required to improve and verify the new side and tip resistance design methods presented herein.
- An Illinois-specific correlation between initial water content and Young's modulus was developed herein for drilled shaft design. Additional data on in situ water content of shale and Yong's modulus should be collected to improve the accuracy of the current relationship.

9.4.1 Illinois Drilled Shaft Load Tests and Future Load Tests

Data for unit side resistance obtained from load tests in Illinois at IL 5 over IL 84 and FAU 6265 sites were reviewed and are summarized in Table 9.1. Unit tip resistance from these sites was not applicable to this study because the drilled shafts at IL 5 over IL 84 bear on massive sandstone and the drilled shafts at FAU 6265 site bear on massive siltstone and sandstone. Data presented in Table 9.1 for FAU 6265 site produce adhesion factors that are lower than values that the existing literature would suggest for drilled shafts in weak cohesive rocks. This is attributed to low shear displacements in this drilled shaft load test that prevented mobilization of the ultimate or maximum unit side resistance. Additional drilled shaft load tests are recommended to confirm the new design method for Illinois shale and to investigate the accuracy of the load test data presented in Table 9.1.

Table 9.1 Illinois Load Test Results for Drilled Shafts in Weak, Cohesive Rocks

Site	Strain Gage Level	Depth (ft.)	Average q_u (ksf)	f_{smax} (ksf)	Displacement at f_{smax} (in.)	Adhesion Factor
John Deere Road (IL 5) over IL 84 (2008)	3 to 2	12.6 to 18.6	5.57	1.4	0.44	0.25
John Deere Road (IL 5) over IL 84 (2008)	2 to 1	18.6 to 24.6	11.7	2.7	0.44	0.23
John Deere Road (IL 5) over IL 84 (2008)	1 to 0-cell	24.6 to 33	55.75	13.3	0.45	0.24
Illinois River Bridge Replacement (FAU 6265) (1996)	7 to 6	18.7 to 25.7	2.65	1.0	0.10	0.37
Illinois River Bridge Replacement (FAU 6265) (1996)	6 to 5	25.7 to 32.7	34	2.2	0.10	0.06
Illinois River Bridge Replacement (FAU 6265) (1996)	5 to 4	32.7 to 39.7	58.8	5.4	0.10	0.09

REFERENCES

AASHTO. 2006. “LRFD highway bridge design specification.” 3rd edition, American Association of State Highway and Transportation Officials, Washington, DC.

ASTM Standard D7012. 2010. “Standard test method for compressive strength and elastic moduli of intact rock core specimens under varying states of stress and temperatures.” ASTM International, West Conshohocken, PA.

ASTM Standard D2166. 2007. “Standard test method for unconfined compressive strength of cohesive soils.” ASTM International, West Conshohocken, PA.

ASTM Standard D6032. 2008. “Standard test method for determining rock quality designation (RQD) of rock core.” ASTM International, West Conshohocken, PA.

ASTM Standard D2216. 2010. “Standard test method for laboratory determination of water (moisture) content of soil and rock by mass.” ASTM International, West Conshohocken, PA.

ASTM Standard D1586. 2008. “Standard test method for standard penetration test (SPT) and split-barrel sampling of soils.” ASTM International, West Conshohocken, PA.

Abu-Hejleh, N., and W. J. Attwooll, *Colorado’s Axial Load Tests on Drilled Shafts Socketed in Weak Rocks: Synthesis and Future Needs*, Final Contract Report No. CDOT-DTD-R-2005-4, Colorado Department of Transportation, Denver, CO, September 2005, 178 p.

Abu-Hejleh, N., M. W. O’Neil, D. Hanneman, and W. J. Attwooll, *Improvement of the Geotechnical Axial Design Methodology for Colorado’s Drilled Shafts Socketed in Weak Rocks*, Final Contract Report No. CDOT-DTD-R-2003-6, Colorado Department of Transportation, Denver, CO, July 2003, 199 p.

ARGEMA, *Design guides for offshore structures: offshore pile design*, Association de recherché en geotechnique marine, P. L. Tirant, ed., Editions Technip, Paris, France, 1992.

Aurora, R. P., and L. C. Reese, *Behavior of Axially Loaded Drilled Shafts in Clay-Shales*, Final Contract Report No. CFHR 3-5-72-176-4, Center for Highway Research, The University of Texas at Austin, Austin, TX, March 1976, 184 p.

Bloomquist, D., and F. C. Townsend, *Development of insitu equipment for capacity determination of deep foundations in Florida limestone*, Report to Florida department of transportation, Gainesville, 1991.

Brown, D. A., and R. Thompson, *Drilled shaft foundation testing and design recommendation: I 65 over Mulberry of the Warrier River*, The State of Alabama Highway Department, Montgomery, Alabama, 1994, 67 p.

Brown, D. A., J. P. Turner, and R. J. Castelli, *Drilled Shafts: Construction Procedure and LRFD Design Methods*, Final Contract Report No. FHWA-NHI-10-016, Federal Highway Administration, Washington, D.C., May 2010, 970 p.

Canadian Geotechnical Society, *Canadian Foundation Engineering Manual*, Friesens Corporation, Altona, MB, 2006, 488 p.

Carter, J. P., and F. H. Kulhawy, *Analysis and design of drilled shaft foundations socketed into rock*, Final Contract Report No. EL-5918, Electric Power Research Institute, Palo Alto, August 1988, 190 p.

Coates, D. F., *Rock Mechanics Principle*, Department of Energy, Mines, and Resources, Canada, 1967, 410 p.

Corps of Engineers, "Investigations for Building Foundations in Expansive Clays," Vol. 1, US Army Engineer District, Forth Worth, TX, 1968.

Deere, D. U., and D. W. Deere, "The Rock Quality Designation (RQD) Index in Practice," *Rock Classification Systems for Engineering Purposes*, ASTM STP 984, L. Kirkaldie, ed., American Society for Testing and Materials, Philadelphia, 1988, pp. 91–101.

Geoke, P. M., and P. A. Hustad, "Instrumented Drilled Shafts in Clay-shale," *Proceedings of Symposium on Deep Foundation*, E. M. Fuller, ed., ASCE National Convention, Atlanta, 1979, pp. 149–164.

Gibson, G. L., Field and laboratory investigation for design of rock-socketed caissons for a multi-storey building founded in sound limestone, Master of Engineering thesis, Carleton University, Ottawa, 1973.

Glos, G. H., and O. H. Briggs, "Rock sockets in soft rock," *ASCE Journal of Geotechnical Engineering*, Vol. 109, No. 4, 1983, pp. 525–535.

Golder, H.Q., and A.W., Skempton, "The Angle of Shearing Resistance in Cohesive Soils for Tests at Constant Water Content," *2nd International Conference on Soil Mechanics and Foundation Engineering*, Rotterdam, 1948, pp. 185–192.

Goodman, R. E., *Engineering Geology: Rock in Engineering Construction*, John Wiley and Sons, Inc., New York, NY, 1993, 432 p.

Goodman R. E., *Introduction to Rock Mechanics*, John Wiley and Sons, Inc., New York, NY, 1989, 576 p.

Gupton, C., and T. Logan, "Design guidelines for drilled shafts in weak rocks of south Florida," *South Florida Annual ASCE Meeting*, 1984.

Hassan, K. M., M. W. O'Neil, S. A. Sheikh, and C. D. Ealy, "Design Method for Drilled Shafts in Soft Argillaceous Rocks," *Journal of Geotechnical and Geoenvironmental Engineering*, Vol. 123, No. 3, 1997, pp. 272–280.

Hendron, A. J., G. Mesri, J. C. Gamble, and J. Way, "Compressibility Characteristics of Shales Measured by Laboratory and In Situ Tests," *Determination of the in situ Modulus of Deformation of Rock*, ASTM STP 477, American Society for Testing and Materials, 1970, pp. 137–153.

Henley, A. D., "Investigation of Side Shear Stress Transfer for Drilled In Foundation Shafts in Weak Rock," *Proceedings of the Fifth Annual Symposium on Engineering Geology and Soils Engineering*, Pocatello, Idaho, April 1967, pp. 141–156.

Horvath, R. G., *Field load test data on concrete-to-concrete rock bond strength drilled pier foundations*, Publication 78-07, Toronto, University of Toronto, 1978.

Horvath, R. G., and T. C. Kenney, "Shaft resistance of rock socketed drilled piers," *Symposium on Deep Foundations*, ed. F.M. Fuller, Atlanta, October 1979, pp. 182–214.

Horvath, R. G., Drilled piers socketed into weak rock – method of improving performance, PhD Dissertation, University of Toronto, Ontario, 1982.

Horvath, R. G., T. C. Kenney, and P. Kozicki, "Methods for improving the performance of drilled piers in weak rock," *Canadian Geotechnical Journal*, Vol. 20, No. 4, 1983, pp. 758-772.

Hummert, J. B., and T. L. Cooling, “Drilled pier test, Fort Collins, Colorado,” *Proceedings of the 2nd International on Case Histories in Geotechnical Engineering*, S. Prakash, ed., 1988, pp. 1375–1382.

Jaeger J. C., N. G. W. Cook, and R. W. Zimmerman, *Fundamentals of Rock Mechanics*, Blackwell Publishing, Ltd., Malden, MA, 2007, 475 p.

Johnston, I. W., and I. B. Donald, *Rock socket pile tests*, Final Contract Report No. 78/6/G, 703 Flinders Street–Spencer Street Overpass. Melbourne underground rail loop project, Monash University, Melbourne, Australia, 1979.

Jubenville, M. D., and R. C. Hepworth, “Drilled pier foundations in shale—Denver, Colorado, area,” *Proceedings of Drilled Piers and Caissons, Session at the ASCE National Convention*, 1981, pp. 66–81.

Kulhawy, F. H., and K. K. Phoon, “Drilled shaft side resistance in clay soil to rock,” In *Design and Performance of Deep Foundations: Piles and Piers in Soil and Soft Rock*, P. P. Nelson, T. D. Smith, and E. C. Clukey, eds., New York, October 24–28, 1993, pp. 172–183.

Kulhawy, F.H., W.A. Prakoso, and S.O. Akbas, “Evaluation of Capacity of Rock Foundation Sockets,” *40th U.S. Symposium on Rock Mechanics*, G. Chen, S. Huang, W. Zhou, and J. Tinucci, eds., Anchorage, Alaska, June 2005, 8 p.

Leach, B. A., J. W. Medland, and H. B. Sutherland, “The ultimate bearing capacity of bored piles in weathered Keuper marl,” *6th European Conference on Soil Mechanics and Foundation Engineering*, Vienna, Vol. 3, 1976, pp. 507–514.

Ladanyi, B., “Friction and end bearing tests on bedrock for high capacity socket design: discussion,” *Canadian Geotechnical Journal*, Vol. 14, 1977, pp. 153-155.

LOADTEST, Inc., *Report on drilled shaft load testing at CH-15 over the Illinois River*, Final Contract Report No. LT-8276, Gainesville, FL, September 1996, 71 p.

LOADTEST, Inc., *Report on drilled shaft load testing at Test Shaft at Sta. 890 + 95 ft.—US 231 over the Ohio River*, Final Contract Report No. LT-8415-2, Gainesville, FL, September 1998, 67 p.

LOADTEST, Inc., *Report on drilled shaft load testing at East test shaft—US 36 over Republican River*, Final Contract Report No. LT-8718-2, Gainesville, FL, April 2001, 58 p.

LOADTEST, Inc., *Report on drilled shaft load testing at Pier 1 West—US 75 at 77th Street*, Final Contract Report No. LT-8733, Gainesville, FL, February 2001, 57 p.

LOADTEST, Inc., *Report on drilled shaft load testing at West test shaft—US 36 over Republican River*, Final Contract Report No. LT-8718-1, Gainesville, FL, April 2001, 59 p.

LOADTEST, Inc., *Report on drilled shaft load testing at Test Shaft #1—US 281 over Solomon River*, Final Contract Report No. LT-8816, Gainesville, FL, October 2001, 54 p.

LOADTEST, Inc., *Report on drilled shaft load testing at Dedicated Test Shaft-I 235 over Des Moines River*, Final Contract Report No. LT-8854, Gainesville, FL, November 2002, 74 p.

LOADTEST, Inc., *Report on drilled shaft load testing at Test shaft- Route 116 over Platte River*, Final Contract Report No. LT-9048, Gainesville, FL, September 2004, 55 p.

LOADTEST, Inc., *Report on drilled shaft load testing at US 75 over Neosho River*, Final Contract Report No. LT-9021, , Gainesville, FL, April 2004, 67 p.

LOADTEST, Inc., *Report on drilled shaft load testing at Test Shaft #1-IL5 over IL 84*, Final Contract Report No. LT-9405, Gainesville, FL, April 2008, 65 p.

Mason, R. C., "Transmission of high loads to primary foundations by large diameter shafts," paper to the ASCE Convention, New Orleans, 1960.

Matich, M. A. J., and P. Kozicki, "Some load tests on drilled cast-in-place concrete caissons," *Canadian Geotechnical Journal*, Vol. 4, No. 4, 1967, pp. 367–375.

McVay, M.C., F. C. Townsend, and R. C. Williams, "Design of socketed drilled shaft in limestone," *Journal of Geotechnical Engineering*, Vol. 118, No. 10, 1992, pp. 1626–1637.

Meigh, A. C., and W. Wolski, "Design parameters for weak rock," *7th European Conference on Soil Mechanics and Foundation Engineering,* Brighton*, 1979,* pp. 59–79.

Mesri, G., and R. Gibala, "Engineering Properties of Pennsylvanian Shale," *Thirteenth Symposium on Rock Mechanics*, E. J. Cording, ed., Illinois, Aug 30–Sep 1, 1972, pp. 57–75.

Millar, W. R., *Results of pile tests on city centre and telephone exchange sites*, Perth, 1976.

Miller, A. D., Prediction of Ultimate Side Shear for Drilled Shafts in Missouri Shales, MS thesis, University of Missouri–Columbia, Missouri, MO, August 2003, 393 p.

Moore, W. W., *Foundation design*, ASCE, Civil Engineering, 1964, pp. 33-35.

O'Neil, M. W., and L. C. Reese, *Drilled Shafts: Construction Procedures and Design Methods*, Final Contract Report No. FHWA-IF-99- 025, Federal Highway Administration, Washington, D.C., 1999, 758 pp.

O'Neil, M. W., F. C. Townsend, K. H. Hassan, A. Buller, and P. S. Chan, *Load Transfer for Drilled Shafts in Intermediate Geomaterials*, FHWA Publication No. FHWA-RD-9-172, Department of Transportation, Federal Highway Administration, McLean, VA, 1996, 790 pp.

Osterberg, J. P., and S. A. Gill, "Load transfer mechanism for piers socketed in hard soils or rocks," *9th Canadian rock mechanics symposium,* Montreal*,* 1973*.*

Palmstrom, A., "The volumetric joint count—a useful and simple measure of the degree of jointing," *International Congress IAEG*, New Delhi, 1982, pp. V.221–V.228.

Pells, P. J. N., D. J. Douglas, B. Rodway, C. Thorne, and B. K. McMahon, *Design loading for foundations on shales and sandstone in the Sydney region*, Research Report No. R 315, The University of Sydney, Sydney, March 1978.

Pells, P. J. N., R. K. Rowe, and R. M. Turner, "An experimental investigation into side shear for socketed piles in sandstone," *International Conference on Structural Foundations on Rock,* P.J.N. Pells, ed., Sydney, May 7–9, 1980, pp. 291–302.

Poulos, H. G., and E. H. Davis, *Elastic Solutions for Soil and Rock Mechanics*, John Wiley and Sons, Inc., New York, NY, 1974, 423 p.

Prakoso, W. A., Reliability-based design of foundations in rock masses, PhD dissertation, Cornell University, Ithaca, 2002.

Prakoso, W.A., and F.H. Kulhawy, "Uncertainty in Capacity Model for Foundations in Rock,"

5th North American Rock Mechanics Symposium, R. Hammah et al., Toronto, 2002, pp. 1241–1248.

Reese, L. C., W. M. Isenhower, and S. T. Wang, *Analysis and Design of Shallow and Deep Foundation*, John Wiley and Sons, Inc., New Jersey, NJ, 2006, 574 p.

Reese, L. C., and M. W. O'Neill, *Drilled shafts: construction procedures and design methods*, Report No. FHWA-HI-88-042, Washington, DC, 1988, 564 p.

Reynolds, R. T., and T. J. Kaderbeck, "Miami limestone foundation design and construction," *Journal of the Geotechnical Engineering Division*, Vol. 107, No. GT7, 1980, pp. 859–872.

Rosenberg, P., and N. L. Journeaux, "Friction and end bearing tests on bedrock for high capacity socket design," *Canadian Geotechnical Journal*, Vol. 13, No. 3, 1976, pp. 324–333.

Rowe, R. K., and H. H. Armitage, *Design of piles socketed into weak rocks*, GEOT -11-84, London, University of Western Ontario, 1984.

Rowe, R. K., and H. H. Armitage, "A design method for drilled piers in soft rock," *Canadian Geotechnical Journal*, Vol. 24, No. 1, 1987, pp. 126–142.

Stroud, M.A., "The Standard Penetration Test in Insensitive Clays and Soft Rocks," *European Symposium on Penetration Testing*, Stockholm, 1974, pp. 367–375.

Santarelli, F. J., and E. T. Brown, "Failure of three sedimentary rocks in triaxial and hollow cylinder compression tests," *International Journal of Rock Mechanics and Mining Sciences*, Vol. 26, No. 5, 1989, pp. 401-413.

Teng, W. C., *Foundation Design*, Prentice-Hall, Englewood Cliffs, NJ, 1962.

Terzaghi K., R. B. Peck, G. Mesri, *Soil Mechanics in Engineering Practice*, John Wiley and Sons, Inc., New York, NY, 1996, 549 p.

Thorburn, S., "Large Diameter Piles Founded on Bedrock," *Institution of Civil Engineers*, 1966, pp. 121–129.

Toh, C. T., T. A. Ooi, H. K. Chiu, S. K. Chee, and W. H. Ting, "Design parameters for bored piles in a weathered sedimentary formation," *12th International Conference on Soil Mechanics and Foundation Engineering*, Rio De Janeiro, August 13–18,1989, pp. 1073–1078.

Turner, J., *Rock-Socketed Shafts for Highway Structure Foundations*, Final Contract Report No. Project 20-5, National Cooperative Highway Research Program, Washington, D.C., 2006, 136 p.

Van Doren, L. M., S. G. Hazard, J. R. Stallings, and D. P. Schnacke, *Drilled Shaft Foundation Test Program*, Final Contract No. 35W-87-I-35W-1(58)48, State Highway Commission of Kansas, Van Doren-Hazard-Stallings-Schnacke Engineers-Architects, Topeka, KS, July 1967.

Vesic, A. S., "Analysis of Ultimate Loads on Shallow Foundations," *Journal of Soil Mechanics and Foundations Division*, Vol. 99, No. SM1, 1973, pp. 45–73.

Vijayvergiya, V. N., W. R. Hudson, and L. C. Reese, *Load Distribution of a Drilled Shaft in Clay-Shale*, Final Contract No. 89-5, Center for Highway Research, The University of Texas at Austin, Austin, TX, 1969.

Walter, D. J., W. J. Burwash, and R. A. Montgomery, "Design of large-diameter drilled shafts

for the Northumberland Strait bridge project," *Canadian Geotechnical Journal*, Vol. 34, No. 4, 1997, pp. 580-787.

Williams, A. F., I. W. Johnston, and I. B. Donald, "Design of socketed piles in weak rock," *The International Conference on Structural Foundations on Rock,* P. J. N. Pells, ed., Sydney, May 7–9, 1980, pp. 327–347.

Williams, A. F., *The design and performance of piles socketed into weak rock,* PhD dissertation, Monash University, Melbourne, Australia, 1980a.

Williams, A. F., "Principle of side resistance development is rock socketed piles," *Third Australia–New Zealand Conference on Geomechanics*, Wellington, May 12–16, 1980b, pp. 87–94.

Williams, A. F., and P. J. N. Pells, "Side resistance of rock sockets in sandstone, mudstone, and shale," *Canadian Geotechnical Journal*, Vol. 18, No. 4, 1981, pp. 502–513.

Wilson, L. C., "Tests of bored piles and driven piles in cretaceous mudstone at Port Elizabeth, South Africa," *Geotechnique*, Vol. 26, No. 1, 1976, pp. 5–12.

Wyllie, D. C., and N. I. Norrish, "Rock Strength Properties and Their Measurement," In TRB Special Report 247, *Landslides—Investigation and Mitigation,* A.K. Turner and L.R. Shuster, ed., Transportation Research Board, National Research Council, Washington, D.C., 1996, pp. 372–390.

Zhang, L., and H. H. Einstein, "End Bearing Capacity of Drilled Shafts in Rock," *Journal of Geotechnical and Geoenvironmental Engineering*, Vol. 124, No. 7, 1998, pp. 574–584.

APPENDIX A FIELD EXPLORATION AT IL 23 OVER SHORT POINT CREEK

A.1 BACKGROUND

Figure A.1 shows location of the IDOT bridge (IL 23) crossing the Short Point Creek, just west of the city of Cornell, Illinois. North and South abutments of this bridge are supported on driven H-piles foundations. Piers 1 and 2, however, are supported on 3-ft diameter drilled shaft foundations that are socketed into weak shale for 21 ft. The weak shale near Pier 1, located near the north abutment, was investigated during this study.

Figure A.1 Location of IL 23 over Short Point Creek.

Figure A.2 shows a plan view of this IL 23 bridge structure over Short Point Creek and the location of borings drilled on 11 July 2012 and 12 July 2012 by the District 3 drilling crew and the UIUC research team. Two borings were advanced near the north abutment and in close proximity to Short Point Creek. These borings were drilled to 6 ft (i.e., two drilled shaft diameters, below the tip of the drilled shafts, which corresponds to elevation of +554 ft). Two shaft diameters below the shaft tip allows determination of weak shale shear strength at the depth where tip resistance (i.e., bearing capacity) will be mobilized. This shear strength is needed to assess tip resistance using existing and proposed predictive methods.

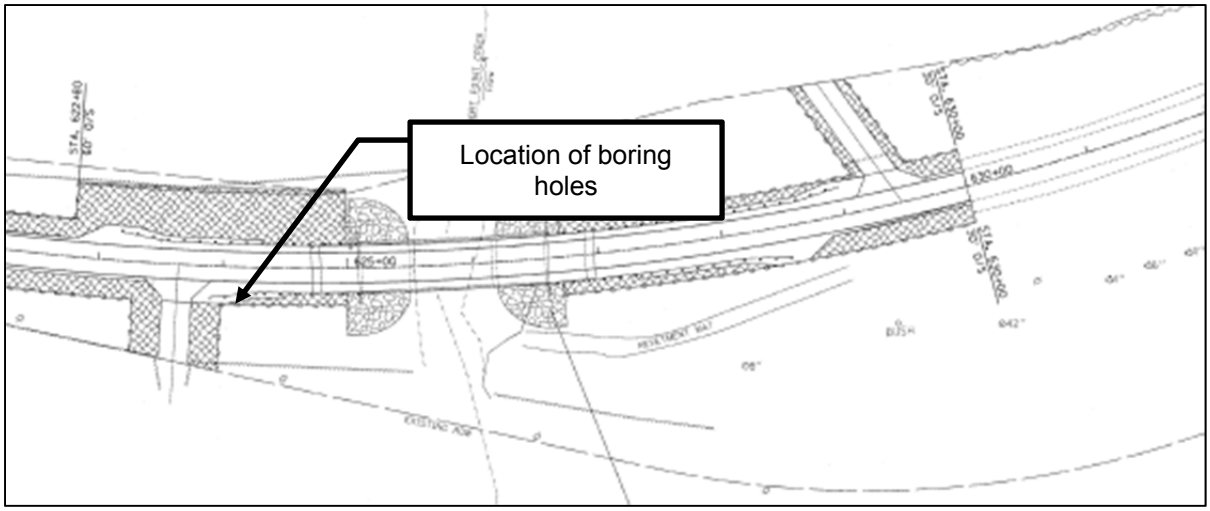

Figure A.2 Location of boring holes for obtaining MSPT blow counts and shale core samples.

One of the two borings was used to obtain shale core samples. Initially rock cores were used for determination of recovery ratio, RQD of the rock mass, and vertical spacing of joints. Afterwards unconfined compression and triaxial compression tests were conducted on representative and comparable shale specimens to study effect of confining pressure on behavior of shale specimens subjected to compressive mode of shear. The in situ water content of the shale specimens used in the triaxial compression tests was also measured for correlation purposes. Triaxial test results were also used to determine the deformability characteristics of shale under undrained loading conditions.

The second boring was used to obtain MSPT blow counts at various depths. This data was used to develop a new correlation between undrained compressive strength of weak shale in Illinois and MSPT penetration rate.

The following sections discuss geology of the bridge site, MSPT test results, and laboratory test results.

A.2 SITE GEOLOGY

The geology at the bridge site consists of stiff brown sandy clay overlying sedimentary bedrock (e.g., shale, and limestone). The ground surface elevation at the two borings is about 602.5 ft. Overburden soil at this site consists of dark brown and stiff silty clay to medium yellow clay loam. A relatively continuous black to gray blocky clay-shale was exposed at an elevation of about 577.5 ft that extends to elevation 552.5 ft where the boring terminated. A layer of black coal (with an approximate thickness of 8 in.) was encountered at elevation 572.5 ft. Thin layers of gray limestone shale were encountered at depths of 564.5 to 563.5 ft and 554.5 to 552.5 ft.

A.3 MODIFIED STANDARD PENETRATION TEST RESULTS

Figure A.3 shows the modified standard penetration test results obtained in one of the borings at IL 23 over the Short Point Creek.

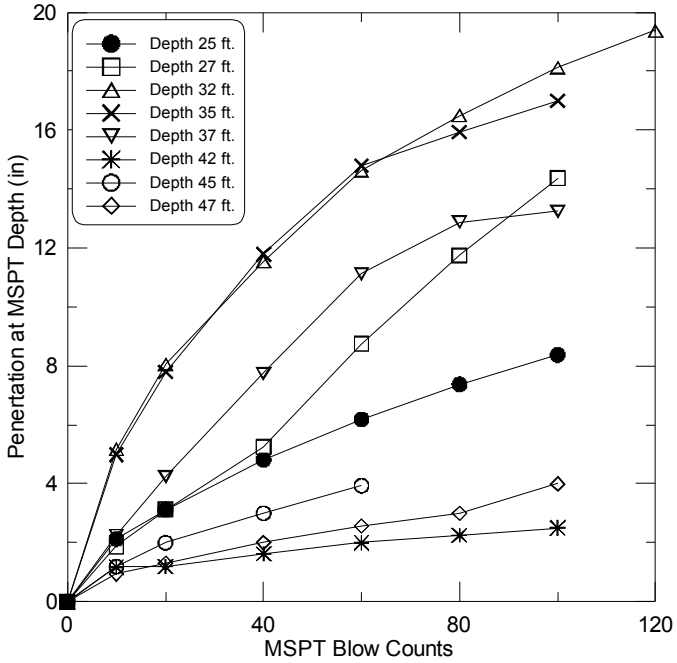

Figure A.3 Modified standard penetration test results.

A.4 LABORATORY TEST RESULTS

A.4.1 Moisture Content and Total Unit Weight

Figure A.4 shows the total unit weight profile at the Short Point Creek site. The total unit weight of shale was computed in accordance with ASTM D 7263.

Shale specimens from unconsolidated undrained and unconfined compressive tests were used for determination of in situ water content. The resulting moisture content profile is shown in Figure A.5. Moisture content of the shale was determined in accordance with ASTM D 2216.

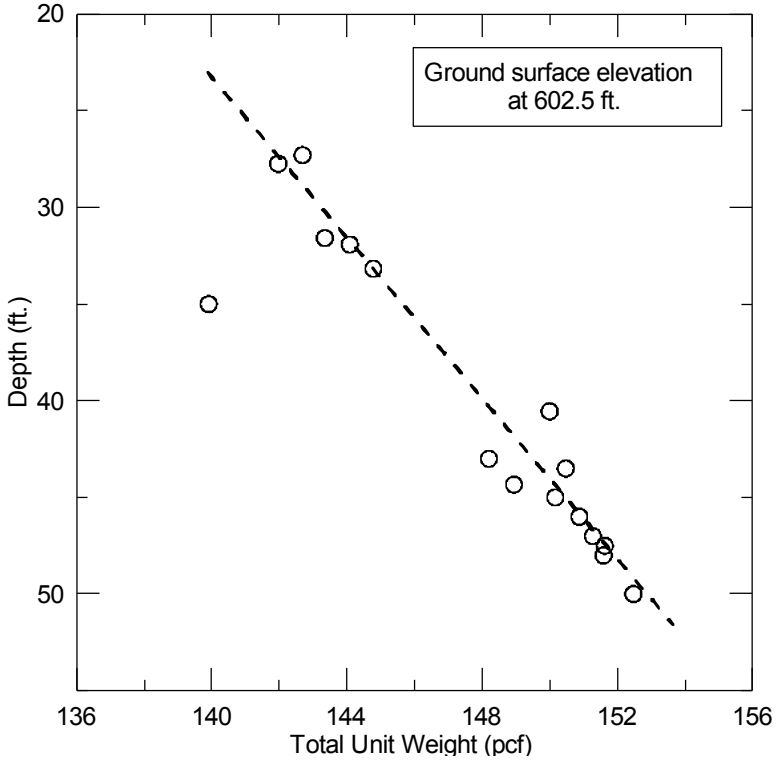

Figure A.4 Total unit weight profile.

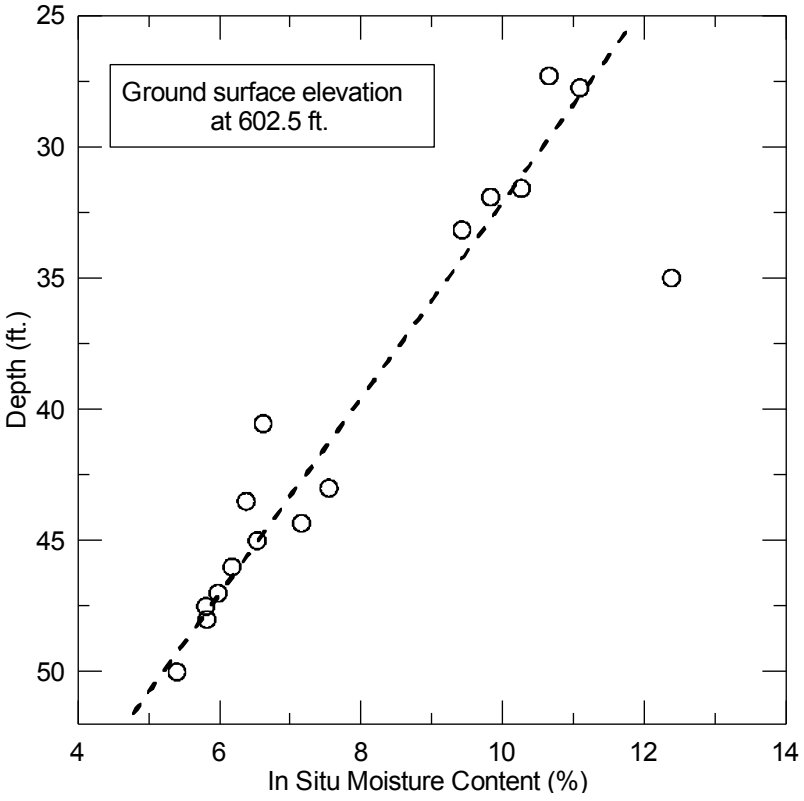

Figure A.5 In situ water content profile.

A.4.2 Triaxial Compression Test Results

Unconfined and confined triaxial compression tests were performed in accordance with ASTM D 7012. The peak deviator stress was used to calculate the undrained compressive strength for each test. The resulting undrained compressive strengths are shown in Table A.1.

A.4.3 Young's Modulus of Shale Specimen

Young's modulus was measured from results of triaxial tests in accordance to ASTM D 7012. In short, the modulus was calculated from the slope of the stress-strain relationships that correspond to 50% of mobilized undrained compressive strength. Figure A.6 shows the relationship between Young's modulus and undrained compressive strength for the shale cores tested from the Short Point Creek site. This data was also used to develop a relationship between undrained Young's modulus and shale natural water content (see Figure A.7). Table A.1 summarizes all of the data obtained from the laboratory testing and evaluation.

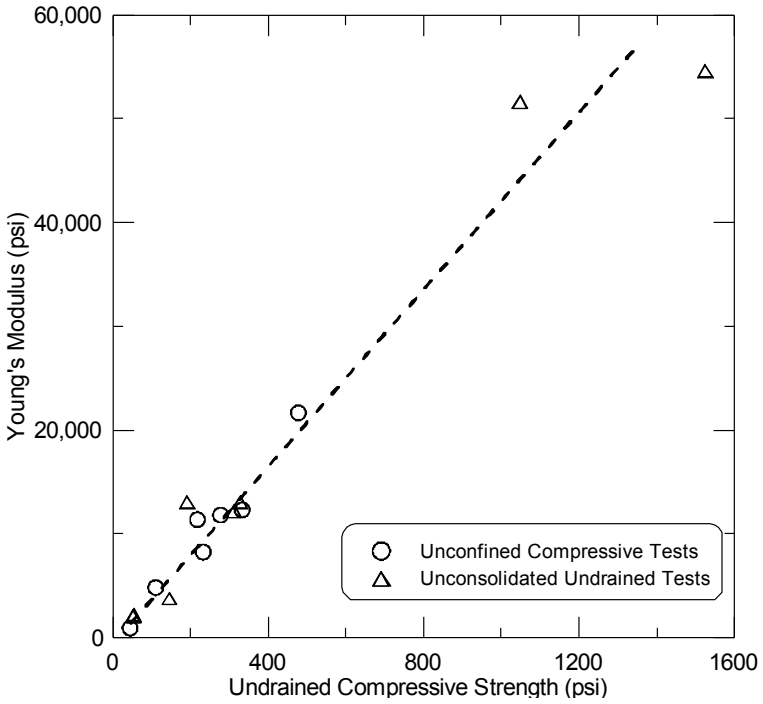

Figure A.6 Relationship between undrained compressive strength and Young's modulus.

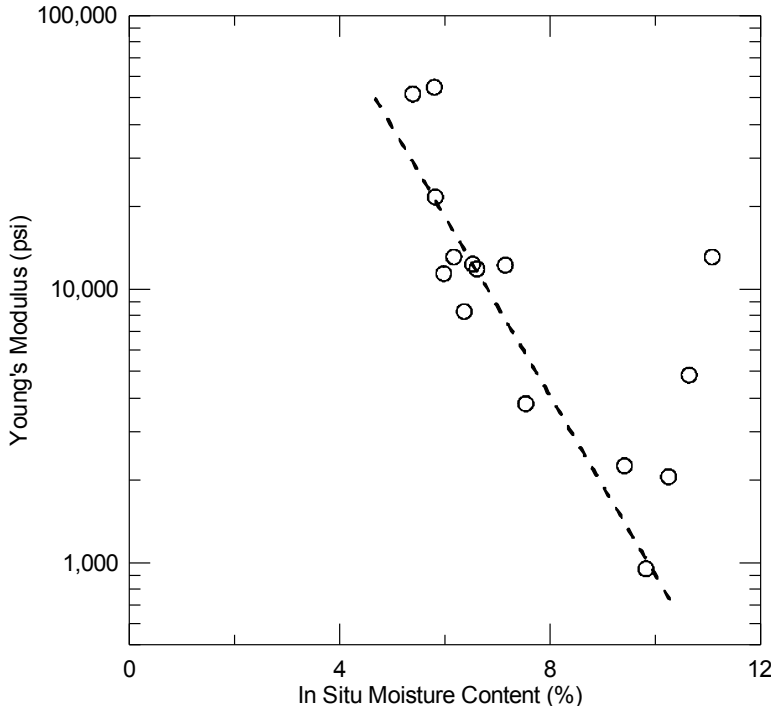

Figure A.7 Relationship between initial water content and Young's modulus.

Table A.1 Laboratory Data Summary at the IL 23 Over Short Point Creek

Specimen Identification	IL 23-S1	IL 23-S2	IL 23-S3
Core Run Number	**1**	**1**	**2**
Depth (ft.)	27.3	27.75	31.6
Initial Water Content (%)	10.7	11.1	10.3
Total Unit Weight (pcf)	142.7	141.9	143.3
Undrained Compressive Strength (ksf)	15.9 (UC)	27.5 (UU)	7.5 (UU)
Strain at Peak Strength (%)	3.3	3.4	7
Young's Modulus (ksf)	698.7	1886	296.7
Recovery (%)	75	75	95
Rock Quality Designation (%)	71	71	82
Joint Average Vertical Spacing (in.)	8	8	2
Sample Description	SHALE, gray and blocky	SHALE, gray and blocky	CLAY-SHALE, Gray and blocky with coal pieces

Specimen Identification	IL 23-S4	IL 23-S5	IL 23-S6
Core Run Number	**2**	**2**	**2**
Depth (ft.)	31.9	33.2	35
Initial Water Content (%)	9.8	9.4	12.4
Total Unit Weight (pcf)	144	145	140
Undrained Compressive Strength (ksf)	6.33 (UC)	7.6 (UU)	—
Strain at Peak Strength (%)	5.0	9.0	—
Young's Modulus (ksf)	137	325	—
Recovery (%)	95	95	95
Rock Quality Designation (%)	82	82	82
Joint Average Vertical Spacing (in.)	5	5	5
Sample Description	CLAY-SHALE, Gray and blocky with coal pieces	CLAY-SHALE, Gray and blocky with coal pieces	CLAY-SHALE, Gray and blocky with coal pieces

Specimen Identification	IL 23-S7	IL 23-S8	IL 23-S9
Core Run Number	**4**	**4**	**4**
Depth (ft.)	40.5	44.3	45
Initial Water Content (%)	6.6	7.15	6.5
Total Unit Weight (pcf)	150	149	150.2
Undrained Compressive Strength (ksf)	40 (UC)	44.8 (UU)	47.8 (UC)
Strain at Peak Strength (%)	2.7	2.7	2.8
Young's Modulus (ksf)	1704	1760	1775
Recovery (%)	100	100	100
Rock Quality Designation (%)	80	80	80
Joint Average Vertical Spacing (in.)	6.5	6.5	6.5
Sample Description	SHALE, with limestone seams, gray to light green	SHALE, gray with limestone inclusions	SHALE, gray with limestone inclusions

Specimen Identification	IL 23-S10	IL 23-S11	IL 23-S12
Core Run Number	**5**	**5**	**5**
Depth (ft.)	46	47	47.5
Initial Water Content (%)	6.2	5.9	5.8
Total Unit Weight (pcf)	150.9	151.3	151.7
Undrained Compressive Strength (ksf)	47 (UU)	31.3 (UC)	219.6 (UU)
Strain at Peak Strength (%)	2.4	2.4	3.1
Young's Modulus (ksf)	1886	1640	7867
Recovery (%)	90	90	90
Rock Quality Designation (%)	74	74	74
Joint Average Vertical Spacing (in.)	6.5	10	10
Sample Description	SHALE, gray to green with limestone seams	SHALE, gray to green with limestone seams	SHALE, gray to green with limestone seams

Specimen Identification	IL 23-S13	IL 23-S14
Core Run Number	**5**	**5**
Depth (ft.)	48	50
Initial Water Content (%)	5.8	5.4
Total Unit Weight (pcf)	151.6	152.5
Undrained Compressive Strength (ksf)	69 (UC)	150 (UU)
Strain at Peak Strength (%)	2.6	2.5
Young's Modulus (ksf)	3122	7430
Recovery (%)	90	90
Rock Quality Designation (%)	74	74
Joint Average Vertical Spacing (in.)	10	10
Sample Description	SHALE, gray to green with limestone seams	SHALE, gray to green with limestone seams

APPENDIX B FIELD EXPLORATION AT US 24 OVER THE LAMOINE RIVER

B.1 BACKGROUND

Figure B.1 shows location of US 24 over the Lamoine River, located in Brown County, just east of village of Ripley, Illinois. This three-span bridge structure carries two-lane highway over the Lamoine River. East and west abutments of this bridge are supported on driven H-pile foundations. Piers 1 and 2, however, are supported on 3.5-ft-diameter drilled shaft foundations that are socketed into weak shale for 13.5 and 19 ft, respectively. The weak shale near Pier 2, located near the east abutment, was investigated during this study.

Figure B.1 Location of US 24 over the Lamoine River.

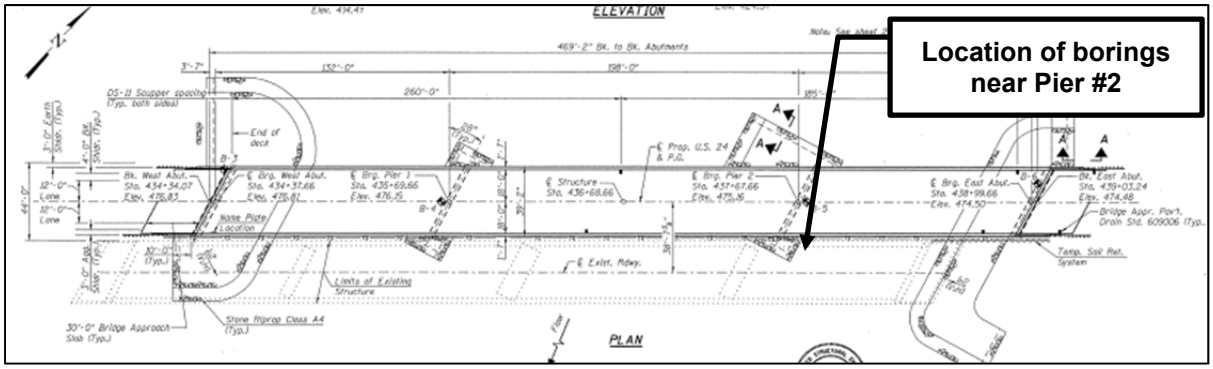

Figure B.2 Location of boring holes at US 24 over the Lamoine River.

Figure B.2 shows a plan view of this US 24 bridge structure over the Lamoine River and the location of borings drilled on 12 September 2012 and 24 October 2012 for by District 6 drilling crew and the UIUC research team. Two borings were advanced near pier #2 and in close proximity to the Lamoine River. These borings were drilled to the elevation of 406 ft. Pier #2 is underlain by limestone whose strength properties are outside of scope of this research and therefore drilling was terminated near the tip elevation of Pier #2.

One of the two borings was used to obtain shale core samples. Initially rock cores were used for determination of recovery ratio, RQD of the rock mass, and vertical spacing of joints. Afterwards unconfined compression and triaxial compression tests were conducted on representative and comparable shale specimens to study effect of confining pressure on behavior of shale specimens subjected to compressive mode of shear. The in situ water content of the shale specimens used in the triaxial compression tests was also measured for correlation purposes. Triaxial test results were also used to determine the deformability characteristics of shale under undrained loading conditions.

The second boring was used to obtain MSPT blow counts at various depths. This data was used to develop a new correlation between undrained compressive strength of weak shale in Illinois and MSPT penetration rates.

The following sections discuss geology of the bridge site, MSPT test results, and laboratory test results

B.2 SITE GEOLOGY

The geology at the bridge site consists of 28 ft of clay with thin seams of loam overlying sedimentary bedrock (e.g., shale, and limestone). The ground surface elevation at Pier #2 (i.e., the two borings) is about 452 ft. Shale was exposed at an elevation of 424 ft. The upper 5 ft (i.e., elevations of 424 to 419) consist of dark gray and very well indurated calcareous shale with unconfined compressive strengths of up to 140 ksf. This relatively strong layer of shale was underlain by 12 ft (i.e., elevation of 419 to 407 ft) of well-indurated clay-shale with unconfined compressive strength of 19 to 80 ksf. An argillaceous gray limestone layer underlies this shale layer. Drilling was terminated at an elevation of 406 ft, (i.e., top of limestone). Laboratory test results are summarized in Table B.1.

B.3 MODIFIED STANDARD PENETRATION TEST RESULTS

Figure B.3 shows the modified standard penetration test results obtained in one of the borings at US 24 over the Lamoine River.

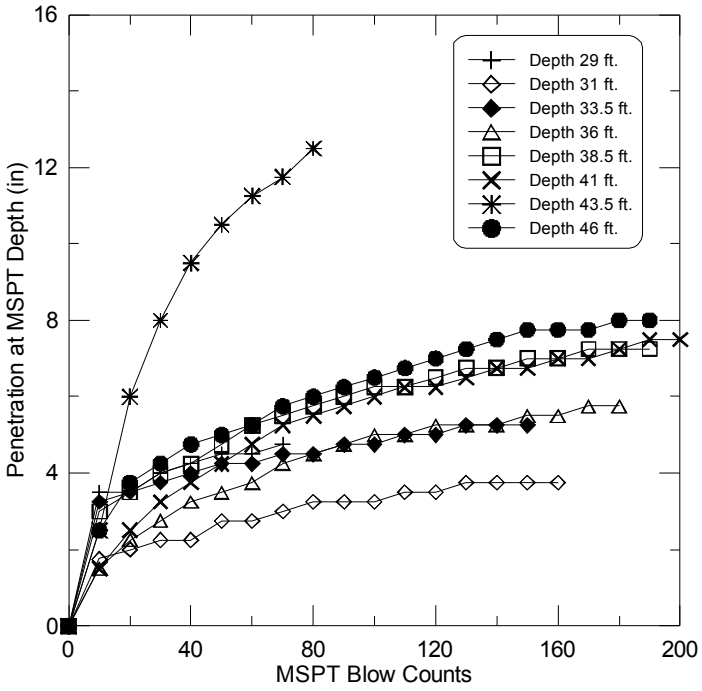

Figure B.3 Modified standard penetration test results.

Twelve in. of penetration was only reached at an elevation of 43.5 where shale was relatively weak and had a low RQD.

B.4 LABORATORY TEST RESULTS

B.4.1 Moisture Content and Total Unit Weight

Figure B.4 shows the total unit weight profile at the US 24 site. The total unit weight of shale was computed in accordance with ASTM D 7263.

Shale specimens from unconsolidated undrained and unconfined compressive tests were used for determination of in situ water content. The resulting water content profile is shown in Figure B.5. Water content of the shale was determined in accordance with ASTM D 2216.

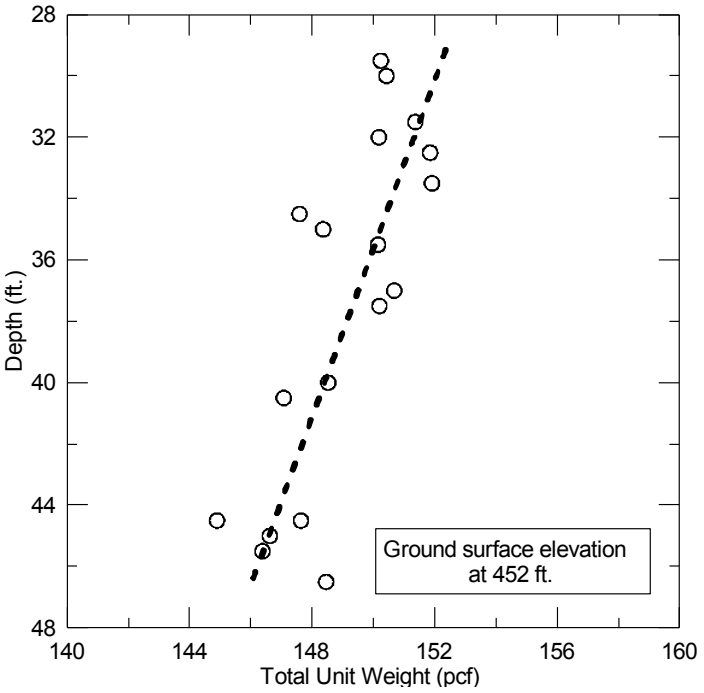

Figure B.4 Total unit weight profile.

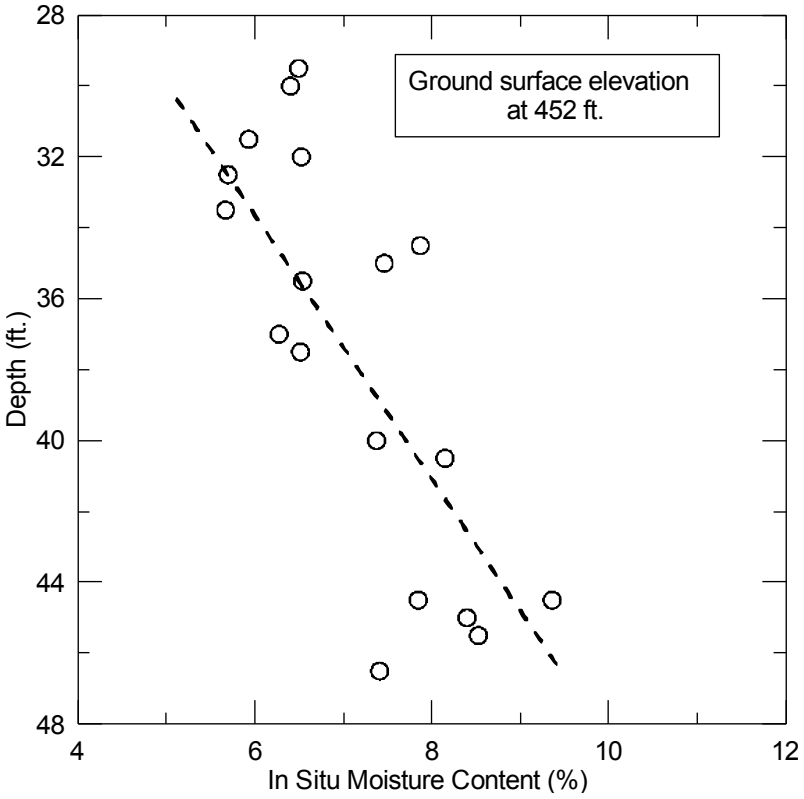

Figure B.5 In situ moisture content profile.

B.4.2 Triaxial Compression Test Results

Unconfined and confined triaxial compression tests were performed in accordance with ASTM D 7012. The peak deviator stress was used to calculate the undrained compressive strength for each test. The resulting undrained compressive strengths are shown in Table B.1.

B.4.3 Young's Modulus of Shale Specimen

Young's modulus was measured from results of triaxial tests in accordance to ASTM D 7012. In short, the modulus was calculated from the slope of the stress-strain relationships that correspond to 50% of mobilized undrained compressive strength. Figure B.6 shows the relationship between Young's modulus and undrained compressive strength for the shale cores tested from the Lamoine River site. This data was also used to develop a relationship between undrained Young's modulus and shale natural water content (see Figure B.7). Table B.1 summarizes all of the data obtained from the laboratory testing and evaluation.

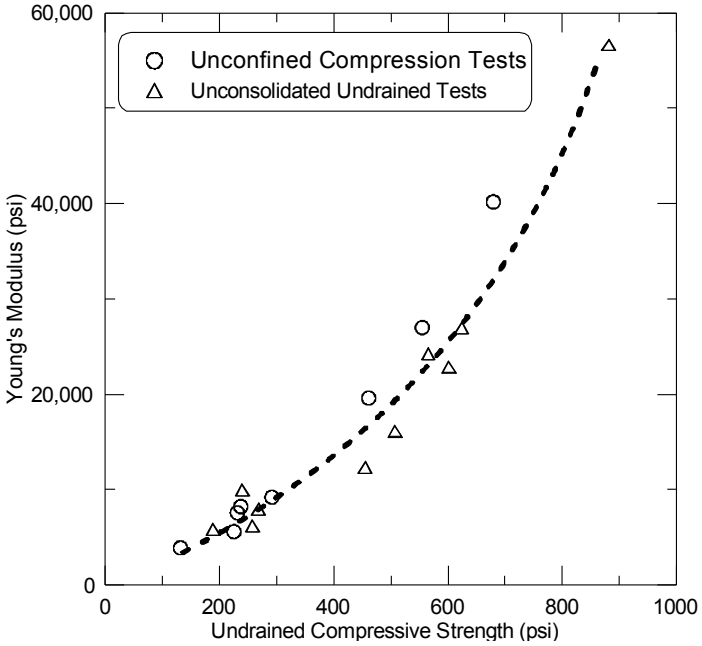

Figure B.6 Relationship between undrained compressive strength and Young's modulus.

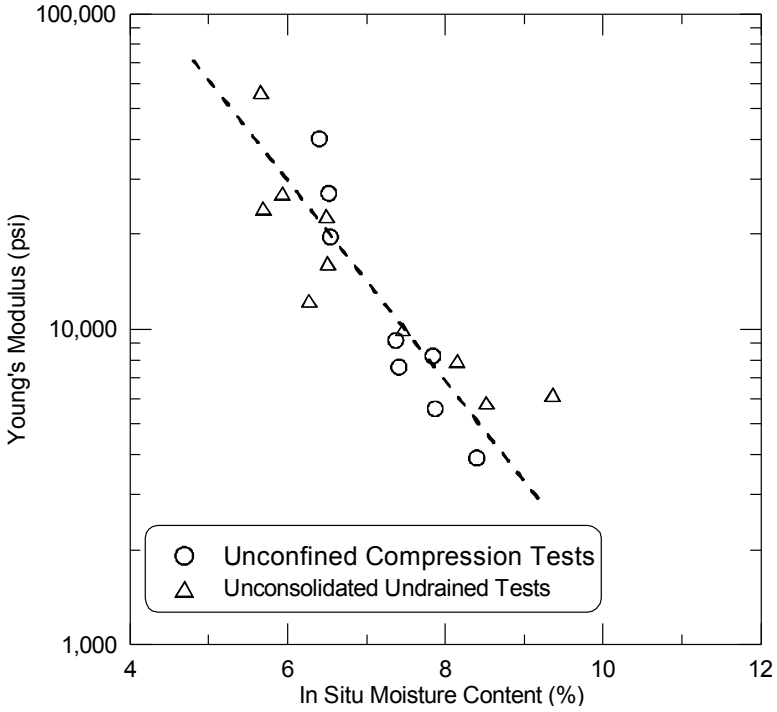

Figure B.7 Relationship between in situ moisture content and Young's modulus.

Table B.1 Laboratory Data Summary at the US 24 Over the Lamoine River

Specimen Identification	**US 24-S1**	**US 24-S2**	**US 24-S3**
Core Run Number	**1**	**1**	**1**
Depth (ft.)	29.5	30	31.5
Initial Water Content (%)	6.5	6.4	5.9
Total Unit Weight (pcf)	150.2	150.4	151.4
Undrained Compressive Strength (ksf)	86.6 (UU)	97.8 (UC)	89.7 (UU)
Strain at Peak Strength (%)	3.9	2.2	2.5
Young's Modulus (ksf)	3295	5786	3888
Recovery (%)	100	100	100
Rock Quality Designation (%)	100	100	100
Joint Average Vertical Spacing (in.)	15	15	15
Sample Description	SHALE, gray and very well indurated	SHALE, gray and very well indurated	SHALE, gray and very well indurated

Specimen Identification	**US 24-S4**	**US 24-S5**	**US 24-S6**
Core Run Number	**1**	**1**	**1**
Depth (ft.)	32	32.5	34.5
Initial Water Content (%)	6.5	5.7	7.9
Total Unit Weight (pcf)	150.2	151.8	147.6
Undrained Compressive Strength (ksf)	80 (UC)	81 (UU)	32.4 (UC)
Strain at Peak Strength (%)	2.3	2.4	5.2
Young's Modulus (ksf)	3888	3497	806
Recovery (%)	100	100	100
Rock Quality Designation (%)	100	100	96
Joint Average Vertical Spacing (in.)	15	15	15
Sample Description	SHALE, gray and very well indurated	SHALE, gray and very well indurated	SHALE, dark and very well indurated

Specimen Identification	US 24-S7	US 24-S8	US 24-S9
Core Run Number	**2**	**2**	**2**
Depth (ft.)	35	35.5	37
Initial Water Content (%)	7.5	6.5	6.3
Total Unit Weight (pcf)	148.4	150.2	150.7
Undrained Compressive Strength (ksf)	34.5 (UU)	66.4 (UC)	65.5 (UU)
Strain at Peak Strength (%)	2.7	3.1	4.8
Young's Modulus (ksf)	1440	2824	1773
Recovery (%)	88	88	88
Rock Quality Designation (%)	85	85	85
Joint Average Vertical Spacing (in.)	10	10	10
Sample Description	SHALE, dark and very well indurated	SHALE, dark and very well indurated	SHALE, dark and very well indurated

Specimen Identification	US 24-S10	US 24-S11	US 24-S12
Core Run Number	**3**	**3**	**3**
Depth (ft.)	40	40.5	44.5
Initial Water Content (%)	7.4	8.15	7.8
Total Unit Weight (pcf)	148.5	147	147.6
Undrained Compressive Strength (ksf)	42 (UC)	38.6 (UU)	34 (UC)
Strain at Peak Strength (%)	3.3	3.6	3.6
Young's Modulus (ksf)	1328	1147	1184
Recovery (%)	32	32	32
Rock Quality Designation (%)	32	32	32
Joint Average Vertical Spacing (in.)	10	N/A	N/A
Sample Description	CLAY-SHALE, Soft with open joints	CLAY-SHALE, Soft with open joints	CLAY-SHALE, Soft with open joints

Specimen Identification	US 24-S13	US 24-S14	US 24-S15
Core Run Number	**3**	**4**	**4**
Depth (ft.)	44.5	45	45.5
Initial Water Content (%)	9.36	8.4	8.52
Total Unit Weight (pcf)	144.9	146.6	146.4
Undrained Compressive Strength (ksf)	37 (UU)	18.91 (UC)	27 (UU)
Strain at Peak Strength (%)	4.7	4.1	3.6
Young's Modulus (ksf)	895	563	844
Recovery (%)	32	100	100
Rock Quality Designation (%)	32	78	78
Joint Average Vertical Spacing (in)	N/A	5.5	5.5
Sample Description	SHALE, dark and very well indurated	CLAY-SHALE, poorly indurated	CLAY-SHALE, poorly indurated

Specimen Identification	US 24-S16	US 24-S17	US 24-S18
Core Run Number	**4**	**2**	**2**
Depth (ft.)	46.5	37.5	33.5
Initial Water Content (%)	7.4	6.5	5.7
Total Unit Weight (pcf)	148.5	150.2	152
Undrained Compressive Strength (ksf)	33 (UC)	73 (UU)	126 (UU)
Strain at Peak Strength (%)	3.5	3.6	1.5
Young's Modulus (ksf)	1092	2331	8160
Recovery (%)	100	88	88
Rock Quality Designation (%)	78	85	85
Joint Average Vertical Spacing (in.)	5.5	10	10
Sample Description	CLAY-SHALE, poorly indurated	SHALE, dark and very well indurated	SHALE, gray and very well indurated

APPENDIX C FIELD EXPLORATION AT FAI 80 OVER AUX SABLE CREEK

C.1 BACKGROUND

Figure C.1 shows location of FAI 80 over Aux Sable Creek, located in Grundy County, just west of city of Minooka, Illinois. This three span bridge structure carries four-lane highway over the Aux Sable Creek. East and west abutments of this bridge as well as Piers 1 and 2 are supported on drilled shaft foundations. Abutments are supported on 2.5-ft-diameter drilled shaft foundations that are socketed into weak shale for 20 ft. The weak shale near east abutment was investigated during this study.

Figure C.1 Location of FAI 80 Over Aux Sable Creek.

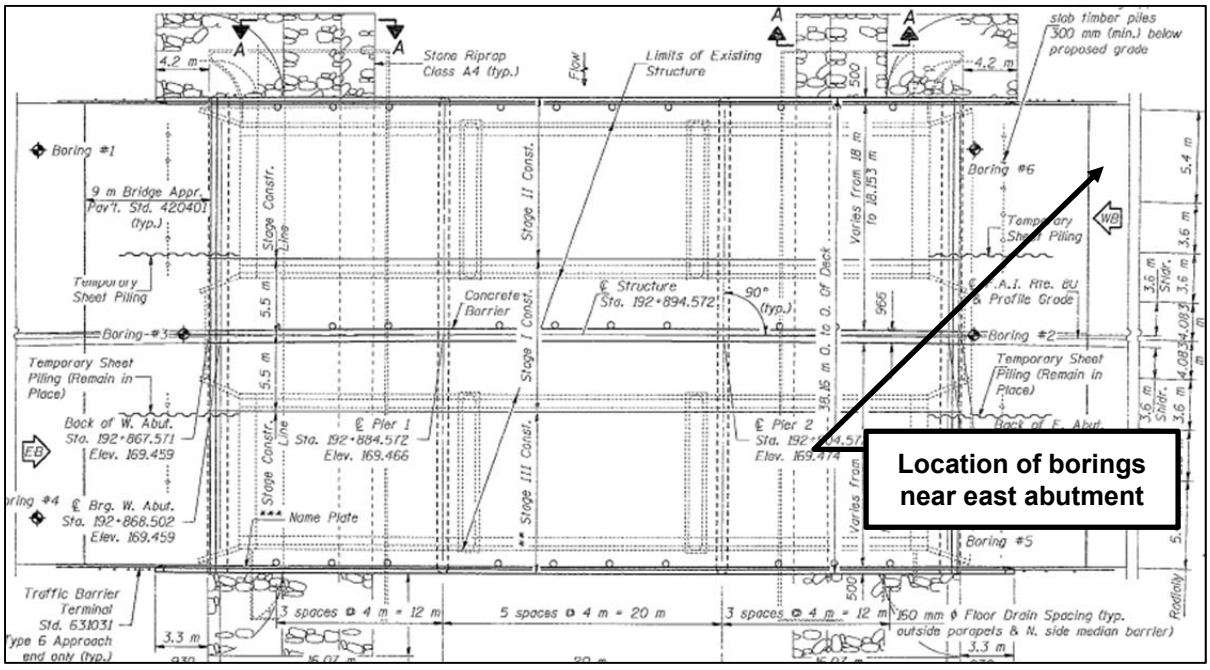

Figure C.2 Location of boring holes at FAI 80 over Aux Sable Creek.

Figure C.2 shows a plan view of this FAI 80 bridge structure over the Aux Sable Creek and the location of borings drilled on 27 November 2012 and 28 November 2012 by Wang Engineering crew and the UIUC research team. Two borings were advanced near east abutment and in close proximity to the Aux Sable Creek. These borings were drilled to the elevation of 521.5 ft. This corresponds to two drilled shaft diameters below the tip of drilled shaft elevation (i.e., 526.5 ft).

One of the two borings was used to obtain shale core samples and to perform pressuremeter tests. Initially rock cores were used for determination of recovery ratio, RQD of the rock mass, and vertical spacing of joints. Afterwards unconfined compression and triaxial compression tests were conducted on representative and comparable shale specimens to study effect of confining pressure on behavior of shale specimens subjected to compressive mode of shear. The in situ water content of the shale specimens used in the triaxial compression tests was also measured for correlation purposes. Triaxial test results were also used to determine the deformability characteristics of shale under undrained loading conditions.

The second boring was used to obtain the MSPT blow counts at various depths. This data was used to develop a new correlation between undrained compressive strength of weak shale in Illinois and MSPT penetration rates.

The following sections discuss geology of the bridge site, MSPT test results, and laboratory test results

C.2 SITE GEOLOGY

The geology at the bridge site consists of 19 ft of stiff to very stiff silty clay overlying sedimentary bedrock (e.g., shale, and limestone). The ground surface elevation at east abutment (i.e., the two borings) is about 554.5 ft. Shale was exposed at an elevation of 535.5 ft. Shale was calcareous and dark gray to black in color. A few thin layers of limestone were present within the shale bedrock. Laboratory test results are summarized in Table C.1.

C.3 MODIFIED STANDARD PENETRATION TEST RESULTS

Figure C.3 shows the modified standard penetration test results obtained in one of the borings at FAI 80 over the Aux Sable Creek.

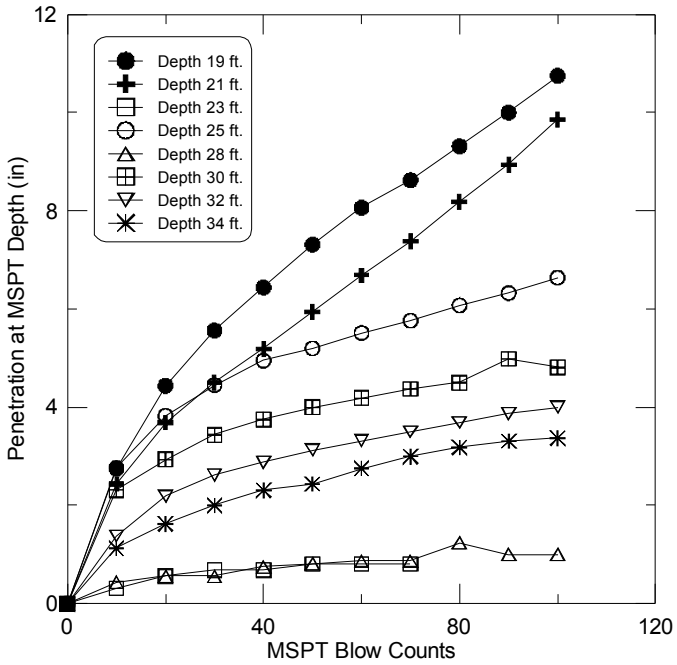

Figure C.3 Modified standard penetration test results.

C.4 LABORATORY TEST RESULTS

C.4.1 Moisture Content and Total Unit Weight

Figure C.4 shows the total unit weight profile at the FAI 80 site. The total unit weight of shale was computed in accordance with ASTM D 7263.

Shale specimens from unconsolidated undrained and unconfined compressive tests were used for determination of in situ water content. The resulting water content profile is shown in Figure C.5. Water content of the shale was determined in accordance with ASTM D 2216.

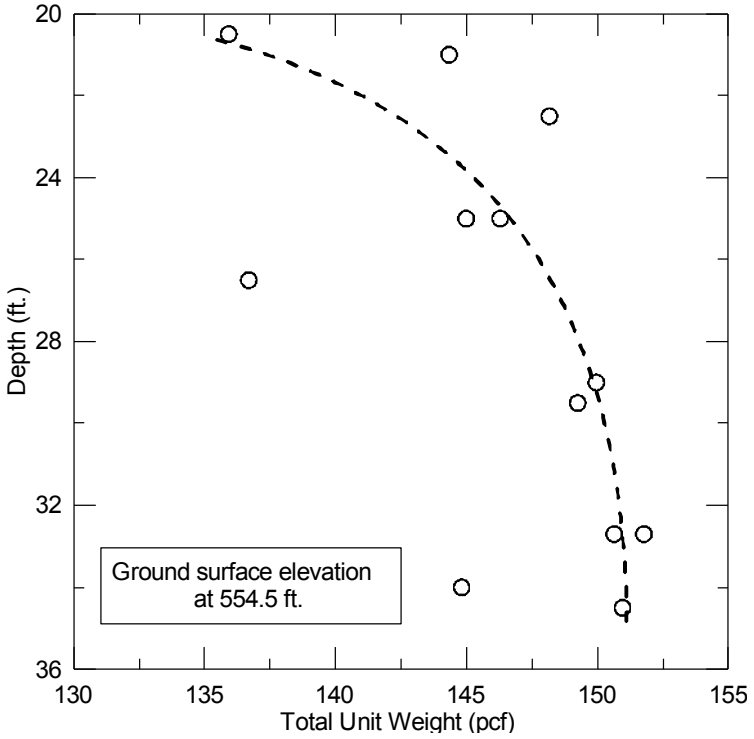

Figure C.4 Total unit weight profile.

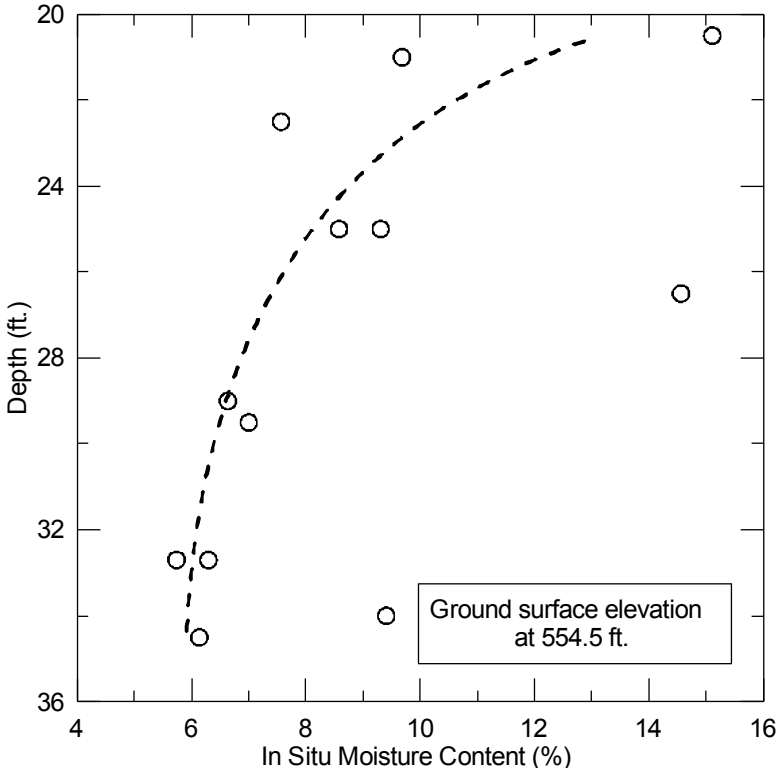

Figure C.5 In situ moisture content profile.

C.4.2 Triaxial Compression Test Results

Unconfined and confined triaxial compression tests were performed in accordance with ASTM D 7012. The peak deviator stress was used to calculate the undrained compressive strength for each test. The resulting undrained compressive strengths are shown in Table C.1.

C.4.3 Young's Modulus of Shale Specimen

Young's modulus was measured from results of triaxial tests in accordance to ASTM D 7012. In short, the modulus was calculated from the slope of the stress-strain relationships that correspond to 50% of mobilized undrained compressive strength. Figure C.6 shows the relationship between Young's modulus and undrained compressive strength for the shale cores tested from the FAI 80 site. This data was also used to develop a relationship between Young's modulus and shale natural water content (see Figure C.7). Table C.1 summarizes all of the data obtained from the laboratory testing and evaluation.

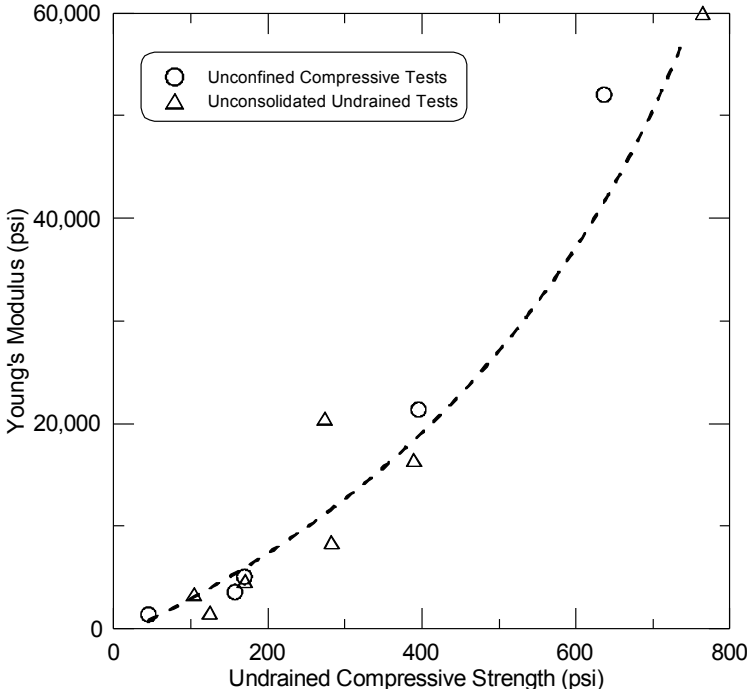

Figure C.6 Relationship between undrained compressive strength and Young's modulus.

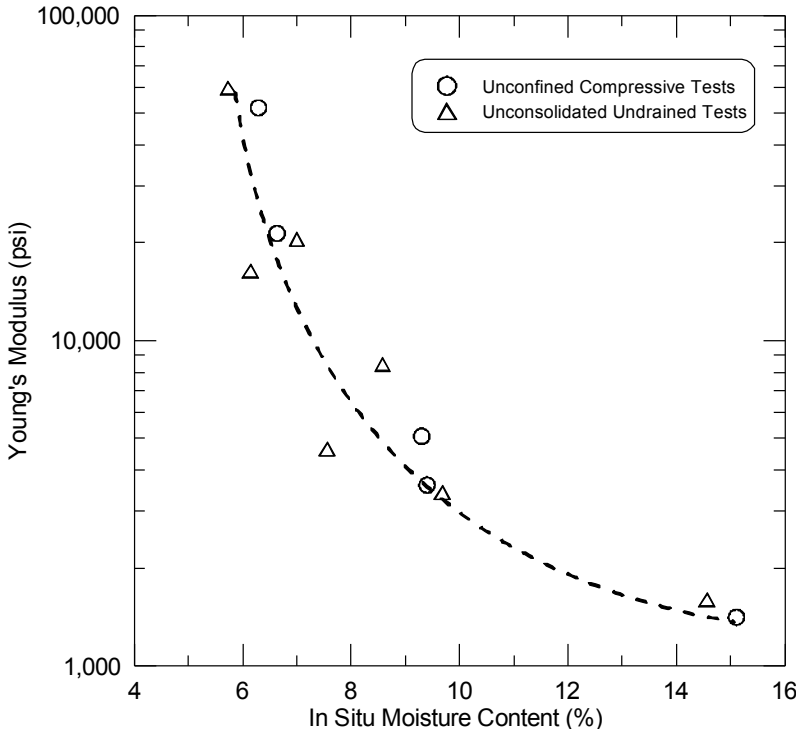

Figure C.7 Relationship between in situ moisture content and Young's modulus.

C.5 PRESSUREMETER TEST RESULTS

Wang Engineering performed three pressuremeter tests at FAI 80 over Aux Sable Creek. These tests were conducted in weathered shale and at depths of 21, 25, and 29 ft. The corrected curves for these three tests are shown in Figure C.8. Pressuremeter modulus and laboratory modulus values are compared in Chapter 4.

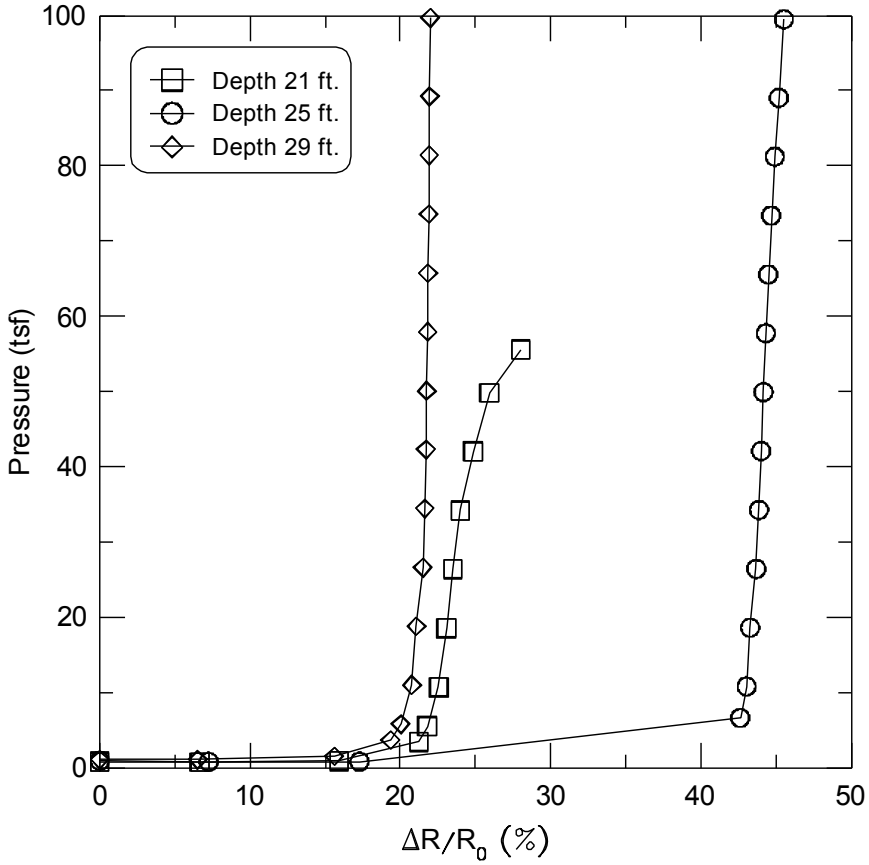

Figure C.8 Pressuremeter results at FAI 80 over Aux Sable Creek.

Table C.1 Laboratory Data Summary at the FAI 80 Over The Aux Sable Creek

Specimen Identification	**FAI 80-S1**	**FAI 80-S2**	**FAI 80-S3**
Core Run Number	**1**	**1**	**1**
Depth (ft.)	20.5	21	22.6
Initial Water Content (%)	15.1	9.7	7.6
Total Unit Weight (pcf)	135.9	144	148
Undrained Compressive Strength (ksf)	6.5 (UC)	15 (UU)	24.5 (UU)
Strain at Peak Strength (%)	3.8	3.3	3.6
Young's Modulus (ksf)	203.5	491	669
Recovery (%)	85	85	85
Rock Quality Designation (%)	61	61	61
Joint Average Vertical Spacing (in.)	4.5	4.5	4
Sample Description	SHALE, dark gray and calcareous	SHALE, dark gray and calcareous	SHALE, dark gray and calcareous

Specimen Identification	**FAI 80-S4**	**FAI 80-S5**	**FAI 80-S6**
Core Run Number	**1**	**1**	**2**
Depth (ft.)	25	25	26.5
Initial Water Content (%)	8.6	9.3	14.6
Total Unit Weight (pcf)	146.3	145	136.7
Undrained Compressive Strength (ksf)	40.7 (UU)	24.4 (UC)	18 (UU)
Strain at Peak Strength (%)	3.4	6.0	9
Young's Modulus (ksf)	1220.9	732.5	230
Recovery (%)	85	85	80
Rock Quality Designation (%)	61	61	77
Joint Average Vertical Spacing (in.)	5	5	5
Sample Description	SHALE, dark gray and calcareous	SHALE, dark gray and calcareous	SHALE, dark gray, laminated

Specimen Identification	FAI 80-S7	FAI 80-S8	FAI 80-S9
Core Run Number	**2**	**2**	**3**
Depth (ft.)	29	29.5	32.7
Initial Water Content (%)	6.6	7	6.2
Total Unit Weight (pcf)	150	149.2	150.6
Undrained Compressive Strength (ksf)	57 (UC)	34.25 (UU)	91.6 (UC)
Strain at Peak Strength (%)	2.5	1.6	1.7
Young's Modulus (ksf)	3078	2955	7495
Recovery (%)	80	80	100
Rock Quality Designation (%)	77	77	92
Joint Average Vertical Spacing (in.)	5	15	15
Sample Description	SHALE, dark gray, laminated	SHALE, dark gray, laminated	SHALE, dark gray, laminated

Specimen Identification	FAI 80-S10	FAI 80-S11	FAI 80-S12
Core Run Number	**3**	**3**	**3**
Depth (ft.)	32.7	34	34.5
Initial Water Content (%)	5.7	9.4	6.1
Total Unit Weight (pcf)	151.8	144.8	151
Undrained Compressive Strength (ksf)	110 (UU)	22.6 (UC)	56 (UU)
Strain at Peak Strength (%)	1.5	6.8	4.3
Young's Modulus (ksf)	8640	518	2367
Recovery (%)	100	100	100
Rock Quality Designation (%)	92	92	92
Joint Average Vertical Spacing (in.)	15	15	6
Sample Description	SHALE, dark gray, laminated	SHALE, dark gray, laminated	SHALE, dark gray, laminated

APPENDIX D FIELD EXPLORATION AT JOHN DEERE ROAD (IL 5) OVER IL 84

D.1 BACKGROUND

Figure D.1 shows location of John Deere Road over IL 84, located in Rock Island County, just east of city of Silvis, Illinois. This two-span bridge structure carries a four-lane highway over the IL 84 Route. South abutment of this bridge is supported on 3.5-ft-diameter drilled shaft foundations that are socketed into weak shale for 20 ft. The weak shale near south abutment was investigated during this study.

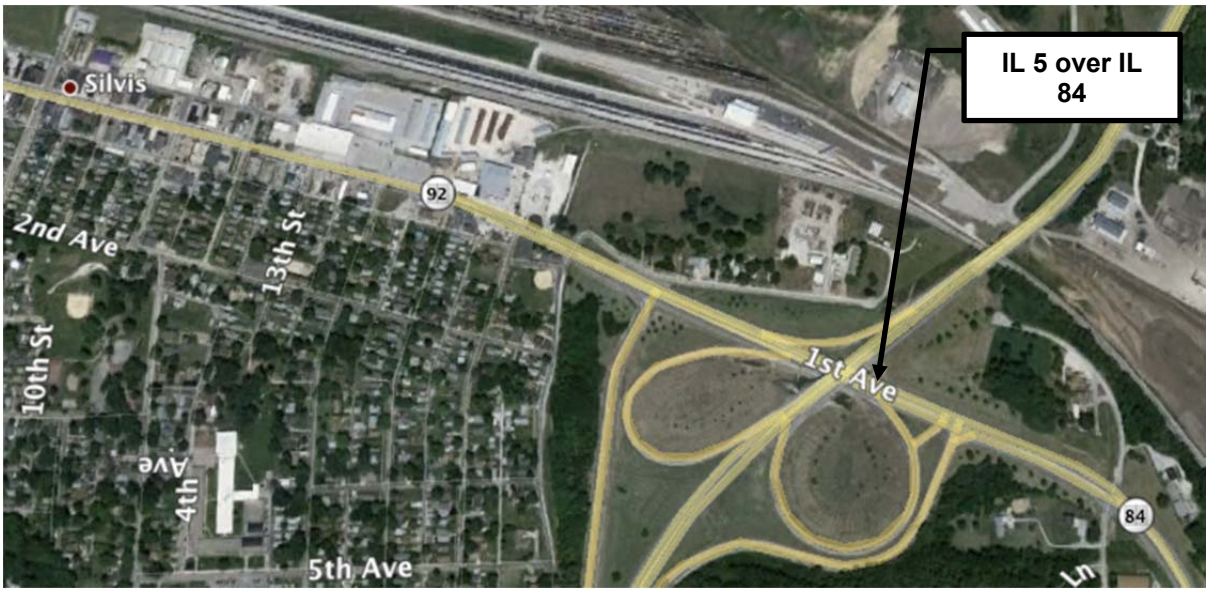

Figure D.1 Location of John Deere Road over IL 84.

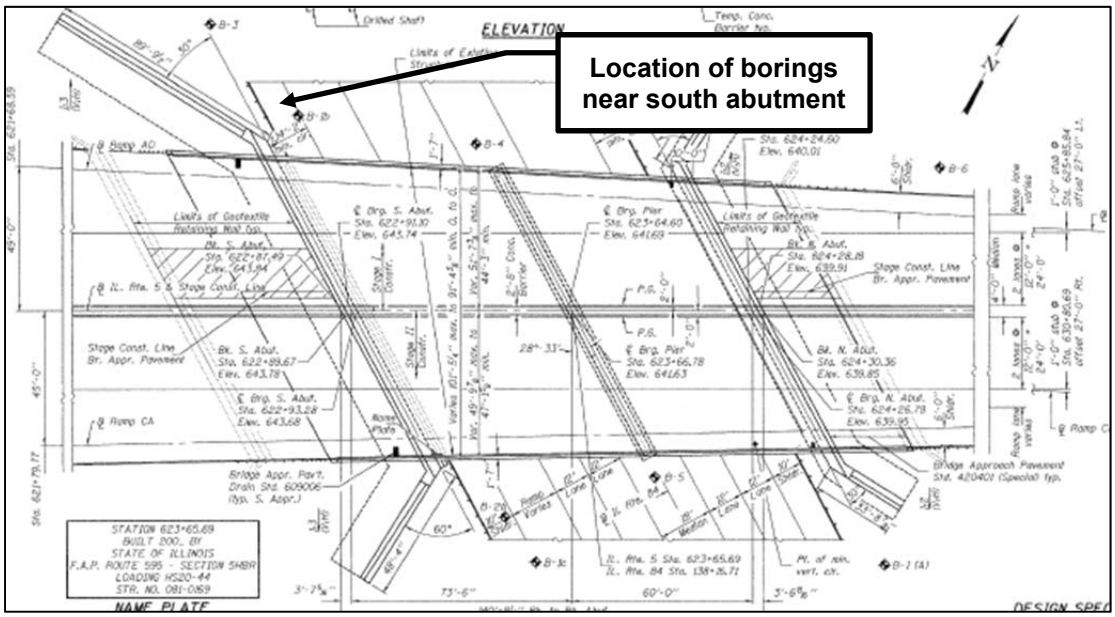

Figure D.2 Location of boring holes at IL 5 over IL 84 Route.

Figure D.2 shows a plan view of IL 5 over IL 84 bridge structure and the location of borings drilled on 5 December 2012 and 6 December 2012 by Wang Engineering crew and the UIUC research team. Two borings were advanced near south abutment and in close proximity to the drilled shaft load test performed in 2007. These borings were drilled to the elevation of 591 ft where a strong sandstone layer was encountered.

One of the two borings was used to obtain shale core samples and to perform pressuremeter tests. Initially rock cores were used for determination of recovery ratio, RQD of the rock mass, and vertical spacing of joints. Afterwards unconfined compression and triaxial compression tests were conducted on representative and comparable shale specimens to study effect of confining pressure on behavior of shale specimens subjected to compressive mode of shear. The in situ water content of the shale specimens used in the triaxial compression tests was also measured for correlation purposes. Triaxial test results were also used to determine the deformability characteristics of shale under undrained loading conditions.

The second boring was used to obtain MSPT blow counts at various depths. This data was used to develop a new correlation between undrained compressive strength of weak shale in Illinois and MSPT penetration rate.

The following sections discuss geology of the bridge site, MSPT test results, and laboratory test results

D.2 SITE GEOLOGY

The geology at the bridge site consists of 5.5 ft of hard, dark gray silt clay overlying sedimentary bedrock (e.g., shale and sandstone). The ground surface elevation at south abutment (i.e., the two borings) is about 620 ft. Hard and dark gray shale was exposed at an elevation of 614.5 ft. Laboratory test results are summarized in Table D.1.

D.3 MODIFED STANDARD PENETRATION TEST RESULTS

Figure D.3 shows the modified standard penetration test results obtained in one of the borings at IL 5 over IL 84.

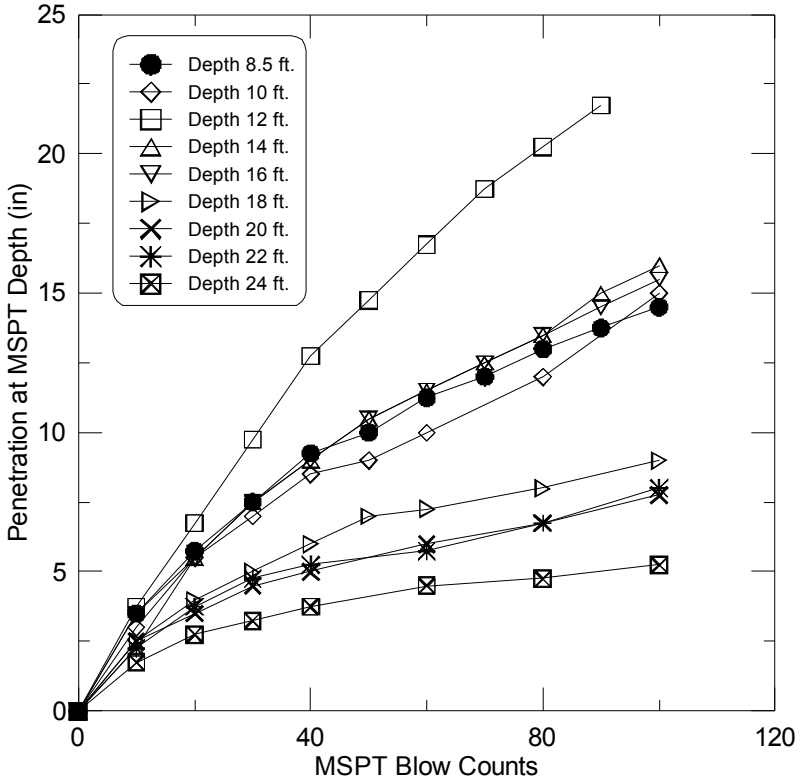

Figure D.3 Modified standard penetration test results.

D.4 LABORATORY TEST RESULTS

D.4.1 Moisture Content and Total Unit Weight

Figure D.4 shows the total unit weight profile at the IL 5 over IL 84 site. The total unit weight of shale was computed in accordance with ASTM D 7263.

Shale specimens from unconsolidated undrained and unconfined compressive tests were used for determination of in situ water content. The resulting water content profile is shown in Figure D.5. Water content of the shale was determined in accordance with ASTM D 2216.

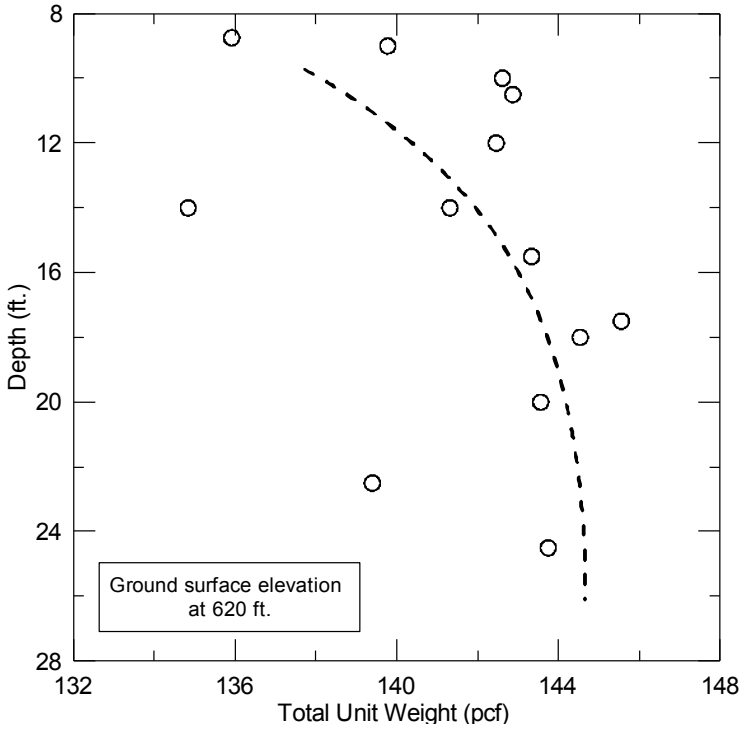

Figure D.4 Total unit weight profile.

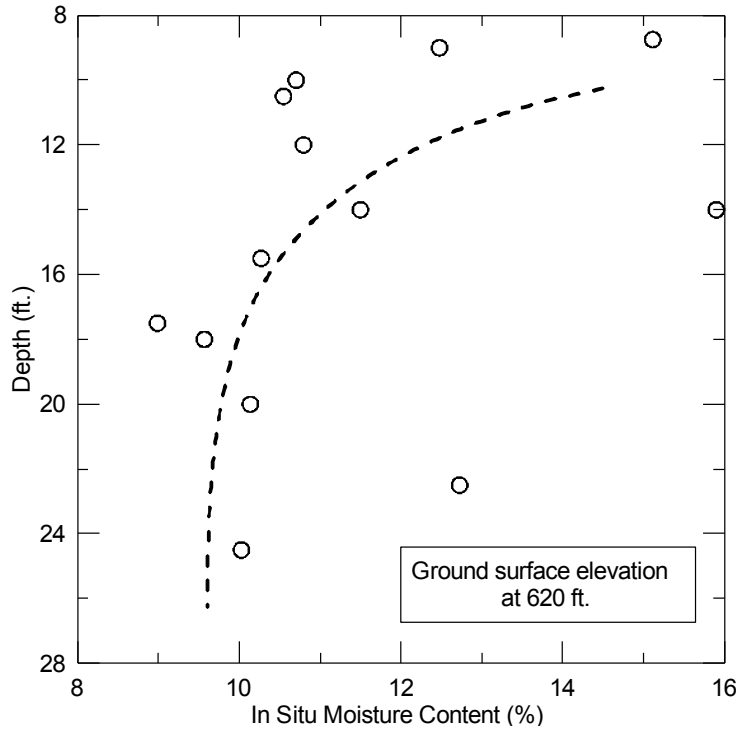

Figure D.5 In situ moisture content profile.

D.4.2 Triaxial Compression Test Results

Unconfined and confined triaxial compression tests were performed in accordance with ASTM D 7012. The peak deviator stress was used to calculate the undrained compressive strength for each test. The resulting undrained compressive strengths are shown in Table D.1.

D.4.3 Young's Modulus of Shale Specimen

Young's modulus was measured from results of triaxial tests in accordance to ASTM D 7012. In short, the modulus was calculated from the slope of the stress-strain relationships that correspond to 50% of mobilized undrained compressive strength. Figure D.6 shows the relationship between Young's modulus and undrained compressive strength for the shale core tested from the IL 5 over IL 84 site. This data was also used to develop a relationship between Young's modulus and shale natural water content (see Figure D.7). Table D.1 summarizes all of the data obtained from the laboratory testing and evaluation.

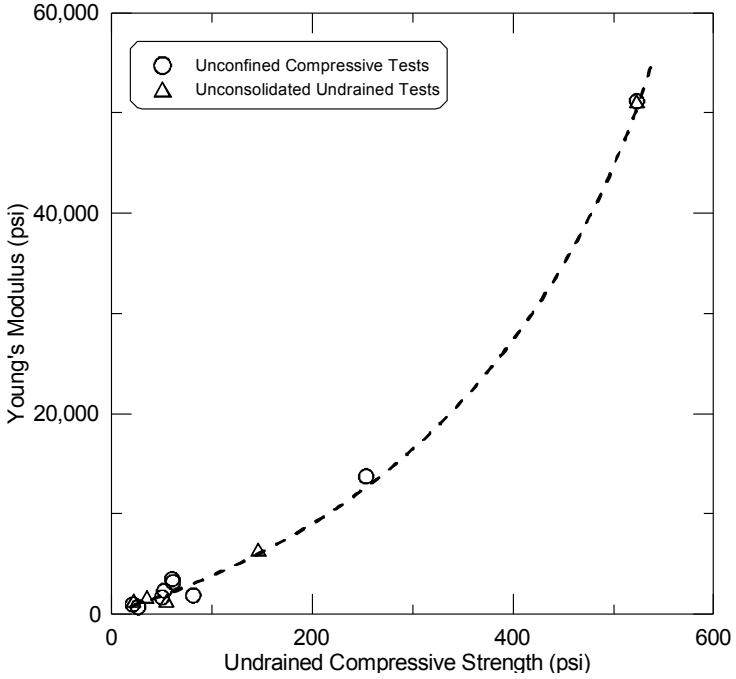

Figure D.6 Relationship between undrained compressive strength and Young's modulus.

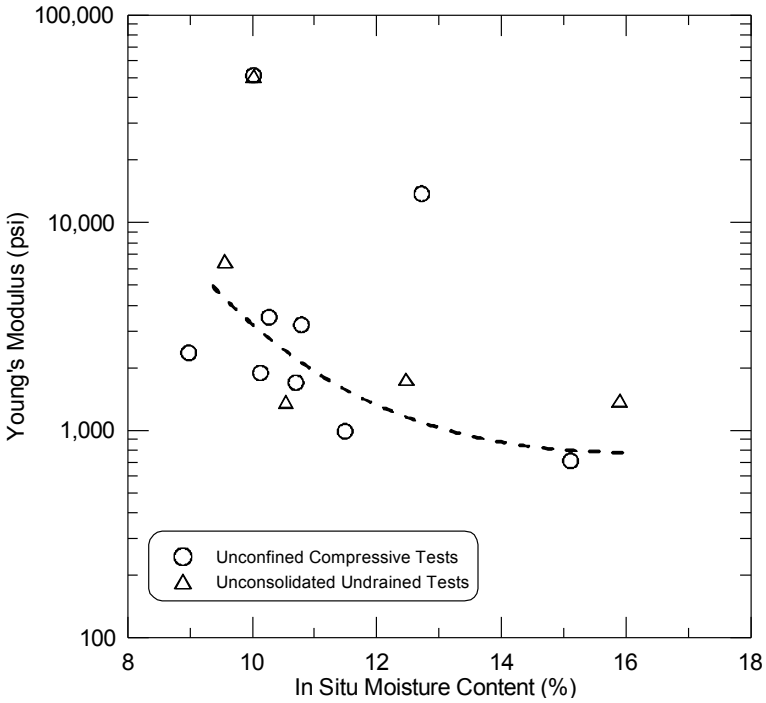

Figure D.7 Relationship between in situ moisture content and Young's modulus.

D.5 PRESSUREMETER TEST RESULTS

Wang Engineering performed three pressuremeter tests at IL 5 over IL 84 in Rock Island County. These tests were conducted in weathered shale and at depths of 13, 17, and 25 ft. The corrected curves for these three tests are shown in Figure D.8. Pressuremeter modulus and laboratory modulus values are compared in Chapter 4.

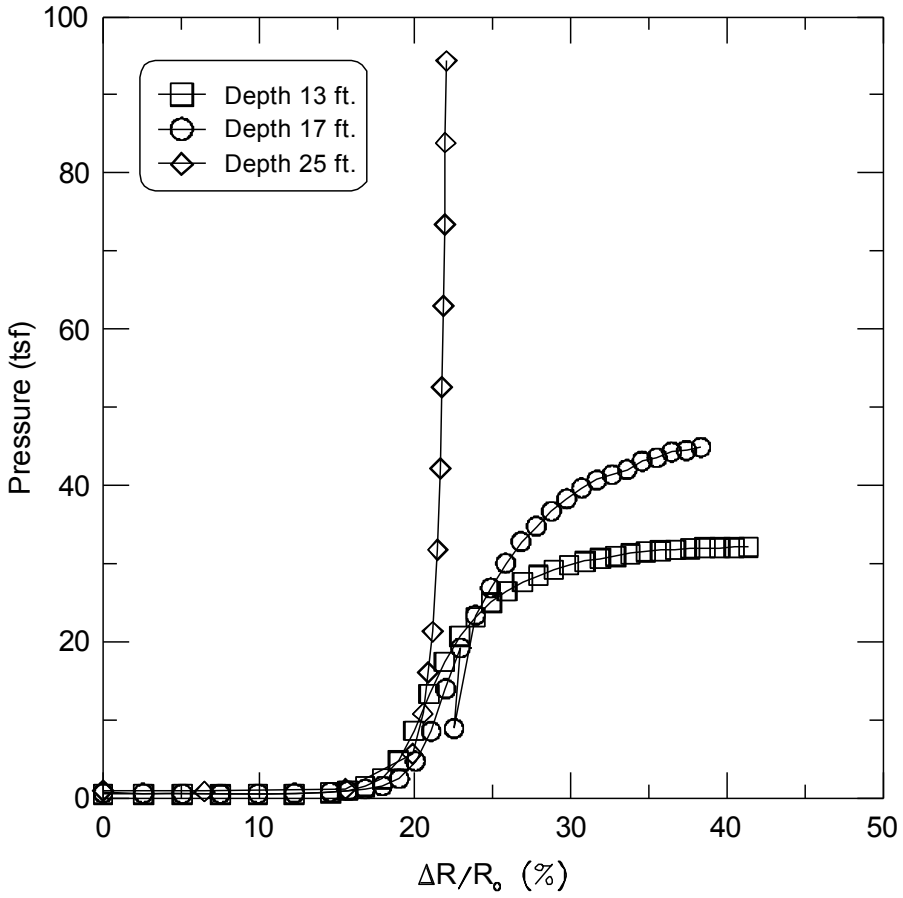

Figure D.8 Pressuremeter results at IL 5 over IL 84.

Table D.1 Laboratory Data Summary at the John Deere Road (IL 5) Over IL 84

Specimen Identification	**IL 5-S1**	**IL 5-S2**	**IL 5-S3**
Core Run Number	**1**	**1**	**1**
Depth (ft.)	8.75	9	10
Initial Water Content (%)	15.1	12.5	10.7
Total Unit Weight (pcf)	135.9	139.8	142.6
Undrained Compressive Strength (ksf)	3.8 (UC)	5 (UU)	7.2 (UC)
Strain at Peak Strength (%)	5.3	3.5	3.4
Young's Modulus (ksf)	102.6	254	244
Recovery (%)	90	90	90
Rock Quality Designation (%)	78	78	78
Joint Average Vertical Spacing (in.)	3 to 20	3 to 20	3 to 20
Sample Description	SHALE, weathered, dark gray	SHALE, weathered, dark gray	SHALE, weathered, dark gray

Specimen Identification	**IL 5-S4**	**IL 5-S5**	**IL 5-S6**
Core Run Number	**1**	**1**	**2**
Depth (ft.)	10.5	12	14
Initial Water Content (%)	10.5	10.8	16
Total Unit Weight (pcf)	143	142.5	134.8
Undrained Compressive Strength (ksf)	8 (UU)	8.8 (UC)	3.1 (UU)
Strain at Peak Strength (%)	3.6	2.9	2.9
Young's Modulus (ksf)	198	463	201
Recovery (%)	90	90	95
Rock Quality Designation (%)	78	78	95
Joint Average Vertical Spacing (in.)	20	20	10
Sample Description	SHALE, weathered, dark gray	SHALE, weathered, dark gray	SHALE, weathered, dark gray

Specimen Identification	IL 5-S7	IL 5-S8	IL 5-S9
Core Run Number	**2**	**2**	**3**
Depth (ft.)	14	15.5	17.5
Initial Water Content (%)	11.5	10.2	8.9
Total Unit Weight (pcf)	141.3	143.3	145.5
Undrained Compressive Strength (ksf)	3 (UC)	8.7 (UC)	7.5 (UC)
Strain at Peak Strength (%)	2.5	1.8	2.2
Young's Modulus (ksf)	142.5	504	339.4
Recovery (%)	95	95	100
Rock Quality Designation (%)	95	95	81
Joint Average Vertical Spacing (in.)	10	10	4 to 7
Sample Description	SHALE, weathered, dark gray	SHALE, weathered, dark gray	SHALE, weathered, dark gray

Specimen Identification	IL 5-S10	IL 5-S11	IL 5-S12
Core Run Number	**3**	**3**	**4**
Depth (ft.)	18	20	22.5
Initial Water Content (%)	9.5	10.1	12.7
Total Unit Weight (pcf)	144.5	143.5	139.4
Undrained Compressive Strength (ksf)	21 (UU)	11.7 (UC)	36.5 (UC)
Strain at Peak Strength (%)	3.1	4.8	2.6
Young's Modulus (ksf)	938	271.7	1981.6
Recovery (%)	100	100	98
Rock Quality Designation (%)	81	81	70
Joint Average Vertical Spacing (in.)	4 to 20	4 to 20	1 to 6
Sample Description	SHALE, weathered, dark gray	SHALE, weathered, dark gray	SHALE, weathered, dark gray

Specimen Identification	IL 5-S13
Core Run Number	4
Depth (ft.)	24.5
Initial Water Content (%)	10
Total Unit Weight (pcf)	143.5
Undrained Compressive Strength (ksf)	75 (UC)
Strain at Peak Strength (%)	1.5
Young's Modulus (ksf)	7369
Recovery (%)	98
Rock Quality Designation (%)	70
Joint Average Vertical Spacing (in.)	1 to 6
Sample Description	SHALE, weathered, dark gray

APPENDIX E FIELD EXPLORATION AT ILLINOIS RIVER BRIDGE REPLACEMENT (FAU 6265)

E.1 BACKGROUND

Figure E.1 shows location of FAU 6265 site, located in LaSalle County, just south of city of Marseilles, Illinois. This eight-span bridge structure carries two-lane highway over the Illinois River. A drilled shaft load test was performed on Pier #2 on the south side of the river when the bridge was constructed in 1996. Pier # 2 is supported on 6-ft-diameter drilled shaft foundations that are socketed into weak shale, mudstone, and siltstone for 57 ft. The weak shale near Pier # 2 was investigated during this study.

Figure E.1 Location of FAU 6265 near city of Marseilles.

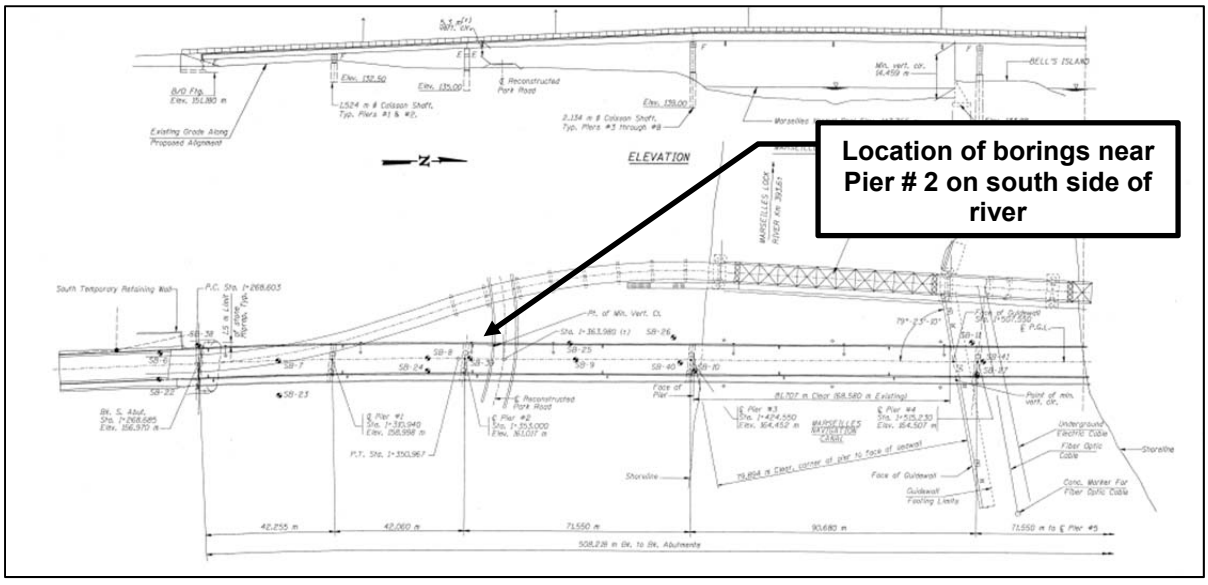

Figure E.2 Location of boring holes at FAU 6265.

Figure E.2 shows a plan view of FAU 6265 bridge structure and the location of borings drilled on 7 December 2012 and 10 December 2012 by Wang Engineering crew and the UIUC research team. Two borings were advanced near Pier # 2 on the south side of river and in close proximity to the drilled shaft load test performed in 1996. These borings were drilled to the elevation of 443 ft.

One of the two borings was used to obtain shale core samples and to perform pressuremeter tests. Initially rock cores were used for determination of recovery ratio, RQD of the rock mass, and vertical spacing of joints. Afterwards unconfined compression and triaxial compression tests were conducted on representative and comparable shale specimens to study effect of confining pressure on behavior of shale specimens subjected to compressive mode of shear. The in situ water content of the shale specimens used in the triaxial compression tests was also measured for correlation purposes. Triaxial test results were also used to determine the deformability characteristics of shale under undrained loading conditions.

The second boring was used to obtain MSPT blow counts at various depths. This data was used to develop a new correlation between undrained compressive strength of weak shale in Illinois and MSPT penetration rate.

The following sections discuss geology of the bridge site, MSPT test results, and laboratory test results.

E.2 SITE GEOLOGY

The geology at the bridge site consists of 10 ft of sandy to clayey loam overlying sedimentary bedrock (e.g., shale, mudstone, and siltstone). The ground surface elevation at Pier # 2 (i.e., the two borings) is about 503 ft. Weathered gray to black shale was exposed at an elevation of 493 ft. Sandstone layer was exposed at elevation of 467.0 ft and extended to elevation of 443.0 ft where drilling was terminated. Laboratory test results are summarized in Table E.1.

E.3 MODIFIED STANDARD PENETRATION TEST RESULTS

Figure E.3 shows the modified standard penetration test results obtained in one of the borings at FAU 6265 for the weathered shale layer.

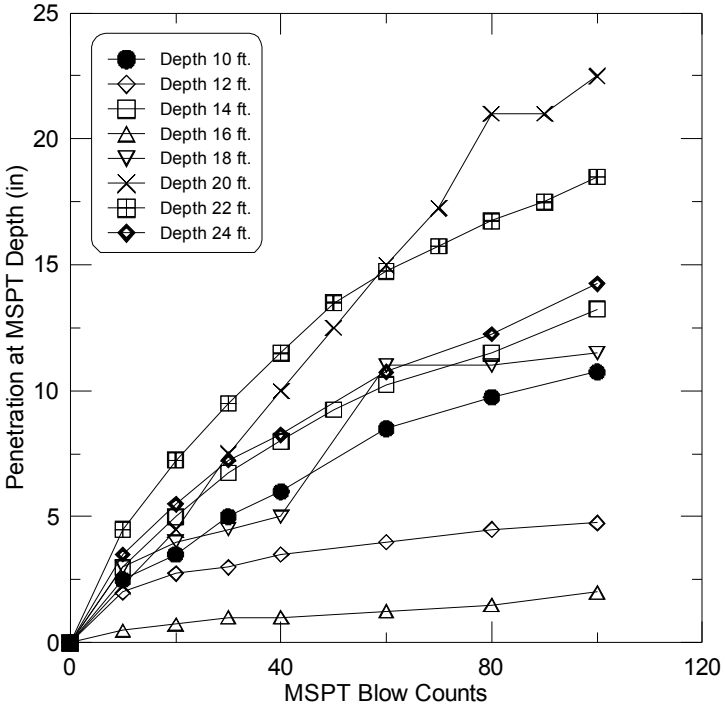

Figure E.3 Modified standard penetration test results.

E.4 LABORATORY TEST RESULTS

E.4.1 Moisture Content and Total Unit Weight

Figure E.4 shows the total unit weight profile at the FAU 6265 site. The total unit weight of shale was computed in accordance with ASTM D 7263.

Shale specimens from unconsolidated undrained and unconfined compressive tests were used for determination of in situ water content. The resulting water content profile is shown in Figure E.5. Water content of the shale was determined in accordance with ASTM D 2216.

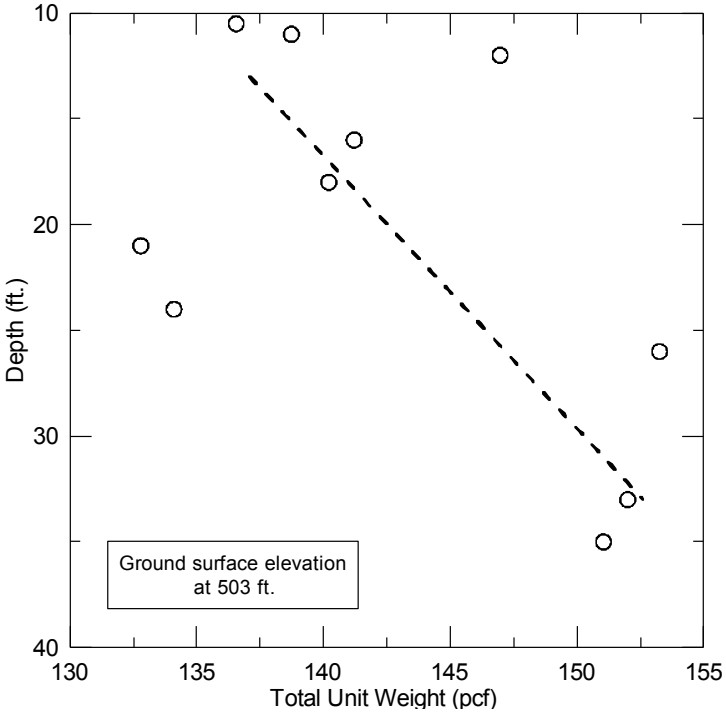

Figure E.4 Total unit weight profile.

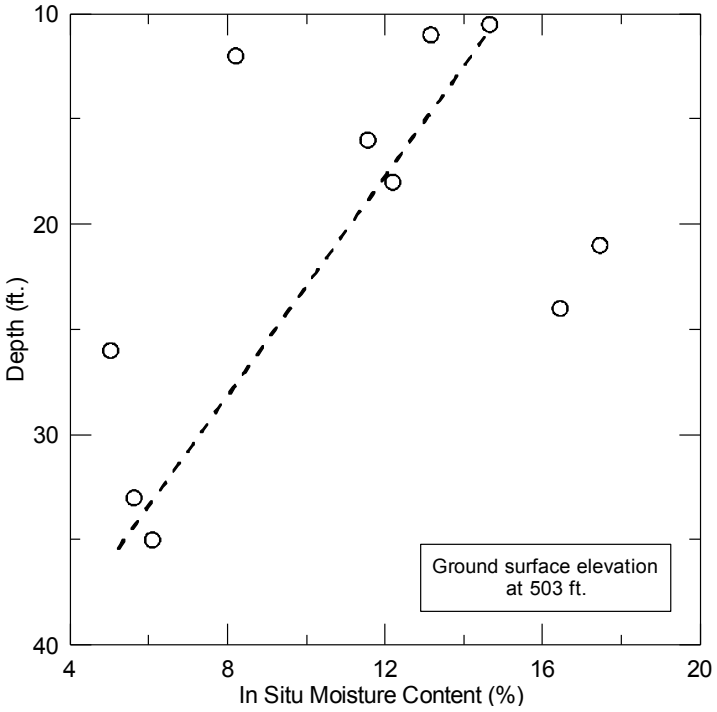

Figure E.5 In situ moisture content profile.

E.4.2 Triaxial Compression Test Results

Unconfined and confined triaxial compression tests were performed in accordance with ASTM D 7012. The peak deviator stress was used to calculate the undrained compressive strength for each test. The resulting undrained compressive strengths are shown in Table E.1.

E.4.3 Young's Modulus of Shale Specimen

Young's modulus was measured from results of triaxial tests in accordance to ASTM D 7012. In short, the modulus was calculated from the slope of the stress-strain relationships that correspond to 50% of mobilized undrained compressive strength. Figure E.6 shows the relationship between Young's modulus and undrained compressive strength for the shale core tested from the FAU 6265 site. This data was also used to develop a relationship between Young's modulus and shale natural water content (see Figure E.7). Table E.1 summarizes all of the data obtained from the laboratory testing and evaluation.

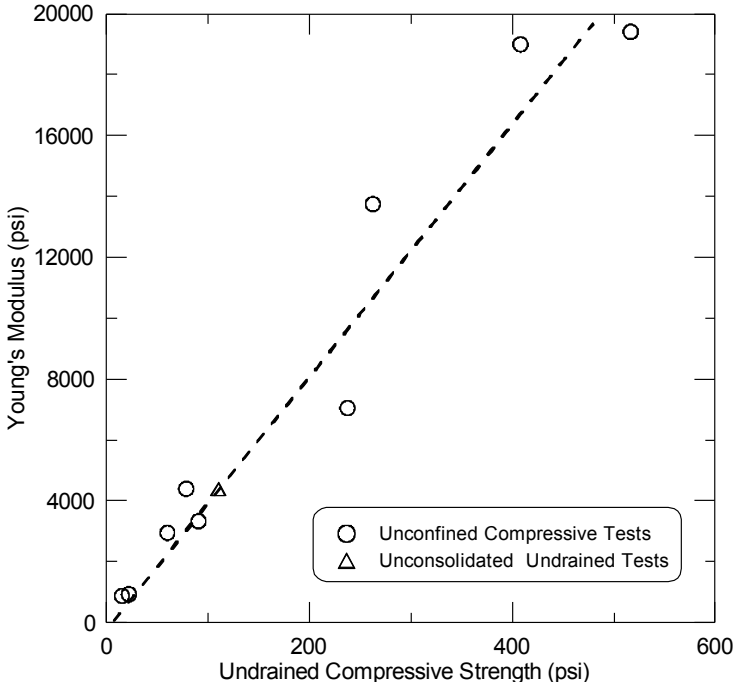

Figure E.6 Relationship between undrained compressive strength and Young's modulus.

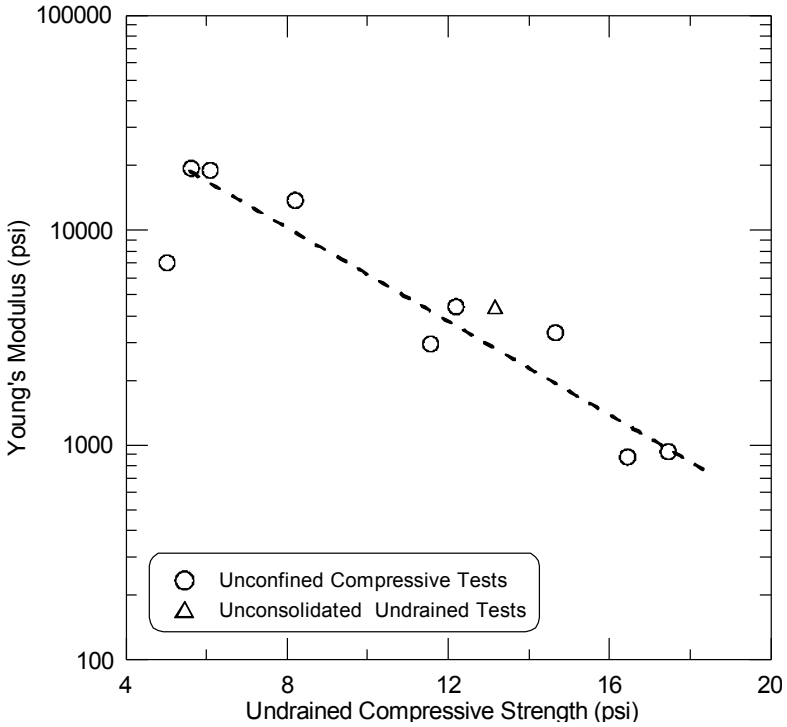

Figure E.7 Relationship between in situ moisture content and Young's modulus.

E.5 PRESSUREMETER TEST RESULTS

Wang Engineering performed two pressuremeter tests at FAU 6265 near Pier # 2 on the south side of Illinois River. These tests were conducted in weathered shale and at depths of 21 and 27.5 ft. The corrected curves for these two tests are shown in Figure E.8. Pressuremeter modulus and laboratory modulus values are compared in Chapter 4.

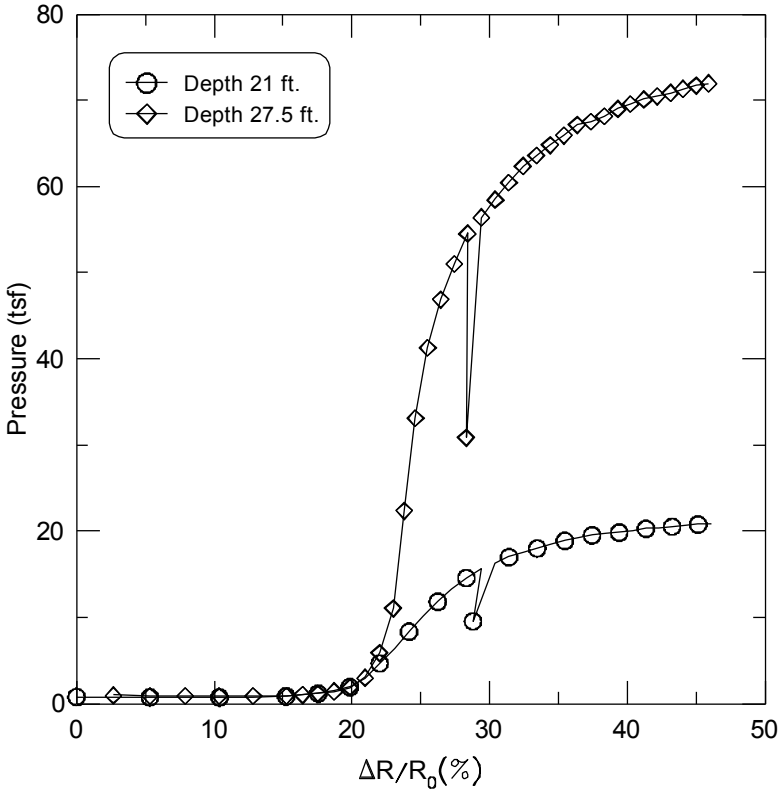

Figure E.8 Pressuremeter results at FAU 6265.

Table E.1 Laboratory Data Summary at the Illinois River Bridge Replacement (FAU 6265)

Specimen Identification	**FAU 6265-S1**	**FAU 6265-S2**	**FAU 6265-S3**
Core Run Number	**1**	**1**	**1**
Depth (ft.)	10.5	11	12
Initial Water Content (%)	14.7	13.2	8.2
Total Unit Weight (pcf)	136.6	138.7	147
Undrained Compressive Strength (ksf)	13 (UC)	16 (UU)	37.8 (UC)
Strain at Peak Strength (%)	3.0	3.5	2.0
Young's Modulus (ksf)	480	631.4	1980
Recovery (%)	82	82	82
Rock Quality Designation (%)	58	58	58
Joint Average Vertical Spacing (in.)	3 to 10	3 to 10	3 to 10
Sample Description	SHALE, weathered, dark gray	SHALE, weathered, dark gray	SHALE, weathered, dark gray

Specimen Identification	**FAU 6265-S4**	**FAU 6265-S5**	**FAU 6265-S6**
Core Run Number	**2**	**2**	**3**
Depth (ft.)	16	18	21
Initial Water Content (%)	11.6	12.2	17.5
Total Unit Weight (pcf)	141.2	140	132.0
Undrained Compressive Strength (ksf)	8.6 (UC)	11.3 (UC)	3.2 (UC)
Strain at Peak Strength (%)	3.4	2.4	2.6
Young's Modulus (ksf)	425	633.6	134
Recovery (%)	100	100	65
Rock Quality Designation (%)	75	75	65
Joint Average Vertical Spacing (in.)	2.5 to 10	2.5 to 10	2.5 to 10
Sample Description	SHALE with inclusions of mudstone, weathered, dark gray	SHALE with inclusions of mudstone, weathered, dark gray	SHALE with inclusions of mudstone, weathered, dark gray

Specimen Identification	FAU 6265-S7	FAU 6265-S8	FAU 6265-S9
Core Run Number	**3**	**4**	**5**
Depth (ft.)	24	26	33
Initial Water Content (%)	16.5	5	5.6
Total Unit Weight (pcf)	134	153	152
Undrained Compressive Strength (ksf)	2.1 (UC)	34 (UC)	74 (UC)
Strain at Peak Strength (%)	3.1	3.4	3.2
Young's Modulus (ksf)	127	1015	2795
Recovery (%)	65	100	96
Rock Quality Designation (%)	65	79	96
Joint Average Vertical Spacing (in.)	3 to 7	3 to 7	3 to 7
Sample Description	SHALE with inclusions of mudstone, weathered, dark gray	SHALE with inclusions of mudstone, weathered, dark gray	SHALE, dark gray

Specimen Identification	FAU 6265-S10	FAU 6265-S11	FAU 6265-S12
Core Run Number	**5**	**6**	**7**
Depth (ft.)	35	40	45
Initial Water Content (%)	6.1	6.0	6.75
Total Unit Weight (pcf)	151	156	158.5
Undrained Compressive Strength (ksf)	58.8 (UC)	200 (UC)	301 (UC)
Strain at Peak Strength (%)	3.1	2.7	3.0
Young's Modulus (ksf)	2736	41234	56752.5
Recovery (%)	96	100	100
Rock Quality Designation (%)	96	90	82
Joint Average Vertical Spacing (in.)	3 to 7	20	20
Sample Description	SHALE, dark gray	Greenish gray sandstone	Greenish gray sandstone

Specimen Identification	FAU 6265-S13	FAU 6265-S14
Core Run Number	**8**	**9**
Depth (ft)	50	55
Initial Water Content (%)	5.5	5.5
Total Unit Weight (pcf)	155	153
Undrained Compressive Strength (ksf)	188 (UC)	205 (UC)
Strain at Peak Strength (%)	3.3	3.9
Young's Modulus (ksf)	40879	39076
Recovery (%)	99	99
Rock Quality Designation (%)	99	85
Joint Average Vertical Spacing (in.)	15	12.5
Sample Description	Greenish gray sandstone	Greenish gray sandstone

APPENDIX F MODIFIED STANDARD PENETRATION TEST FOR WEAK COHESIVE ROCKS

F.1 INTRODUCTION

The standard penetration test (SPT) is widely used by practicing engineers for assessment of in situ properties of granular materials for design of deep foundations because it is easy to perform and widely available, and test results are easy to interpret. The use of SPT blow counts for deep-foundation design in cohesive material is not widespread. However, use of this test method is expected to reduce design time and costs by reducing or eliminating soil or rock sampling and laboratory triaxial compression testing. The SPT requires 18 in. of penetration but only the blow counts associated with the last 12 in. of penetration are used to calculate the blows per foot because they are considered trepresentative of the in situ geomaterials and used for design. Because weak rocks are significantly stronger than soils, the SPT is advantageous for sites where the weak rock or shale is highly weathered or fractured, so sufficient penetration is achieved for a reasonable number of blow counts. The SPT is also advantageous in these materials because it is difficult to obtain high-quality rock cores for laboratory triaxial compression tests due to the weathered and fractured nature of the material.

Previous investigators (e.g., Stroud 1974; Terzaghi et al. 1996; Abu-Hejleh 2003) have attempted to develop correlations between SPT blow counts of weak rocks or stiff clays and undrained compressive strength for drilled shaft design. Available SPT data in weak rocks (e.g., Abu-Hejleh et al. 2003; Stark et al. 2013) show that 18 in. of penetration is often not achieved or is difficult to achieve in weak cohesive sedimentary rocks. For example, SPT data developed herein shows that penetration is often less than 8 to 10 in. for 100 blows using an automatic trip hammer (60% to 70% of theoretical energy). Interpretation of test results for weak rocks, however, is difficult and requires engineering judgment because 12 in. of penetration is often not obtained in weak rocks.

To eliminate the difficulties in interpretation of results of standard penetration tests in weak rocks, the SPT procedure was modified herein to eliminate the need for obtaining 18 in. of penetration while achieving sufficient data for drilled shaft design.

F.2 EXISTING DESIGN PROCEDURES

Stroud (1974) and Terzaghi et al. (1996) indicate that values of blow count (blows for final 12 in. of penetration) in an SPT on saturated insensitive cohesive material are related to undrained compressive strength. As a result, some relationships between undrained compressive strength and SPT blow count have been developed; these design procedures are briefly reviewed before the modified SPT (MSPT) is described.

F.2.1 Stroud (1974)

Stroud (1974) presents SPT results obtained from some 70 boreholes at 18 sites in the London area, where standard penetration tests were performed at frequent depth intervals. The maximum depth of the 70 boreholes is 50 m. Stroud (1974) concludes that SPT blow counts, N-values, and results of undrained triaxial compression tests on 102 mm specimens of London stiff and fissured clays are related.

F.2.2 Terzaghi et al. (1996)

Terzaghi et al. (1996) summarize ratios of S_u to N_{60} for a variety of clays and weak rocks, including 31 sites in London clay. N_{60} is defined as the blow count corresponding to

60% of the theoretical maximum energy applied by a 140-lb weight falling 30 in. to drive a split-spoon sampler the last 12 in. Terzaghi et al. (1996) conclude that as the stiff clay becomes stiffer or harder, the weakening effect of fissures becomes more significant on values of S_u than values of N_{60}. They also conclude that the ratio of S_u to N_{60} is independent of fissure spacing up to at least 200 mm.

F.2.3 Abu-Hejleh et al. (2003)

Abu-Hejleh et al. (2003) conducted standard penetration tests on soil-like claystone bedrock and proposed a correlation between SPT blow counts and unconfined compressive strength, q_u. The proposed correlation is based on only four SPT results from two sites in Colorado:

$$q_u = 0.24 * N$$

where

q_u = unconfined compressive strength, ksf

N = standard penetration blow counts, blows per foot (bpf)

The unconfined compressive strength of the weak rocks tested by Abu-Hejleh et al. (2003) are all less than 18 ksf. An attempt was made to conduct standard penetration tests on hard sandy claystones, but 18 in. of penetration was not obtained in any of the tests. Therefore, this empirical correlation cannot be applied to intermediate geologic material with q_u greater than 18 ksf, such as Illinois shales. During the subsurface investigations conducted herein, obtaining 18 in. of penetration in Illinois shales was difficult to impossible. As a result, a new SPT procedure is presented below to correlate penetration rate to unconfined compressive strength of Illinois shales at IDOT bridge sites.

F.3 SHORTCOMINGS OF STANDARD PENETRATION TEST

Standard penetration test procedure (ASTM D 1586) requires 18 in. of penetration of a 2-in. outside and 1-3/8-in. inside diameter split-spoon sampler in soil or rock. Blow counts for the final 12 in. of penetration are designated as an SPT N-value of blow count and are commonly used to infer in situ shear strength of the soil. Blow counts are mainly used for soil strength characterization because of the difficulties of obtaining 12 in. of penetration in weak rock. Some of the other shortcomings of standard penetration tests in weak rocks are as follows:

- Standard penetration tests reported in literature (e.g., Abu-Hejleh et al. 2003) and SPT tests performed by authors in weak cohesive sedimentary rocks show 18 in. of penetration is difficult to impossible to obtain.
- SPT penetrations are commonly less than 10 in. for a total of 100 blows using an automatic trip hammer.
- Interpretation of SPT results in weak rocks involves engineering judgment and uncertainty because 18 in. of penetration is not often obtained and extrapolation of test data is required.
- Most drillers do not like to apply more than 100 blows because of time and equipment constraints, so development of a procedure that obtains a useful penetration rate after 100 blows regardless of penetration distance was sought herein.

F.4 MODIFIED STANDARD PENETRATION TEST (MSPT)

The standard penetration test (SPT) was modified herein to improve its performance and test results in weak cohesive sedimentary rocks. Penetration rate ($\dot{N}$) is measured in this test instead of or in addition to N and is correlated to unconfined compressive strength of weak rock. In short, penetration rate ($\dot{N}$) is the inverse of the slope of the penetration versus blow count data plot, which is discussed in detail below. As shown later in Figure F.2, this slope varies during the initial portion of the test due to changes in rock strength and stiffness during the test and then becomes approximately constant. The improvements in the SPT, new test procedure, and new analysis procedure are discussed below. The new test procedure is called the modified standard penetration test (MSPT), and it is anticipated that the new procedure will be submitted to ASTM for balloting and possible acceptance.

F.4.1 Improvements and Advantages

The MSPT is based on penetration rate ($\dot{N}$) and eliminates the shortcomings of the conventional standard penetration test (ASTM D 1586) in weak rocks and problems associated with obtaining 18 in. of penetration. Test results indicate that penetration rate ($\dot{N}$) becomes a constant after 4 to 5 in. of penetration. With this new test procedure, 18 in. of penetration is no longer required for successful completion of the test. Modified standard penetration tests performed at five IDOT sites investigated herein show penetration rate ($\dot{N}$) is related to unconfined compressive strength of weak cohesive rocks.

F.4.2 MSPT Procedure

The new test procedure is outlined below and is subsequently used to develop a correlation between MSPT penetration rate ($\dot{N}$) and unconfined compressive strength of weak shales in the state of Illinois.

1. Drill to the desired depth of the MSPT. Insert the MSPT sampler and necessary drill rod.
2. Measure the initial length of the rod segment between the top of borehole and the top of rod, L (see Figure F.1).
3. Apply 10 blows to the top of the drill rod using the 140-lb hammer falling 30 in. and then stop the test.
4. Measure the new length of rod segment between the top of borehole and the top of rod.
5. Subtract the rod length in Step 3 from the rod length in Step 2 to obtain amount of penetration that was obtained for the first 10 blows. Repeat Steps 1 through 4 to obtain penetration distances for 20, 30, 40, 50, 60, 70, 80, 90, and 100 blows. Table F.1 is a sample data sheet that can be used to record the penetrations and MSPT blow counts at each desired MSPT depth.
6. If the penetration distance is not changing substantially after 40 blows have been applied to the drill rod, the number of blows per penetration measurement can be increased to 20 to accelerate the test, which results in the following blows being applied: 10, 10, 10, 10, 20, 20, 20 for a total of 100 blows.

7. Plot the penetration distances versus the associated blow counts as is shown in Figure F.2.

Once a plot of MSPT penetration versus blow counts is constructed at each desired depth, the proposed analysis procedure presented in Section F.4.3 of this appendix can be used to interpret the test results.

Figure F.1 MSPT procedure.

Table F.1 MSPT Data Sheet

MSPT Depth									
Initial Exposed Rod Length from Ground Surface to Top of Rod (in.)									
Blow Counts	**Exposed Rod Length (in.)**								
10									
20									
30									
40									
50									
60									
70									
80									
90									
100									

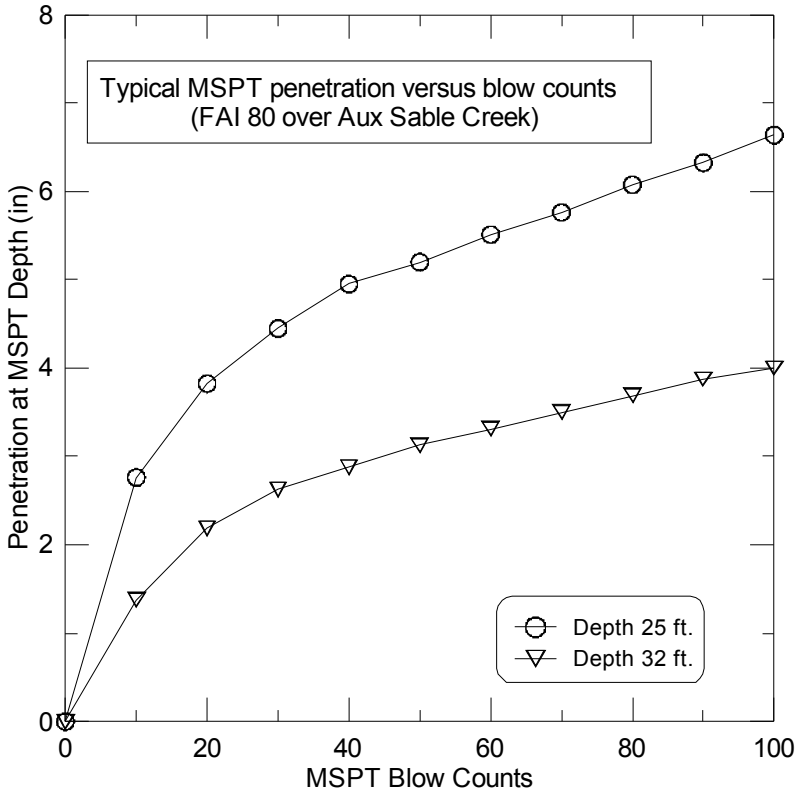

Figure F.2 MSPT penetration versus blow count relationship.

F.4.3 MSPT Analysis Procedure

The MSPT utilizes the concept of penetration rate ($\dot{N}$) to estimate the unconfined compressive strength of weak cohesive rocks (e.g., shales). The step-by-step procedure for determining the penetration rate ($\dot{N}$) from the plot of penetration versus MSPT blow counts (Figure F.2) is as follows:

1. Follow the procedures outlined in Section F.4.2 to construct the penetration versus MSPT blow counts graph (Figure F.2).
2. Find the linear portion of penetration versus MSPT blow count relationship after the initial portion of the relationship—that is, 4 to 5 in. of penetration, where the resistance is variable due to disturbance, loose material in the boring, and reduced confining pressure (Figure F.3),
3. Draw a tangent line to this linear portion of penetration versus MSPT blow count relationship to determine the slope of the less disturbed portion of the relationship (Figure F.3).
4. The inverse of the slope obtained in Step 3 is the penetration rate ($\dot{N}$) and is defined as the following:

$$\dot{N} = \frac{1}{\frac{\Delta \text{Penetration Distance}}{\Delta \text{MSPT Blowcount per foot}}}$$

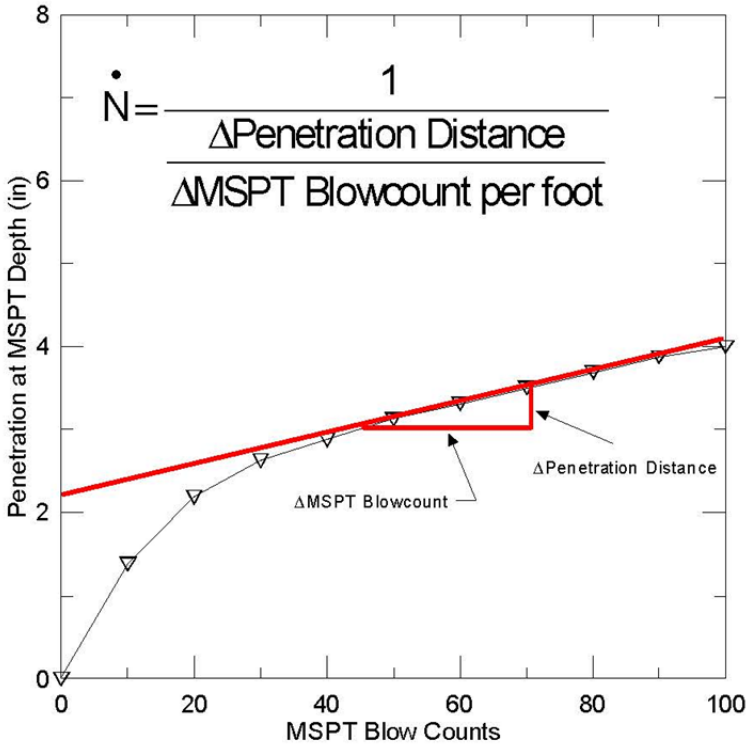

Figure F.3 Graphical method for determining penetration rate.

F.5 PROPOSED CORRELATION BETWEEN PENETRATION RATE AND UNCONFINED COMPRESSIVE STRENGTH FOR WEAK COHESIVE ROCKS

For this study, five IDOT bridge sites where bridge piers or abutments are supported on drilled shaft foundations were investigated. These drilled shafts were partially socketed in weak shales. Modified standard penetration tests (MSPTs) were performed at various depths in weathered shales in accordance with Section F.4.2 of this report. Test results are presented in Appendices A through E. MSPT results were analyzed in accordance with Section F.4.3 to determine MSPT penetration rates ($\dot{N}$). Resulting penetration rates and unconfined compressive strengths at each depth are shown in Table F.2. Unconfined compressive strength versus MSPT penetration rates ($\dot{N}$) are plotted in Figure F.4 along with the line of best fit to the observed trend. This correlation is expected to significantly reduce the amount of rock coring in the field and laboratory triaxial compression tests required for characterization of weak shales for drilled shaft design in Illinois.

Table F.2 Data from Modified Standard Penetration
Tests Conducted at Five IDOT Bridge Sites

Site	Depth of MSPT (ft)	Geomaterial Type	MSPT Penetration Rate (bpf)	Unconfined Compressive Strength (ksf)
IL 23 over Short Point Creek	27	Shale	78.4	15.9
IL 23 over Short Point Creek	32	Shale	153.7	6.33
IL 23 over Short Point Creek	47	Shale	443	31.3
US 24 over Lamoine River	36	Shale	693	66.4
US 24 over Lamoine River	41	Shale	712	42
US 24 over Lamoine River	46.5	Shale	589	33
FAI 80 over Aux Sable Creek	25	Shale	461	24.4
FAI 80 over Aux Sable Creek	29.5	Shale	689	57
John Deere Road (IL 5) over IL 84	10	Shale	106.7	7.2
John Deere Road (IL 5) over IL 84	12	Shale	53	8.8
John Deere Road (IL 5) over IL 84	16	Shale	109.6	8.7
John Deere Road (IL 5) over IL 84	20	Shale	267	11.7
John Deere Road (IL 5) over IL 84	22	Shale	223	36.5
John Deere Road (IL 5) over IL 84	24	Shale	387	75
Illinois River Bridge Replacement (FAU 6265)	10.5	Shale	176	13
Illinois River Bridge Replacement (FAU 6265)	12	Shale	585	37.8
Illinois River Bridge Replacement (FAU 6265)	20	Shale	51	3.2
Illinois River Bridge Replacement (FAU 6265)	22	Shale	133	3.2
Illinois River Bridge Replacement (FAU 6265)	24	Shale	126	2.1
Illinois River Bridge Replacement (FAU 6265)	32	Shale	986	74

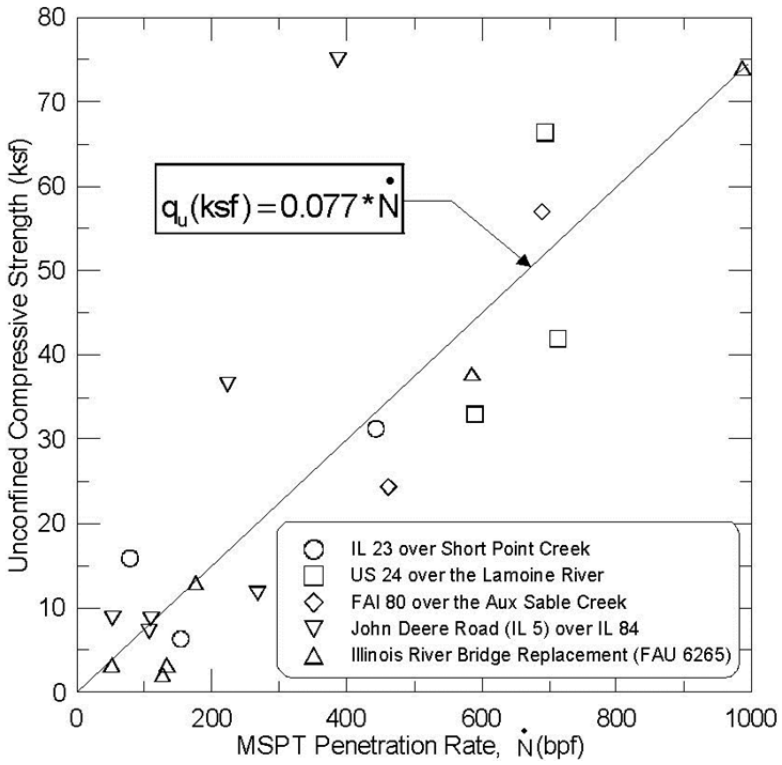

Figure F.4 Proposed correlation between MSPT penetration rate and unconfined compressive strength for weak Illinois shales.

The proposed correlation for prediction of unconfined compressive strength of weak shales from MSPT penetration rate ($\dot{N}$) is shown in Figure F.4 and is presented below:

$$q_u(ksf) = \zeta * \dot{N}$$

where

q_u = unconfined compresive strength, ksf

$\dot{N}$ = MSPT penetration rate, bpf

$\zeta = 0.077$ = empirical factor relating MSPT penetration rate and q_u, ksf / bpf

Figure F.4 shows some scatter between the trend line and the data that is due to only five sites being used to develop the correlation. Additional MSPT and triaxial compression testing has been proposed, and it is anticipated that the additional data will result in a refinement of the correlation and greater confidence in the use of the correlation for drilled shaft design in Illinois.

APPENDIX G RE-DESIGN OF DRILLED SHAFTS AT IDOT BRIDGES

G.1 INTRODUCTION

A new design method was proposed in Chapter 8 for design of drilled shafts in weak cohesive IGMs. This design method is based on a new criterion for side resistance and tip resistance. The proposed design criterion for side resistance is:

$$f_s(\text{ksf}) = 0.30 * q_u \leq 30 \text{ ksf}$$

where

f_s = unit side resistance of drilled shafts socketed in weak rocks, kips/square foot (ksf)

q_u = average unconfined compressive strength of rock along socket wall, ksf

0.30 = empirical adhesion factor, dimensionless

The proposed design criterion for tip resistance correlation is:

$$q_t = \frac{3.2 * \delta / D}{\delta / D + 1.3} * q_u * d_c \leq 2.5 * q_u * d_c$$

where

q_t = tip resistance, ksf

q_u = unconfined compressive strength, ksf

δ = tip movement, inch

D = tip diameter, inch

d_c = Vesic's depth correction factor = $1.0 + 0.4 * k$, dimesionless

$$k = \begin{cases} k = L/D & L/D \leq 1 \\ k = \tan^{-1}(L/D) & L/D > 1 \end{cases}$$

L = embedment depth in weak rock, inch

Three IDOT bridge sites where drilled shafts are used were selected to demonstrate the effectiveness of the proposed criterion for side and tip resistance. These IDOT sites are:

1. IL 23 over the Short Point Creek bridge
2. US 24 over the Lamoine River
3. John Deere Road (IL 5) over IL 84

Description of subsurface condition, existing drilled shaft geometry, and new design drilled shaft dimensions are discussed for each case to evaluate the conservatism and cost savings that may be realized by using the new side and tip resistance criteria presented above.

G.2 RE-DESIGN FOR IL 23 OVER SHORT POINT CREEK

Pier number 1 of IDOT bridge at IL 23 over Short Point Creek was studied. This pier is supported on four drilled shafts. Each of these drilled shafts has a diameter of 3 ft and is embedded 21 ft in the weathered shale. The axial factored load per drilled shaft is 349 kips. The unconfined compressive strength values of the weathered shale for this site are presented in Appendix A and were used to design the drilled shaft using the proposed side and tip resistance design criteria.

Because the new drilled shaft method accounts for strain compatibility between side and tip resistance, it was assumed that side and tip resistance contribute to the total axial capacity. A conservative value of tip displacement to tip diameter of 0.75% was used for estimating tip resistance. A resistance factor of 0.5 was applied to the predicted axial resistance.

The new design criteria results in needing a drilled shaft with a diameter of only 2.5 ft and an embedment of 8 ft into shale instead of 3-ft diameter and 21 ft of embedment. This combination yields a design-factored resistance per drilled shaft of 470 kips, which is greater than the factored service load of 349 kips. Statistics show that the cost for rock drilling has averaged about $\$105/ft^3$ of rock drilled since 2007. The new method therefore can save approximately $12,000 per drilled shaft at this site. Eight drilled shafts were used at this site for support of the two bridge piers; thus, a total of $96,000 of savings can be realized for this bridge project.

G.3 RE-DESIGN FOR US 24 OVER THE LAMOINE RIVER

Pier number 2 of the bridge at US 24 over the Lamoine River site was studied. This bridge pier is supported on three drilled shafts. Each of the drilled shafts has a diameter of 3.5 ft and is embedded 19 ft in the weathered shale. The axial factored load per drilled shaft is 740 kips. The unconfined compressive strength values of the weathered shale for this site are presented in Appendix B and were used to design the drilled shaft using the proposed side and tip resistance design criteria.

Because the new drilled shaft method accounts for strain compatibility between side and tip resistance, it was assumed that side and tip resistance contribute to the total axial capacity. A conservative value of tip displacement to tip diameter of 0.75% was used for estimating tip resistance. A resistance factor of 0.5 was applied to the predicted axial resistance.

The new design criteria results in needing a drilled shaft diameter of only 2.5 ft and an embedment of 13 ft into shale instead of 3.5 ft diameter and 21 ft of embedment. This combination yields a design-factored resistance per drilled shaft of 767 kips, which is greater than the factored service load of 740 kips. Statistics show that the cost for rock drilling has averaged about $\$105/ft^3$ of rock drilled since 2007. The new method therefore can save approximately $12,500 per drilled shaft at this site. Six drilled shafts were used to support two bridge piers; thus, a total of $75,000 of savings can be realized for this bridge project.

G.4 RE-DESIGN FOR JOHN DEERE ROAD (IL 5) OVER IL 84

The south abutment of the bridge at John Deere Road over IL 84 site was studied . This bridge abutment is supported on two rows of drilled shafts. The front row of drilled shafts is under compressive loads and back rows are under tensile loads. Each of these drilled shafts has a diameter of 3.5 ft and is embedded 20 ft in the weathered shale. The axial factored load per drilled shaft is 626 kips. The unconfined compressive strength values

of the weathered shale for this site are presented in Appendix D and were used to design the drilled shaft using the proposed side and tip resistance design criteria.

Because the new drilled shaft method accounts for strain compatibility between side and tip resistance, it was assumed that side and tip resistance contribute to the total axial capacity. A conservative value of tip displacement to tip diameter of 0.75% was used for estimating tip resistance. A resistance factor of 0.5 was applied to the predicted axial resistance.

The new design criteria results in needing a drilled shaft of only 2.5 ft and an embedment of 16.75 ft into shale instead of 3.5-ft diameter and 20 ft of embedment. This combination yields a design-factored resistance per drilled shaft of 669 kips, which is greater than factored service load of 626 kips. Statistics show the cost for rock drilling has averaged about $\$105/ft^3$ of rock drilled since 2007. The new method therefore can save approximately $11,500 per drilled shaft at this site. Thirty-two drilled shafts were used in the front row of shaft group at the south abutment of this bridge; thus, a total of $350,000 of savings can be realized for the drilled shafts in the front row of the south abutment. The back row of drilled shafts is under tensile loading, which is outside the scope of this research project and therefoere was not analyzed .

G.5 SUMMARY

Table G.1 summarizes the dimensions of the constructed drilled shafts compared to the drilled shaft dimensions estimated using the new design criteria presented in this report. Table G.1 also presents the savings per bridge pier or bridge abutment that could be achieved using the new side and tip design criteria and a total foundation support cost savings for the structure. The cost savings are significant and do not reflect the savings that would be experienced by the reduced amount of rock coring and laboratory testing due to use of the new MSPT and unconfined compressive strength of weak cohesive rock.

Table G.1 Summary of Drilled Shaft Dimensions and Cost Savings Using Proposed Design Criteria

Site	Existing Diameter (ft)	Existing Embedment Depth (ft)	New Diameter (ft)	New Embedment Depth (ft)	Cost Savings Using New Design Criteria
IL 23 over Short Point Creek	3	21	2.5	8	$12,000/shaft or $48,000 for one bridge pier
US 24 over the Lamoine River	3.5	19	2.5	13	$12,500/shaft or $37,500 for one bridge pier
John Deere Road (IL 5) over IL 84	3.5	20	2.5	16.75	$11,500/shaft or $350,000 for the front row shafts


Illinois Department
of Transportation


ILLINOIS
UNIVERSITY OF ILLINOIS AT URBANA-CHAMPAIGN